

EQUIVALENT MODEL OF PERFECTLY CONDUCTING RANDOM CYLINDERS

By
Muhammad Aqueel Ashraf

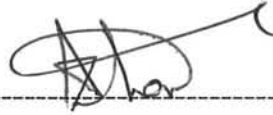
SUBMITTED IN PARTIAL FULFILLMENT OF THE
REQUIREMENTS FOR THE DEGREE OF
DOCTOR OF PHILOSOPHY
AT
QUAID-I-AZAM UNIVERSITY
ISLAMABAD, PAKISTAN
MAR 2009

© Copyright by Muhammad Aqueel Ashraf, 2009



CERTIFICATE

It is certified that Mr. Muhammad Aqueel Ashraf carried out the work contained in this dissertation, under my supervision.

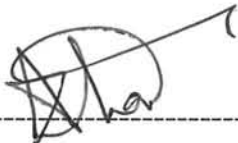


Dr. Azhar Abbas Rizvi

Professor and Chairman

Department of Electronics,

Quaid-I-Azam University Islamabad, Pakistan.



Submitted through

Prof. Dr. Azhar Abbas Rizvi

Professor and Chairman

Department of Electronics,

Quaid-I-Azam Univeristy, Islamabad, Pakistan.



Table of Contents

Table of Contents	i
Abstract	iii
Acknowledgements	iv
1 Introduction	1
2 The Random Cylinder	13
2.1 Periodic Random Process	14
2.2 Gaussian Cylinder	25
2.3 Lognormal Cylinder	31
2.4 Maximum Radius	35
2.5 Lateral Width	40
3 Scattering	51
3.1 Scattered Field	54
3.2 Coherent Scattering Amplitude	65
3.3 Optical Theorem Test	68
3.4 Total Scattering Cross Section	71
3.5 Equivalent Radius	79
3.6 Scatter Diagram	88
3.7 Joint Probability Density Function	101
3.8 Summary	104
4 Equivalent Elliptic Cylinder	108
4.1 Total Scattering Cross Section	110
4.1.1 Analytical Solution	111
4.1.2 Numerical Solution	113



4.2	Equivalent Elliptical Cylinder	115
4.3	Prediction of Total Scattering Cross Section.	125
4.4	Summary	130
5	Conclusion	133
A	Sum of Stationary Processes	140
	Reference	142

Abstract

The problem of electromagnetic scattering due to perfectly electrically conducting (PEC) random angularly corrugated cylinder, placed in free space, has been solved numerically with the help of method of moments. The field is normally incident with parallel polarization of the electric field. Two models of arbitrarily shaped cylinder are given. Statistics of geometrical properties such as root mean square area, circumference, maximum radius and lateral width of these cylinders are also determined. Scattered field due to arbitrarily shaped cylinder is obtained numerically. Its reliability is determined using optical theorem. An ensemble of fifty thousand cylinders is used for each simulation. Considering total scattering cross section as the invariant parameter, it is shown that a circular cylinder is better equivalent than a strip. It has also been shown that equivalent radius is bounded by isoperimetric inequality and can be approximated from the bounding values. Total scattering cross section is highly correlated with lateral width and the joint pdf of these two quantities is approximately Gaussian.

An elliptical cylinder is introduced as an equivalent model. Parameters of equivalent elliptic cross section are obtained using lateral width and total scattering cross section of random cylinder. It is observed that the two axes of equivalent elliptic cylinder are inversely proportional with each other and area of mean radius circular cylinder is the proportionality constant. It is concluded that if lateral width and mean radius of random cylinder is known then one can predict total scattering cross section of random cylinder with the help of equivalent elliptical cylinder.

Chapter 1

Introduction

Electromagnetic wave travelling in a homogenous medium gets scattered if it is obstructed by any inhomogeneity placed in its path. This inhomogeneity is commonly called a scatterer. Scattering of electromagnetic field is an important area of research. It has remained a field of interest since long due to its vast applications in different areas of science, such as remote sensing, radar applications and scattering from buried objects. In general, the study of scattering parameters of a scatterer depend upon the shape of the scatterer, its constituent material and the geometry in which it is placed. Scattering problems involving scatterer shapes varying from one dimensional surface to three dimensional objects with materials ranging from low contrast to perfectly conducting and placed in countless different geometries have been attempted by researchers over the years. Several analytical methods and numerical techniques have been developed to solve such scattering problems.

Geometry around a scatterer is an important factor because any other obstruction in its close proximity affects the scattered field. Object of any material other than the material of space surrounding the scatterer can be considered as another obstruction. These obstructions could be of any shape and material. In such cases, electric field is

multiply scattered back and forth between the scatterer and its surrounding obstructions. Hence, determining the scattered field becomes complicated. The complication increases as the complexity of surrounding increases. Over the years scattering problems with scatterer in different surroundings have been solved. In the absence of any other inhomogeneity, which can disturb the scattered field, the scatterer is said to be placed in free space. Free space scattering problem is relatively simple to solve for a given scatterer.

Besides surrounding of a scatterer, its constituent material is another important parameter in a scattering problem. The material properties of a scatterer can vary from low contrast to electrically opaque. A low contrast scatterer is one whose material properties are close to its surroundings whereas an opaque scatterer consists of perfect electrically conducting material. The material of the scatterer can also be anisotropic or inhomogeneous. Scattering problems with different material properties have also been solved. Solving a scattering problem with a perfect electrically conducting (PEC) scatterer is perhaps simplest among all.

Apart from material and surrounding of the scatterer, its shape is also an important factor in the study of its scattering properties. Like the other two parameters, shape of a scatterer can also be very diverse. Most of the complex shaped scatterers are usually approximated or modelled by simple canonical shapes, such that an approximate analytical solution can be obtained. The shape of a scatterer can be deterministic or random. Sizeable amount of scientific work has been carried out on studying the scattering properties of scatterers having deterministic shape. A good amount of work on scattering from deterministic boundaries has been compiled by

Bowman et.al. [1] and can be found in the references therein. Compared to deterministic scatterers, very little work on scattering from random shapes is found in literature.

Work on scattering from random boundaries has been reported as early as 1950s [2, 3]. In recent history most of the work on scattering from random boundaries is found to be on planar random surfaces. A brief description of work on PEC planar random surfaces begins with work of Ogura and his associates. In more than fifteen years of their work, in the field of scattering from random surfaces, they have developed a stochastic functional approach to obtain an approximate analog solution of the scattered field for both Dirichlet and Neumann boundary conditions. A probabilistic approach is developed in [4]. This approach is extended for scattering of scalar and EM waves from slightly rough surfaces [5, 6, 7, 8]. In [9], stochastic representation of Green's function is obtained and stochastic analog of optical theorem is developed. Stochastic functional theory is used and the scattered field is represented in terms of Weiner-Hermite functions in [10]. The stochastic functional method is then extended to two dimensional random surface [11].

A summary of analytic solutions for the scattering from random planar surface found in literature is as follows. Manninen [12] has developed a surface with multi-scale roughness using autocorrelation function to study the backscattered field. Chiu and Sarabandi [13] have applied a reciprocity based technique to study the scattered field from a dielectric cylindrical structure placed near a slightly rough planar surface. A mass operator representing multiple scattering effects is introduced in the theory of wave scattering from a slightly random surface by Tamura and Nakayama [14]. A non-Gaussian model for sea surface is introduced to obtain the scattering cross

section using geometric optics by Tatarskii and Tatarskii [15, 16]. Bistatic scattering characteristics from randomly rough surfaces along different azimuth angles based upon integral equation model with multiple scattering is studied by Hsieh [17]. Other analytical techniques developed to study different scattering parameters are Kirchhoff approximations used by Luo et.al. [18], small slope approximations, applied by Bourlier and Berginc [19] and small perturbation theory, by Soriano and Saillard [20].

Numerical techniques are also reported to have been applied to determine scattered field from random planar surfaces. A numerical solution for scattering of a narrow beam from a randomly rough Gaussian surface, using Dirichlet boundary condition and multiple reflection approach is obtained by Macaskill and Cao [21]. Wagner et.al. [22] has developed a numerical technique consisting of Fast multipole and Fast Fourier transform methods to compute the scattering from a two dimensional rough surface. Moments Method(MM) has been widely applied to determine scattered field from random planar surfaces. Zhang et.al. [23] has developed a hybrid statistical parametric maps and moments method (SPM/MM) technique to obtain scattered field from a conducting sphere above a rough surface. An iterative MM based solution is given by Donolve et.al. [24]. MM method with different basis and weighting functions is applied to obtain scattered field from planar random structures by Baudier and Dusseaux [25] and by Dusseaux and Oliveira [26]. Numerical solutions for scattering from numerous different random surfaces and random media are given by Tsang et.al. [27]. A numerical solution for scattered field by rough surface based on curvilinear coordinate system approach is given by Granet et.al. [28].

Complex manipulation of spherical functions in the perturbation calculus and lack of techniques to handle field on a random sphere are the two primary reasons

that very little work is found on electromagnetic scattering from three dimensional objects with random surface. Ogura and Takahashi [29] have extended the stochastic functional theory, developed by them, for scattering from planar surface to the case of a random spherical surface. Fung et.al. [30] have given numerical results using FD-TD method for three dimensional randomly rough surfaces. Scattering from randomly placed spherical structures has been discussed by Tsang et.al. [31]. The problem of scattering of electric field in random medium has also been attempted by Blaunstein et.al. [32] and Tseng et.al. [33].

Little work is found on electromagnetic scattering from two dimensional random cylindrical structures. In circular cylindrical coordinates, i.e., r , θ and z , three different types of random cylinders can be defined. A circular random cylinder, is a circular cylinder whose radius, r , is a random variable. An ensemble of such random cylinders consist of circular cylinders of different radii. Another type of random cylinders is axially corrugated random cylinder. The radius, $r(z)$, of these random cylinders is a stochastic process with parameter z . Cross section of these cylinders is circular with different radius at different values of z . Third type of random cylinders is called angularly corrugated random cylinders [34]. Radius of an angularly corrugated random cylinder is different at different angles and is a stochastic function of azimuthal angle, θ . The cross section of angularly corrugated random cylinders does not vary along cylindrical axis. Of all these random cylinders a circular random cylinder is easiest to generate and modelling of angularly random cylinder is most difficult. The difficulty is due to the fact that a periodic random process is needed to generate angularly corrugated cylinders. In this thesis, angularly corrugated cylinders are considered only. Henceforth, in this thesis, the term random cylinder will be used for angularly

corrugated random cylinder and cylinder with constant cross sectional radius will be referred to as circular cylinder.

Ogura and Nakayama [35, 36] have used the stochastic function approach to determine the average scattered field from random cylinder. Infinite Fourier series with two coefficients is used to define a cyclic stochastic process. One coefficient of the series is a zero mean complex Gaussian random variable and other is used to control variance of the resultant process. Vertical polarization of the incident electric field is considered in [35] whereas horizontal polarization case is solved in [36]. Solutions for scattered electric field are obtained for both Dirichlet and Neumann boundary conditions using cylindrical wave expansion of plane wave and Wiener–Hermite functions. Expressions for coherent and incoherent scattered field as well as total scattering cross section are given in terms of an infinite series of unknown coefficients. Second order solution for scattered field is obtained. Optical theorem test is used to validate the results for scattered field. The optical theorem test shows that the reliability of the scattered electric field obtained by this method decreases as the randomness increases.

All the above mentioned three types of random cylinders are used by Eftimiu [34, 37], while solving scattering problem from PEC random cylinders. The random process used to define angularly corrugated cylinder in [34] is a zero mean Gaussian process which is periodic, even and has stationary correlation function. The scattered field for all these models of random cylinders is obtained using perturbation theory. In general, scattered field for both horizontal and perpendicular polarizations of incident field is formulated. Solutions are obtained for average scattered electric field for small perturbation only. A comparison is given between average scattered field and the field scattered by a mean radius circular cylinder.

Skaropoulos and Chrissoulidis [38] have used the same model of random cylinder as used by Ogura and Nakayama [35], while tackling the scattering problem from random cylinders. Stochastic functional method is adopted to determine the scattered field. Coefficients of terms of order higher than those obtained by Ogura and Nakayama [35] for orthogonal Wiener–Hermite series are obtained. Average scattered field is obtained in all directions of observation. Stochastic optical theorem, defined by Ogura [9], is applied to show that higher order solution obtained in [38] is better than that given in [35]. Scattered field obtained in [38] does not satisfy optical theorem if the randomness is large. Skaropoulos and Chrissoulidis [39] have also attempted to obtain the scattered field from a random cylindrical surface in terms of cylindrical waves. The coefficients of the cylindrical wave expansion are expressed as an asymptotic series in the root-mean-square of surface randomness. These coefficients are determined with the help of Taylor series expansion of the Dirichlet boundary condition. Second and fourth order approximate solution for the scattered electric field are obtained.

In the above cited work on random cylinders two different angularly corrugated random cylinder models are used. Both of these models are defined as a sum of mean radius and a zero mean periodic stochastic process. Ogura and Nakayama [35] have used an infinite Fourier series to define a stochastic process. Fourier series ensures the periodicity. Random coefficients make the process a cyclic random process. A product of two numbers is used as coefficients in the Fourier series. One is a complex Gaussian random variable and other controls variance of the resultant periodic Gaussian process. Since there is no bound on Gaussian coefficients, it is difficult to ensure that radius of all random cylinders in an ensemble will always be greater than

zero, i.e., the value of the stochastic process will not be less than mean radius of the cylinder. Eftimiou [34] has defined a random process by defining its correlation function. The correlation function has to be periodic for a periodic process. There is no direct control available on the shape of random cylinders. Therefore, even with this model, it cannot be ensured that radius of all random cylinders will always be positive. Another drawback of this model is that the solution is valid for small variance in radius.

In all the above mentioned work on random cylinders, models of random cylindrical surfaces are defined in terms of their statistical averages. The shape and other geometrical parameters of the random cylinders are not specified. It is difficult to determine statistics of geometrical parameters such as area, circumference, etc. of random cylinder using the given definitions. Emphasis in these works is given on determining scattered field from random cylinders. Optical theorem test shows that their solutions are reliable only when the variance of random cylinder is small. The random scattered field is not analyzed further by any of the authors cited above. Therefore, no detailed analysis on the random cylinder or on the scattered field is available in literature.

In previous available work on random cylinders the statistical averages of scattered field from the whole ensemble are determined. In these solutions there is no procedure to determine scattered field from a single random cylinder. Hence, it is difficult to determine one to one correspondence between the random cylinder and corresponding scattered field with the help of earlier reported work. It is of interest that scattered electric field from a single random cylinder should be obtained. Scattered field from an individual random cylinder will help to better understand that how variation in

shape effects the scattered field. It is also desirable to develop a procedure for reliably determining the scattered field from random cylinders even if the variance is large.

To develop any relation between the two random processes i.e., random cylinder and scattered field, it is important that detailed statistics of the individual process should be known. Thus statistics of few important parameters of random cylinder, such as area, circumference and lateral width are also desirable to be known. It is difficult to obtain statistics of such parameters from the given models of random cylinder. Hence a new random cylinder model needs to be defined such that statistics of its other geometrical parameters can also be determined. This new random process will be better if it has no restriction on ensembles, i.e., random cylinders should not be restricted by choices of correlation function or its variance. Thus random cylinders can be generated of shapes significantly different from circular cylinders.

Is it possible to estimate the scattered field from a single random cylinder without solving the electromagnetic scattering problem, i.e., can one predict the scattered field or any scattering parameter of a random cylindrical structure from its geometrical parameters? This question can be answered in affirmative if an equivalent model can be obtained for random cylinder. An equivalent model of a structure is one which helps to predict certain parameter(s) of the actual structure [40]. In general, a circular cylinder has been used as an equivalent model [41, 42]. Does a better equivalent model exist for random cylinders? A model which can better approximate the scattered field or any other scattering parameter of random cylinders than circular cylinder. Another aspect to search is cross sectional shape of these equivalent cylinders, i.e., a shape whose scattering properties are close to the average scattering properties of the ensemble.

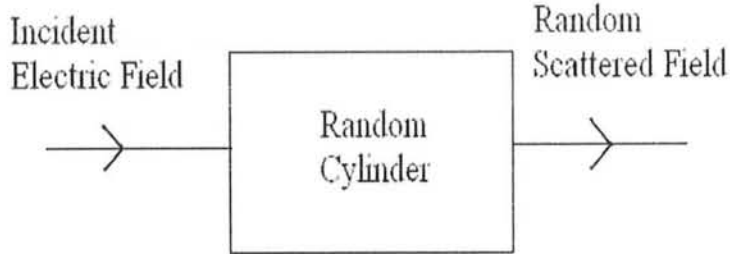


Figure 1.1: An equivalent linear system model for scattering from random cylinders.

The problem of determining an equivalent shape can be considered as a system identification problem. An analogy of the above problem with signals and systems can be made by considering the incident plane wave as input to the system, random cylinder as the system and scattered field as the output of the system, as shown in the Figure 1.1. Input to the system is deterministic but the system is a random process and so is the output. It is of interest to determine the system from its output, i.e., infer about the scatterer from its scattered field. Although there is a one to one correspondence between the random cylinder and scattered field but scattered field is complicated function of scatterer's shape.

In the previously reported work, the cylinder model is defined in terms of its statistical averages and statistical averages of the output scattered field are obtained. Statistics of different geometric parameters are needed in order to determine any correspondence between scatterer and scattered field. To obtain statistics of different

geometrical parameters of random cylinders, i.e., functions of a random process, either the probability density function(pdf) or infinite moments of the random process should be known. Hence, it is difficult to determine the statistics of any geometrical parameter of random cylinders if only mean and covariance of the radius are known. If with mean and covariance matrix the radius is classified as Gaussian then the ensemble of random cylinder are restricted. Further, due to average operation on the scattered field all the information about scattered field from an individual sample function is lost. Therefore, it is impossible to predict equivalent shape or the system using the earlier reported procedures.

To be able to predict the equivalent shape of random cylinders a new model is used to define random cylinders. In chapter two of this thesis, a zero mean periodic stationary stochastic process is first defined with the help of finite Fourier series. Characteristic function and k^{th} statistical moment of finite Fourier series are obtained. It is shown that the stochastic Fourier series is stationary and its pdf is determined. Two different models of random cylinders are obtained using this stochastic process. Average area and circumference due to rms differential length are obtained for both these models. Out of the two models only one is used to study its scattering properties. Probability density of maximum radius and lateral width are obtained for the selected model.

Scattered field from random cylinders and its analysis are presented in chapter three of this thesis. The scattered field from random cylinder is obtained numerically using Method of Moments(MM). Considering the random nature of the scatterer and the error introduced by MM, the number of segments are carefully determined for MM. Optical theorem is used to verify the reliability of the numerically obtained

scattered field. Average scattered field is also determined and compared with the previously documented results for reliability. Equivalent canonically shaped models, such as circular cylinder and strip, are obtained keeping average total scattering cross section of random cylinders as the invariant parameter. Bounds on the values of radius of equivalent circular cylinder and on average total scattering cross section are obtained. Scatter plots are obtained between lateral width and total scattering cross section of random cylinders and the joint pdf of these two random variables is estimated. In chapter four of this thesis a cylinder with elliptic cross section is considered and its scattering properties are analyzed. An equivalent elliptic cylinder model is obtained. Further analysis is performed to determine any relation between the equivalent elliptical model parameters and the ensemble statistics of random cylinder. In the last chapter some concluding remarks about the work are given.

Chapter 2

The Random Cylinder

An angularly corrugated cylinder is the one whose cross section is random but does not vary along the cylindrical axis. If it is represented in circular cylindrical coordinates then radius r has to be a periodic random process with parameter θ and independent of cylindrical z axis. Two slightly different models of random cylindrical structure are found in literature. Both of these models are expressed as periodic stationary Gaussian stochastic processes. One of these models of random cylindrical structure, presented by Eftimiu [34], is defined with the help of mean and correlation of the process. The correlation of the stochastic process is taken to be even, periodic and translational invariant. The other model is given by Ogura and Nakayama [35]. Stochastic function for this model is written in terms of infinite complex Fourier series, with normalized orthogonal complex coefficients. The coefficients consist of a product of two numbers, one is a complex Gaussian random variable and other is used to control variance of the process. As discussed in previous chapter, these cylinder models have a few shortcomings.

In this chapter a new random cylinder model is defined with the help of a stochastic process. A random process can only be used to define a random cylinder if it is

periodic and continuous at 2π . It shall always be greater than zero and shall not be a multi-valued function. Electromagnetic boundary conditions are difficult to apply at sharp edges, therefore, randomness should not introduce any sharp edges or jump discontinuity in the resultant cylinder. All these requirements are met in two steps, first an auxiliary random function is defined and with the help of auxiliary process a model of random cylinder is obtained.

An auxiliary process is defined such that it is a zero mean cyclic random process. It is defined with the help of finite Fourier series. Using this auxiliary random process two different models of random cylinder are obtained. These models are named as Gaussian and Lognormal cylinders. Geometrical parameters such as mean area, circumferential length, equivalent area radius and equivalent circumferential length are determined for both these models. Out of these two models one is selected to study its scattering properties. Later in this chapter the probability distributions of maximum radius and lateral width of selected random cylinder are estimated.

2.1 Periodic Random Process

In this section an auxiliary random process is defined. It will be helpful in expressing radius of random cylinders. Characteristics of the auxiliary random process should be such that it can be used to model random cylinder. Hence, certain conditions which are imposed on this auxiliary random process are that auxiliary process has to be periodic, smooth and continuous at 2π . It also should not be a multiple valued function. An auxiliary random process defined in terms of Fourier series fulfills all the above mentioned requirements. Fourier series ensures that the process is periodic and single valued. Smoothness is achieved by truncating the Fourier series to finite

number of terms.

Randomness in the auxiliary random process is introduced by randomizing the coefficients of the series. A random phase component is also introduced in each harmonic of the series. Addition of random phase is important as it helps to make the statistics of the random process independent of azimuthal angle. Mathematically this auxiliary random process is given as,

$$\mathbf{p}(\theta) = \sum_{n=1}^N \mathbf{A}_n \cos(n\theta + \Psi_n) \quad (2.1.1)$$

where \mathbf{A}_n and Ψ_n are all independent and identically distributed(i.i.d.) random variables. Probability distributions of both the random variables are taken to be uniform, such that random variable \mathbf{A}_n is distributed between $[-B, B]$ and the range for random variable Ψ_n is $[-\pi, \pi]$.

To better understand the behaviour of auxiliary process $\mathbf{p}(\theta)$ statistical moments of this process are obtained first. The k^{th} statistical moment of $\mathbf{p}(\theta)$ can be written as,

$$E[\mathbf{p}(\theta)^k] = E \left[\left(\sum_{n=1}^N \mathbf{A}_n \cos(n\theta + \Psi_n) \right)^k \right]. \quad (2.1.2)$$

Using the independence of all the random variables the above equation can be written as,

$$E[\mathbf{p}(\theta)^k] = \sum_{n=1}^N E[\mathbf{A}_n^k] E[\cos^k(n\theta + \Psi_n)] \quad k > 0 \quad (2.1.3)$$

The k^{th} statistical moment of random variable \mathbf{A} can be given as

$$\begin{aligned} E[\mathbf{A}_n^k] &= \int_{-B}^B \frac{1}{2B} A_n^k dA_n \\ &= \begin{cases} B^k/(k+1) & k = 2, 4, 6, \dots \\ 0 & k \text{ odd,} \end{cases} \end{aligned} \quad (2.1.4)$$

and for even values of k ,

$$\begin{aligned} E[\cos^k(n\theta + \Psi_n)] &= \frac{1}{2^k} \sum_{m=0}^k \binom{k}{m} e^{in(2m-k)\theta} E[e^{i(2m-k)\Psi_n}] \\ &= \frac{1}{2^k} \binom{k}{k/2}. \end{aligned} \quad (2.1.5)$$

Therefore, the k^{th} moment of $\mathbf{p}(\theta)$ is given as,

$$E[\mathbf{p}(\theta)^k] = \begin{cases} \binom{k}{k/2} \frac{NB^k}{2^{k(k+1)}} & k = 2, 4, 6, \dots \\ 0 & k \text{ odd.} \end{cases} \quad (2.1.6)$$

The above equation shows that mean of the auxiliary random process, \mathbf{p} , is zero and its variance, $\sigma_{\mathbf{p}}^2$, is equal to $NB^2/6$.

Autocorrelation function $R_{\mathbf{p}}(\theta_1, \theta_2)$ of the auxiliary process is given as

$$\begin{aligned} R_{\mathbf{p}}(\theta_1, \theta_2) &= E[\mathbf{p}(\theta_1)\mathbf{p}(\theta_2)] \\ R_{\mathbf{p}}(\tau) &= \frac{B^2}{6} \sum_{n=1}^N \cos(n\tau) \end{aligned} \quad (2.1.7)$$

where $\tau = \theta_1 - \theta_2$ is the difference between two angles. Since mean value of the process is zero therefore its covariance is equal to its correlation. It is important to note that mean value of the auxiliary process is zero and its correlation depends on the relative interval of the two angles hence the process \mathbf{p} is at least wide sense stationary.

An important statistical parameter which can be determined with the help of statistical moments is the characteristic function of a random process. It is defined as[43],

$$\Phi_{\mathbf{p}}(\omega) = \sum_{k=0}^{\infty} \frac{(j\omega)^k}{k!} E[\mathbf{p}^k], \quad (2.1.8)$$

The characteristic function of the auxiliary random process $\mathbf{p}(\theta)$ can be written by employing its statistical moments, which have been obtained in equation (2.1.6), in the above equation as,

$$\Phi_{\mathbf{p}}(\omega) = 1 + \sum_{k=1}^{\infty} \frac{(j\omega)^{2k}}{(k!)^2} \frac{(6 \sigma_{\mathbf{p}}^2)^k}{2^{2k}(2k+1)N^{k-1}} \quad (2.1.9)$$

In principle, first-order density function of a random process can be obtained by taking inverse Fourier transform of the characteristic function. Characteristic function of this random process is convergent for a finite value of ω , therefore, for a fixed finite value of ω , its inverse Fourier transform can be evaluated by truncating the series at suitably large value of k . Whereas, for $\omega \rightarrow \infty$ the series is not convergent and its inverse Fourier transform cannot be evaluated for large values of ω . Therefore, it is difficult to write a close form first-order pdf of the random process \mathbf{p} from its characteristic function.

First-order density function of the auxiliary function $\mathbf{p}(\theta)$ can also be determined from the density function of a single harmonic in the Fourier series and using independence of each harmonic in Fourier series. Probability distribution function of a single harmonic, $\mathbf{p}_n(\theta)$, in the Fourier sum is obtained as follows,

$$\mathbf{p}_n(\theta) = \mathbf{A} \cos(n\theta + \Psi) = \mathbf{A}\mathbf{Q} \quad (2.1.10)$$

where random variable, \mathbf{Q} , is a function of Ψ and its pdf is given as [44]

$$f_{\mathbf{Q}}(Q) = \frac{1}{\pi \sqrt{1 - Q^2}}. \quad (2.1.11)$$

Since \mathbf{A} and Ψ are independent, \mathbf{A} and \mathbf{Q} are also independent. Joint pdf of random variables \mathbf{A} and \mathbf{Q} can thus be written as the product of their individual pdfs,

$$f_{\mathbf{A}\mathbf{Q}}(A, Q) = f_{\mathbf{A}}(A) \frac{1}{\pi \sqrt{1 - Q^2}}. \quad (2.1.12)$$

Using the transformation for a product of random variables [43], one obtains pdf of \mathbf{p}_n from the joint pdf of \mathbf{A} and \mathbf{Q} as follows,

$$f_{\mathbf{p}_n}(p_n) = \int_{-\infty}^{\infty} \frac{1}{\pi \sqrt{1-Q^2}} f_{\mathbf{A}}\left(\frac{p_n}{Q}\right) \frac{dQ}{|Q|}. \quad (2.1.13)$$

Random variable \mathbf{Q} is a cosine function of real argument and $f_{\mathbf{A}}(A)$ is uniformly distributed between $[-B, B]$, therefore, random variable \mathbf{Q} will be zero outside the interval $|p_n|/B \leq |Q| \leq 1$. Hence the pdf of \mathbf{p}_n is written as

$$\begin{aligned} f_{\mathbf{p}_n}(p_n) &= \int_{-1}^{-|p_n|/B} \frac{1}{2\pi B|Q|\sqrt{1-Q^2}} dQ + \int_{|p_n|/B}^1 \frac{1}{2\pi B|Q|\sqrt{1-Q^2}} dQ \\ &= \frac{1}{\pi B} \ln \left| \frac{p_n}{B - \sqrt{B^2 - p_n^2}} \right|. \end{aligned} \quad (2.1.14)$$

The above equation shows that the pdf is symmetric around zero and has a spread of $\pm B$. It is important to note that $f_{\mathbf{p}_n}(p_n)$ has an integrable singularity at $p_n = 0$ and it is not a function of θ . Since the phase term in a single harmonic, \mathbf{p}_n , is uniformly distributed between $[-\pi, \pi]$ and is independent of amplitude of the harmonic, the joint density of its amplitude and phase can be written as

$$f_{\mathbf{A}\Psi}(A, \Psi) = f_{\mathbf{A}}(A) \frac{1}{2\pi} \quad (2.1.15)$$

therefore, the process \mathbf{p}_n is strict sense stationary as well [43].

Random variables \mathbf{A}_n and Ψ_n are all i.i.d., therefore, each harmonic \mathbf{p}_n in the Fourier series is statistically independent and identically distributed. The pdf of $\mathbf{p}(\theta)$ for N independent harmonics is therefore, N^{th} order convolution of the pdf of \mathbf{p}_n . It is difficult to obtain a close form solution of the N^{th} order convolution of the expression on right hand side of equation (2.1.14), hence the pdf of \mathbf{p} is approximated with the help of Central Limit Theorem (CLT). Central Limit Theorem states that

the sum of large number of independent random variables tends to be a Gaussian random variable, irrespective of the probability densities of the variables added. Can CLT be applied to determine pdf of process \mathbf{p} , given that the pdf of process \mathbf{p}_n has an integrable singularity at zero? A sufficient condition for applicability of CLT on identically distributed random variables is that the third absolute central moment of individual pdf, i.e., $E[|\mathbf{p}_n - E[\mathbf{p}_n]|^3]$, remains bounded. The third absolute moment of \mathbf{p}_n is given as,

$$\begin{aligned} E[|\mathbf{p}_n|^3] &= E[|\mathbf{A} \cos(n\theta + \Psi)|^3] \\ &= E[|\mathbf{A}|^3] E[|\cos(n\theta + \Psi)|^3] \leq B^3/4. \end{aligned} \quad (2.1.16)$$

It is finite, therefore, CLT can be applied to approximate the pdf of the auxiliary random process \mathbf{p} .

Applicability of CLT can also be verified by evaluating the characteristic function of the random process \mathbf{p} as N approaches infinity. The characteristic function of \mathbf{p} , given by equation (2.1.9), in the limit $N \rightarrow \infty$ and for finite $\sigma_{\mathbf{p}}$ will become

$$\lim_{N \rightarrow \infty} \Phi_{\mathbf{p}}(\omega) = 1 - \frac{\omega^2 \sigma_{\mathbf{p}}^2}{2}, \quad (2.1.17)$$

which is the characteristic function of a Gaussian probability density function. Therefore, for large N , the pdf of \mathbf{p} can be approximated as normal pdf, having zero mean and variance equal to $\sigma_{\mathbf{p}}^2$, i.e., $N(0, \sigma_{\mathbf{p}}^2)$

$$f_{\mathbf{p}}(p) = \frac{1}{\sigma_{\mathbf{p}} \sqrt{2\pi}} e^{-\frac{1}{2}(p/\sigma_{\mathbf{p}})^2}. \quad (2.1.18)$$

Boundedness of the third absolute moment of individual pdfs only fulfills sufficient condition on applicability of CLT. On the other hand, the characteristic function above has shown that the pdf of \mathbf{p} becomes Gaussian when the number of terms in Fourier sum is large.

Theoretically, the pdf of \mathbf{p} is Gaussian if the number of terms, N , tends to infinity but as N increases higher order harmonics will be added in the Fourier sum. With the introduction of higher order harmonics the random process tends to be like a Gaussian noise process. Surfaces defined using such processes are referred to as rough surfaces. As discussed in previous chapter, scattering characteristics of such surfaces have been largely studied. Noise like Gaussian random process is undesirable in this work, therefore, N has to be kept sufficiently low and it becomes important to determine the minimum number of terms needed to approximate pdf of $\mathbf{p}(\theta)$ as Gaussian. Minimum number of terms are determined with the help of numerical simulation. Numerical code is written in Fortran programming language. The statistics of the random process are estimated with the help of standard software tools. To have faith in the process of generation and analysis of the random process, these estimated parameters are compared with the exact analytical results. Exact analytical results are available only for a single term of the random process \mathbf{p}_n , therefore, a single term of the Fourier sum is simulated first.

Random numbers with uniform pdf have been generated using RNUNF(\cdot) function from standard IMSL library. Hundred thousand samples of $\mathbf{p}_n(\theta)$ have been generated for a single simulation. Values of the generated process have been recorded for different fixed values of θ . Probability density function is estimated from the numerical data for each value of θ . These estimates of pdf are first compared with each other. They are found to be same for every θ , thus validating the stationarity of the simulated process. One of these pdfs is then compared with the analytically determined pdf, given by equation (2.1.14). Figure 2.1 shows the analytic pdf and the pdf estimated from numerical data for $B = 1$. Both the plots in Figure 2.1 are in

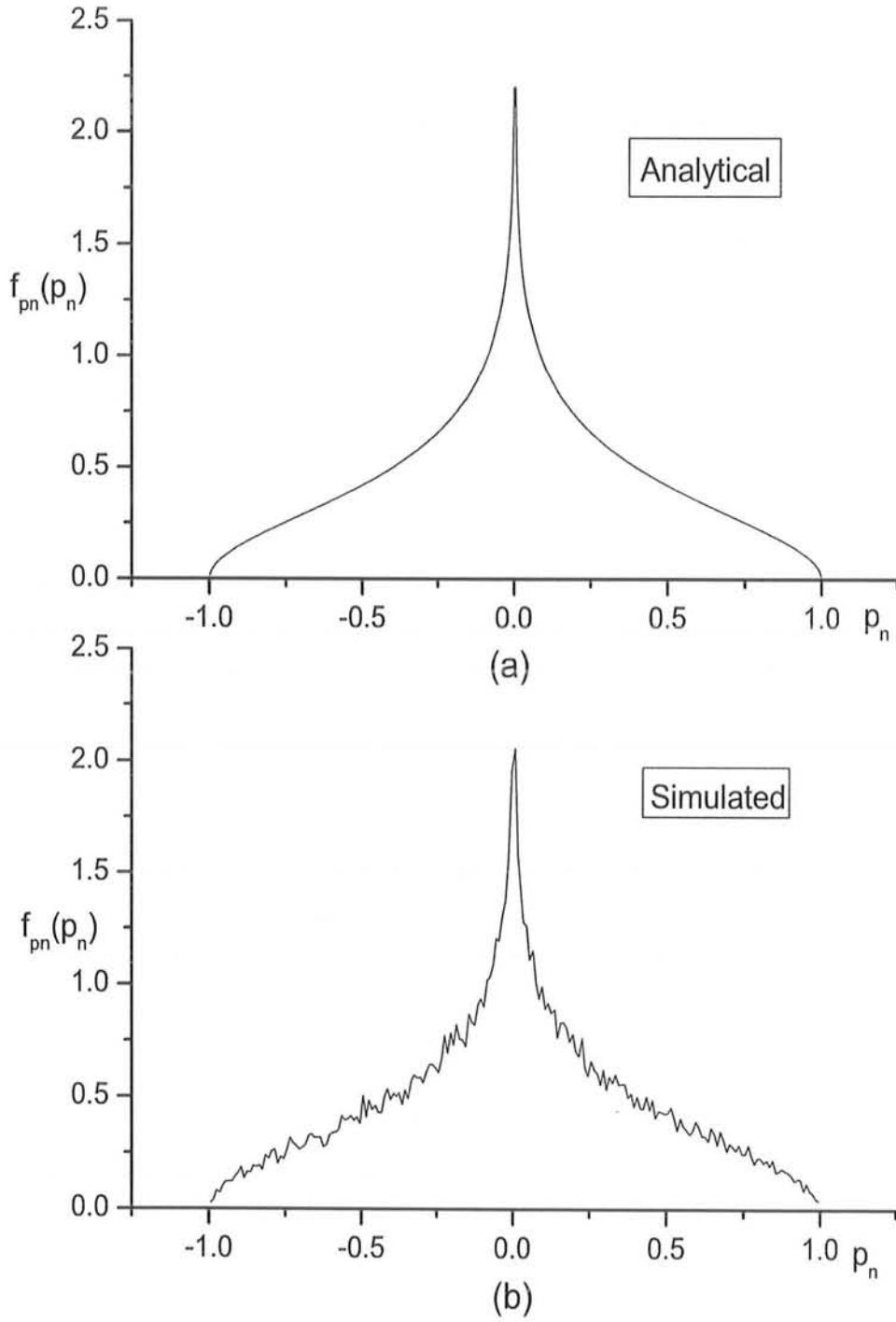


Figure 2.1: Probability density function of $\mathbf{p}_n(\theta)$, $f_{\mathbf{p}_n}(p_n)$, for $N = 1$ and $B = 1$. (a) Analytical, (b) Simulated.

good agreement with each other. Therefore, the procedure of generation of random process and estimation of its pdf is reasonably reliable.

After gaining confidence in numerical procedure, random process $\mathbf{p}(\theta)$ is simulated for different values of N and a fixed value of θ . Probability density functions have been estimated from the recorded data for each value of N . A Gaussian curve is fitted on these estimated pdfs to determine how close these curves are to a Gaussian and is shown in Figure 2.2. The Figure shows pdfs of \mathbf{p} estimated from numerical data and Gaussian fitted curves for $B = 1$ and $N = 2, 3, 4$ and 5 . Broken lines in the Figure are the estimated pdfs of numerical data and solid lines are Gaussian curves fitted to the estimated pdf. In curve fitting procedure, two parameters of the Gaussian, i.e., mean and standard deviation are optimized to better match the pdf estimated from the numerical data. Analytic mean of the process \mathbf{p} is zero and so is the estimated mean from the data. Since it does not depend on number of terms, therefore, it is not useful for determining minimum number of terms.

Standard deviation of the random process depends on number of terms in the Fourier sum. Therefore, standard deviation for fixed values of N obtained from analytical expression and its estimated value from simulated data as well as from the fitted Gaussian curve are tabulated in Table 2.1. A comparison between tabulated standard deviations can answer the question of minimum number of terms required in the Fourier sum for $f_{\mathbf{p}}(p)$ to be approximated as Gaussian. In Table 2.1 column labelled χ^2 shows the goodness of fit parameter. It is defined as

$$\chi^2 = \frac{1}{M - p} \sum_{n=1}^M [y_n - f(x_n)]^2, \quad (2.1.19)$$

where M is total number of bins used while estimating the pdf from numerical data, y is measured value, i.e., bin count, $f(x)$ is the fitted expression and p is total number

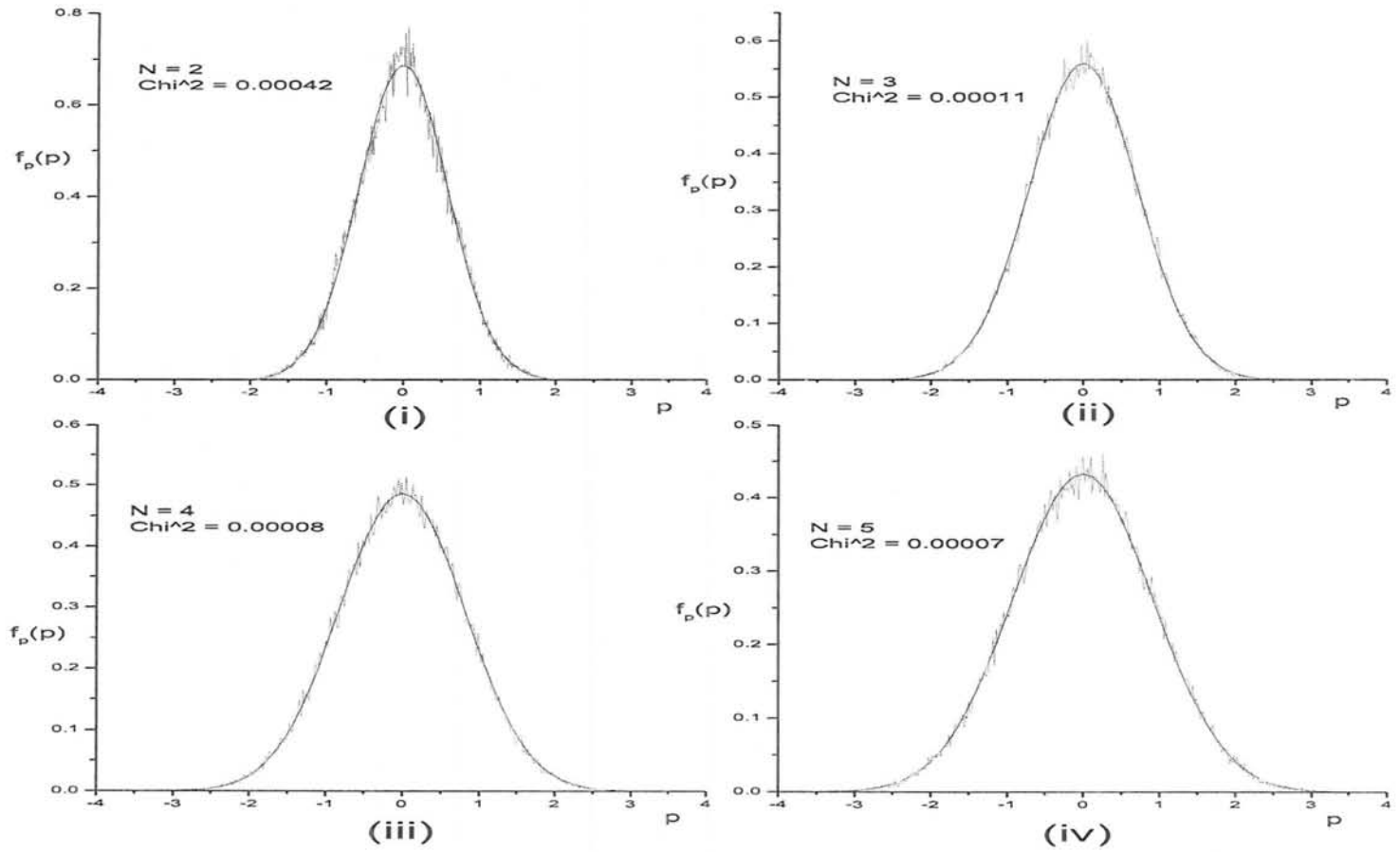


Figure 2.2: Probability density function of $p(\theta)$, $f_p(p)$, for $B = 1$ and $N =$ i) 2, ii) 3, iii) 4 and iv) 5. (---) Numerically estimated and (—) Gaussian curve fitted to estimated pdf.

N	Analytic σ_p^2	Simulated data σ_p^2	Gaussian fit σ_p^2	χ^2
2	0.57735	0.57644	0.58171	0.00042
3	0.70711	0.70691	0.71352	0.00011
4	0.81649	0.81615	0.82057	0.00008
5	0.91287	0.91561	0.92202	0.00007
6	0.99990	0.99856	1.00175	0.00007
7	1.08012	1.08017	1.08702	0.00005
8	1.15470	1.16039	1.16580	0.00005
9	1.22474	1.22528	1.23022	0.00004

Table 2.1: Standard deviations of $f_{\mathbf{P}}(p)$ obtained analytically, estimated from simulated data, of Gaussian fitted curve and goodness of fit parameter for different number of terms, N .

of parameters in the fitted expression which are to be determined to minimize χ^2 [45]. This column indicates that as N increases, χ^2 decreases showing a better fit to the Gaussian Curve. Hence, goodness of fit is chosen as the parameter to determine the minimum value of N for which $f_{\mathbf{P}}(p)$ can be considered Gaussian. The estimated pdf is said to be Gaussian for all values of χ^2 less than 10^{-4} . It is therefore concluded from the Table 2.1 and graphs in Figure 2.2 that N should be greater than 3 for $f_{\mathbf{P}}(p)$ to be approximately Gaussian.

Hence, pdf of the random process defined in terms of Fourier series with uniformly varying random amplitudes and phases will be considered Gaussian if the number of terms, N , is greater than 3. The process \mathbf{p} is sum of processes \mathbf{p}_n and it has been shown that \mathbf{p}_n is a strict sense stationary, therefore process \mathbf{p} is also stationary, Appendix A. This auxiliary random function fulfills most of the requirements for radius of random cylinder. Randomness of the auxiliary function can be controlled by choosing suitable values of N and B . This process has both negative as well as

positive values, i.e., it is not positive definite hence cannot be directly used as radius of random cylinder, which is always positive. The requirement that the random process should always be positive, for it to be used as radius of random cylinder, can be met with two different ways. Hence there are two choices to define the radius of a random cylinder using this auxiliary random function. These choices of random cylinders are named Gaussian and Lognormal. Each of the two types of random cylinders and their statistical properties are presented in subsequent sections.

2.2 Gaussian Cylinder

Most of the requirements of the radius of random cylinder are met by auxiliary random process \mathbf{p} and only the negative values of the process hinders it to be called as radius of random cylinder. Hence a useful model for random cylinder can be defined by only shifting mean of the random process \mathbf{p} . Mean of the process is shifted by adding a constant value in the auxiliary process. Mathematically it is given as

$$\mathbf{r}(\theta) = r_d + \mathbf{p}(\theta) \quad (2.2.1)$$

where r_d is the desired mean of the random cylinder. Cylinders with radius defined by above equation will be referred to as Gaussian cylinders. Probability density function of radius, $f_{\mathbf{r}}(r)$, is normal, $N(r_d, \sigma_{\mathbf{p}}^2)$, where $\sigma_{\mathbf{p}}^2$ is given by equation (2.1.6). One advantage of defining a random cylinder in this manner is that a desired mean value of the radius can be obtained without affecting any other parameter.

Variance of Gaussian random cylinder $\sigma_{\mathbf{p}}^2$ can be changed to any desired value by either properly selecting N and B or by scaling the random variable \mathbf{r} . Variance depends upon total number of terms used to define the random radius, N and the

value of B according to equation (2.1.6). Number N is an integer whereas B is a real number. A particular value of σ_p^2 can be obtained by using different values of N and B , therefore, the value of N used to obtain a particular value of variance also needs to be mentioned together with the variance of random cylinder to unambiguously represent an ensemble of random cylinders.

Autocorrelation of radius of Gaussian cylinders is given as

$$R_g(\theta_1, \theta_2) = E[\mathbf{r}(\theta_1)\mathbf{r}(\theta_2)] = r_d^2 + \frac{B^2}{6} \sum_{n=1}^N \cos\{n(\theta_1 - \theta_2)\} \quad (2.2.2)$$

Second term in the above equation is the auto-covariance of the auxiliary function \mathbf{p} , given by equation (2.1.7). Therefore, the above equation can also be expressed as

$$R_g(\tau) = r_d^2 + R_p(\tau) \quad (2.2.3)$$

Let τ_1 be the angle where first zero of auto-covariance function, $R_p(\tau)$, occurs and the angle between first nulls of the auto-covariance function, $2\tau_1$, be the correlation angle of the process $\mathbf{r}(\theta)$. The angle τ_1 for auto-covariance function given by equation (2.1.7), is equal to $\pi/(N+1)$. A plot of normalized covariance is shown in Figure 2.3 for $N = 5$ and 10, showing that as N increases the correlation angle decreases. Other statistical parameters of \mathbf{r} are similar to that of random process $\mathbf{p}(\theta)$.

A similar definition of random cylinder has been used by Ogura et.al. [35]. An infinite complex Fourier series with complex Gaussian random coefficients is used to obtain the random process. Advantage of using Gaussian coefficients is that the resultant process is Gaussian. One of its disadvantages is that there is no limit on maximum and minimum values of the random process. Whereas with uniform variate random coefficients of a finite Fourier series the resultant process is always confined

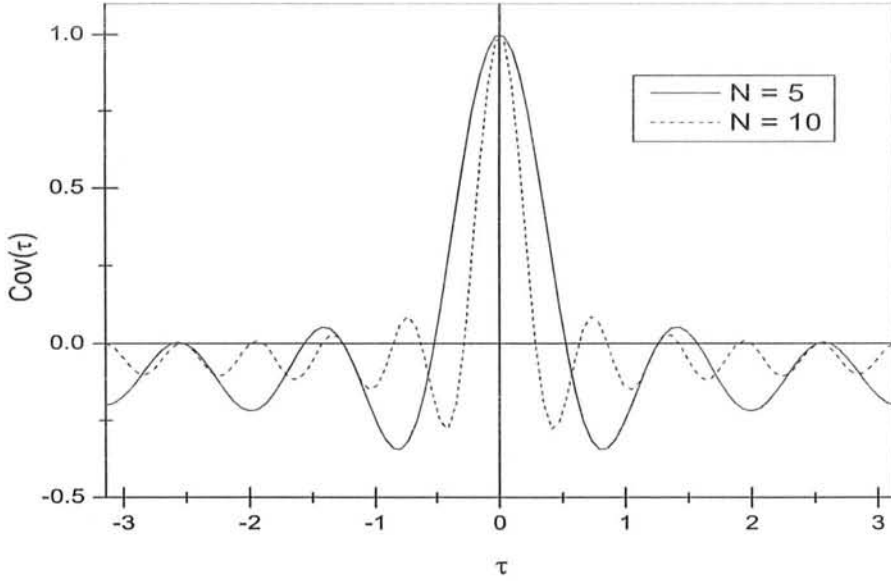


Figure 2.3: Normalized covariance of Gaussian cylinder.

to $\pm NB$ and it has almost Gaussian distribution. An advantage of the limited range of the random process is that no random cylinder will ever have negative radius at any angle if input parameters, r_d , N and B are properly chosen. If the choice of N and B is such that there is a finite probability of radius to become negative then it is proposed to reject all those cylinders whose radius is negative for any value of θ . The pdf of radius of such Gaussian cylinders will be a conditional distribution $f_{\mathbf{r}}(r|\mathbf{r} > 0)$. This pdf will also be Gaussian with its tail truncated for $\mathbf{r} < 0$.

Since radius of the random cylinder is random, therefore, the cross sectional area will also be random. Average cross sectional area of a random cylinder is written as,

$$E[\text{Area}] = \frac{1}{2} \int_0^{2\pi} E[\mathbf{r}(\theta)^2] d\theta \quad (2.2.4)$$

The second moment of $\mathbf{r}(\theta)$ is given as

$$E[\mathbf{r}(\theta)^2] = r_d^2 + \sigma_{\mathbf{p}}^2 \quad (2.2.5)$$

where $\sigma_{\mathbf{p}}^2$ is the variance of random process \mathbf{p} . Hence mean area of Gaussian cylinder is $\pi(r_d^2 + \sigma_{\mathbf{p}}^2)$. Let equivalent area radius, r_{ea} , be defined as the radius of a circle which occupies the same area as average area of random cylinder and is given as $r_{ea} = \sqrt{E[\mathbf{Area}]/\pi}$. It is equal to $\sqrt{(r_d^2 + \sigma_{\mathbf{p}}^2)}$ for a Gaussian cylinder. Circumferential length of random cylinder is another geometrical quantity of interest. In parametric form, the differential arc length, dl , of a curve, i.e., the length of the arc subtended by angle $d\theta$, is given as

$$dl = \sqrt{r^2 + \left(\frac{dr}{d\theta}\right)^2} d\theta \quad (2.2.6)$$

Integrating above equation with respect to (w.r.t.) the parameter θ over the range $[0 - 2\pi]$ gives total circumferential length of a convex shaped closed structure.

The statistical averages of circumference due to rms differential length of random cylinders are obtained as follows. It is difficult to determine the expected value of differential length, $d\mathbf{l}$ from the statistics of \mathbf{r} , due to a square operator in equation (2.2.6). On the other hand, it is relatively easy to determine the root mean square value of $d\mathbf{l}$, i.e., $\sqrt{E[(d\mathbf{l})^2]}$. According to equation (2.2.6) the root mean square of $d\mathbf{l}$ is written as,

$$\sqrt{E[(d\mathbf{l})^2]} = \left\{ E[\mathbf{r}^2] + E\left[\left(\frac{d\mathbf{r}}{d\theta}\right)^2\right] \right\}^{1/2} d\theta \quad (2.2.7)$$

For Gaussian cylinder, $E[\mathbf{r}^2]$ is given by equation (2.2.5) and with the help of Fourier sum used to define \mathbf{r} , $E[(d\mathbf{r}/d\theta)^2]$ can be obtained as

$$E\left[\left(\frac{d\mathbf{r}}{d\theta}\right)^2\right] = \frac{\sigma_{\mathbf{p}}^2(N+1)(2N+1)}{6} \quad (2.2.8)$$

Values of $E[r^2]$ and $E[(dr/d\theta)^2]$ show that rms differential length of Gaussian cylinder is independent of parameter θ . Integrating equation (2.2.7) w.r.t. parameter θ over the range $[0 - 2\pi]$ gives a measure of circumferential length of Gaussian cylinder, as

$$l = 2\pi \left[r_d^2 + \sigma_p^2 \left(1 + \frac{(N+1)(2N+1)}{6} \right) \right]^{1/2} \quad (2.2.9)$$

This circumference is due to rms differential length of Gaussian cylinder.

It is important to note that circumference due to rms differential length of Gaussian cylinder depends on mean radius, variance and total number of terms in the Fourier sum, whereas its average area does not depend on total number of terms, N . Variance of random cylinders marks deviation of its shape from circular cylinder. An increase in number of terms N , while keeping variance constant, makes the surface of Gaussian cylinder rougher, a surface with large number of small peaks. Thus average area of the Gaussian cylinder remains constant and the circumference due to rms differential length of Gaussian cylinder increases with increase in N and equation (2.2.9) gives good estimate of the circumference due to rms differential length of Gaussian cylinders. Let equivalent circumferential radius, r_{ec} , be the radius of a circle whose circumference is equal to the circumference of a non circular cylinder. For random cylinders it can be written as $\sqrt{E[l^2]}/2\pi$. The equivalent circumferential radius of Gaussian cylinder is

$$r_{ec} = \left[r_d^2 + \sigma_p^2 \left(1 + \frac{(N+1)(2N+1)}{6} \right) \right]^{1/2} \quad (2.2.10)$$

which is the root mean square length of random cylinder per unit radian of angle.

Of all geometric shapes a circle requires minimum perimeter length to enclose a given area. For a given area, if the perimeter length is different from of a circle then the shape of the object could not be a circle. In a class of convex shaped structures a thin

strip requires largest perimeter length to enclose a given area. Similarly the perimeter length of rough or non convex closed structures will also be greater than that of a circle required to enclose same area. Therefore as a measure of deformation in the shape of random cylinders from a circular cylinder a quantity called equivalent radii ratio is defined herein. An Equivalent radii ratio(EQRR) is the ratio of equivalent circumferential and equivalent area radii.

$$EQRR = \frac{r_{ec}}{r_{ea}} \quad (2.2.11)$$

The minimum value of equivalent radii ratio is one, which is for a circular cross section. Higher values of this ratio show deviation from circular cross section, either elongated or rough. The higher the values of this ratio larger is the deviation of the cross sectional shape from a circle.

Equivalent radii ratio for Gaussian cylinder can be written as

$$\frac{r_{ec}}{r_{ea}} = \left[1 + \frac{\sigma_p^2}{\sigma_p^2 + r_d^2} \frac{(N+1)(2N+1)}{6} \right]^{1/2} \quad (2.2.12)$$

The above relation shows that equivalent radii ratio of Gaussian cylinder depends on mean and variance of the radius as well as on number of terms N . The equivalent radii ratio for a Gaussian cylinder with mean radius, $r_d = 3$, $B = 0.5$ and $N = 5$ is 1.1175. A representative Gaussian cylinder with these input parameters is shown in Figure 2.4. It can be seen that the cylinder is smooth and its cross section does not deviate markedly from a circular cylinder. It can also be observed from the figure that Gaussian cylinder is not double valued at any angle. Another important observation is that the number of maxima of radius is equal to the number of terms N . The largest number of maxima a Gaussian cylinder can have is equal to the number of terms in the Fourier sum. For a given mean radius and variance, as circumference

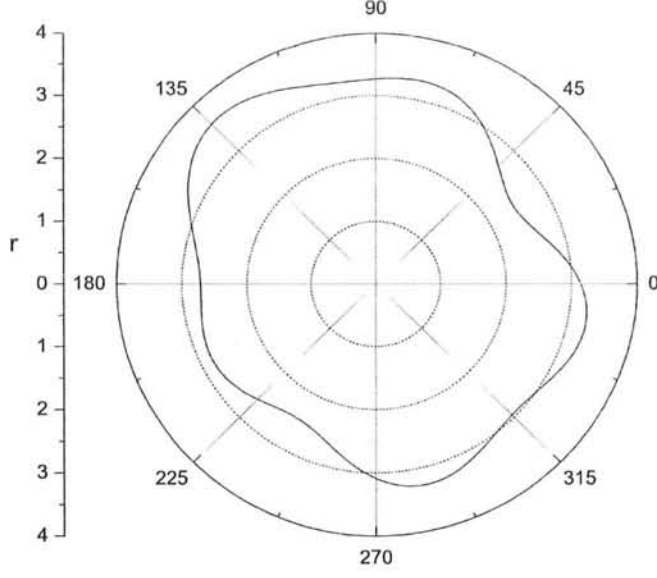


Figure 2.4: A Gaussian cylinder with $r_d = 3\lambda$, $B = 0.5$ and $N = 5$.

due to rms differential length increases the surface becomes rougher and rougher and resultant Gaussian cylinder will have more maxima and less deviation from the mean radius.

2.3 Lognormal Cylinder

Considering the fact that radius of any physical cylinder cannot be negative another possible definition of random cylinder using auxiliary random process $\mathbf{p}(\theta)$ can be given as

$$\mathbf{r}(\theta) = e^{\mathbf{p}}. \quad (2.3.1)$$

The probability density of $\mathbf{r}(\theta)$ is lognormal as $\log(\mathbf{r})$ is normally distributed. This model of random cylinder has been used for studying light scattering from heavenly

bodies, such as comets [46]. Mischenko et.al. [46] has referred to this model as Gaussian cylinder whereas, in this thesis, it will be referred to as lognormal cylinder. The k^{th} order statistical moment of radius of lognormal cylinder \mathbf{r} is given as

$$E[\mathbf{r}^k] = \int_{-\infty}^{\infty} (e^p)^k \frac{1}{\sigma_{\mathbf{p}} \sqrt{2\pi}} e^{-p^2/2\sigma_{\mathbf{p}}^2} dp = e^{(k\sigma_{\mathbf{p}})^2/2} \quad (2.3.2)$$

Mean radius of lognormal cylinder is therefore given as $e^{\sigma_{\mathbf{p}}^2/2}$ and its variance is $\{e^{2\sigma_{\mathbf{p}}^2} - e^{\sigma_{\mathbf{p}}^2}\}$.

Average cross sectional area, given by equation (2.2.4), of lognormal cylinder is $\pi e^{2\sigma_{\mathbf{p}}^2}$ and its equivalent area radius, r_{ea} , is therefore given as $e^{\sigma_{\mathbf{p}}^2}$. According to equation (2.2.6), second moment of radius \mathbf{r} and its derivative with respect to θ , $d\mathbf{r}/d\theta$, are needed to determine the mean square differential length of lognormal cylinders. Second moment of \mathbf{r} , i.e., $E[\mathbf{r}^2]$ can be obtained from equation (2.3.2). The second moment of $d\mathbf{r}/d\theta$, i.e., $E[(d\mathbf{r}/d\theta)^2]$ is obtained with the help of autocorrelation function of $d\mathbf{r}/d\theta$. The statistics of radius \mathbf{r} of lognormal cylinder are determined first in order to obtain the autocorrelation function of first derivative of \mathbf{r} .

The autocorrelation of radius \mathbf{r} of lognormal cylinder can be expressed as

$$R_1(\theta_1, \theta_2) = E[\exp\{\mathbf{p}(\theta_1) + \mathbf{p}(\theta_2)\}] \quad (2.3.3)$$

The autocorrelation of an exponential function of a stationary, zero mean normal stochastic process \mathbf{p} is given by [44], as

$$R_1(\tau) = \exp\{\sigma_{\mathbf{p}}^2(1 + r_{cp}(\tau))\} \quad (2.3.4)$$

where r_{cp} is the correlation coefficient of process \mathbf{p} and is given as

$$r_{cp}(\tau) = \frac{R_{\mathbf{p}}(\tau)}{\sigma_{\mathbf{p}}^2} = \frac{1}{N} \sum_{n=1}^N \cos(n\tau) \quad (2.3.5)$$

Since $R_1(\tau)$ is a function of $\tau = \theta_1 - \theta_2$, therefore, the process \mathbf{r} is at least wide sense stationary.

The process \mathbf{r} if passed through a differentiator yields another random process $\mathbf{v} = d\mathbf{r}/d\theta$. Since \mathbf{r} is a wide sense stationary process, therefore, autocorrelation of \mathbf{v} can be written as [44],

$$\begin{aligned} R_{\mathbf{v}}(\tau) &= -\frac{d^2 R_1(\tau)}{d\tau^2} \\ &= -R_1\left\{\left(-\frac{1}{N} \sum_{n=1}^N n \sin n\tau\right)^2 - \frac{1}{N} \sum_{n=1}^N n^2 \cos n\tau\right\}. \end{aligned} \quad (2.3.6)$$

As \mathbf{v} is a zero mean process, therefore, its variance is $R_{\mathbf{v}}(0)$ and it is given as

$$E[\mathbf{v}^2] = E\left[\left(\frac{d\mathbf{r}}{d\theta}\right)^2\right] = \frac{(N+1)(2N+1)}{6} \exp\{2\sigma_{\mathbf{p}}^2\} \quad (2.3.7)$$

which is the desired quantity needed to determine the mean square differential length given by equation (2.2.7).

Root mean square differential length of lognormal cylinder is therefore written as

$$\sqrt{E[(d\mathbf{l})^2]} = \left[1 + \frac{(N+1)(2N+1)}{6}\right]^{1/2} \exp\{\sigma_{\mathbf{p}}^2\} d\theta \quad (2.3.8)$$

The circumference of lognormal cylinder due to rms differential length can easily be determined by integrating the above equation with parameter θ over the range $[0 - 2\pi]$. The Equivalent circumferential radius, r_{ec} , of lognormal cylinders can thus be written as

$$r_{ec} = \left[1 + \frac{(N+1)(2N+1)}{6}\right]^{1/2} \exp\{\sigma_{\mathbf{p}}^2\} \quad (2.3.9)$$

The above equation shows that equivalent circumferential radius r_{ec} increases exponentially with increase in variance $\sigma_{\mathbf{p}}^2$ and approximately linearly with number of

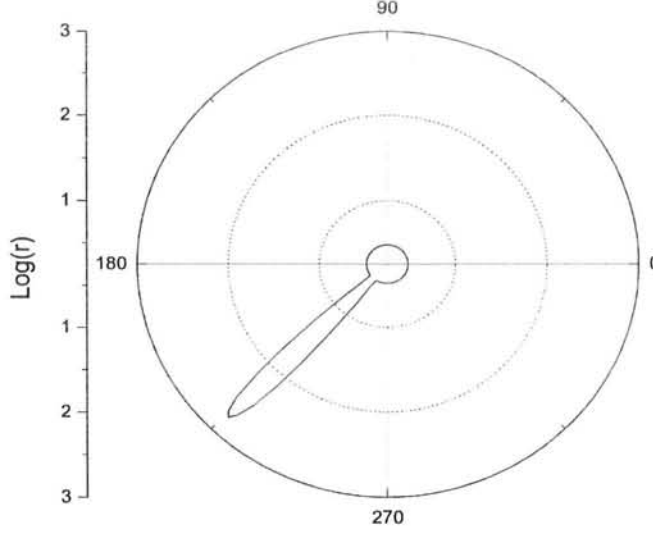


Figure 2.5: A Lognormal cylinder with a long tail.

terms N . It implies that for a given value of σ_p^2 and N equivalent circumference due to rms differential length of lognormal cylinder is greater than Gaussian cylinder.

Equivalent radii ratio for lognormal cylinder can be written as

$$\frac{r_{ec}}{r_{ea}} = \left[1 + \frac{(N+1)(2N+1)}{6} \right]^{1/2}. \quad (2.3.10)$$

It is important to note that the above ratio depends only on number of terms N . For a given value of N , the cross sectional shape of lognormal cylinder will deviate more from circular cylinder as compared to cross section of Gaussian cylinder. Therefore, Lognormal cylinders have tendency to have cross sections deviating markedly from a circle. At times the cylinder is so deformed that it appears as if the cylinder has a long tail. Figure 2.5 shows a flat lognormal cylinder. In this figure the radius is plotted on logarithmic scale, even on this scale the tail is very prominent. These tails at times are so sharp that the sampling of these tails becomes difficult with a

finite precision machine. These cylinders appear more like a large strip with a round edge rather than a perturbed circular cylinder. Therefore, it is not a good model for studying electromagnetic scattering from structure resembling circular cylinder. Hence this model is not used any further and hereafter the term random cylinder will be used for a Gaussian cylinder only.

2.4 Maximum Radius

Radius of a random cylinder varies randomly. As the radius of a given sample function varies along θ , it traces crests and troughs. One of these crests has the highest value of that sample function. Highest valued crest is the global maximum radius, \mathbf{R}_M , in that realization. Global maximum radius of random cylinder and its angle of occurrence Θ_M both are random. The range of values of global maximum radius \mathbf{R}_M is between mean radius, r_d , and upper limiting value, $r_d + NB$, of the ensemble. The pdf of global maximum radius gives an estimate of how frequently a particular value of global maximum occurs and how long the bulge of Gaussian cylinder could be. Global Maximum radius, \mathbf{R}_M , can occur at any angle, as the random process $\mathbf{r}(\theta)$ is stationary, therefore pdf of Θ_M has to be uniform $[-\pi, \pi]$.

To obtain the pdf of global maximum radius \mathbf{R}_M , the probability distribution function of local maxima of the radius, $f_{\text{lmx}}(r)$, is determined first. The pdf of local maxima is determined with the help of the joint pdf of \mathbf{r} , its first and second derivatives, i.e., $f_{\mathbf{rva}}(r, v, a)$. Random variables \mathbf{v} and \mathbf{a} are first and second derivative of \mathbf{r} w.r.t. θ respectively. At a given angle θ , $f_{\mathbf{rva}}(r, v, a)drdvda$ represents the probability that the random variables \mathbf{r} , \mathbf{v} and \mathbf{a} lie between $[r_0, r_0 + dr]$, $[v_0, v_0 + dv]$ and $[a_0, a_0 + da]$ respectively. Maximum of a process is an event when its first derivative

is zero and second derivative is negative. Therefore, the pdf of local maxima can be written as [47]

$$f_{\text{lmx}}(r) = \int_{-\infty}^0 |a| f_{\text{rva}}(r, 0, a) da. \quad (2.4.1)$$

For Gaussian process the pdf of maxima has been obtained by Rice [48] and it is given as,

$$\begin{aligned} f_{\text{lmx}}(r) = & \sqrt{1 - \epsilon^2} \Phi\left(\frac{(r - r_d)\sqrt{1 - \epsilon^2}}{\epsilon\sigma_{\mathbf{p}}}\right) \frac{(r - r_d)}{\sigma_{\mathbf{p}}^2} \exp\left\{-\frac{(r - r_d)^2}{2\sigma_{\mathbf{p}}^2}\right\} \\ & + \frac{\epsilon}{\sigma_{\mathbf{p}}\sqrt{2\pi}} \exp\left\{-\frac{(r - r_d)^2}{2(\epsilon\sigma_{\mathbf{p}})^2}\right\} \end{aligned} \quad (2.4.2)$$

where,

$$\Phi(q) = \frac{1}{\sqrt{2\pi}} \int_{-\infty}^q e^{-u^2/2} du,$$

$$\epsilon = \sqrt{\frac{M_0 M_4 - M_2^2}{M_0 M_4}}$$

and

$$M_n = r_0^2 \delta_n + \frac{\sigma_A^2}{2} \sum_{p=1}^N p^n.$$

Function $\Phi(\cdot)$, in the above equation, is the cumulative normal probability function and M_n is the n^{th} spectral moment of radius. The above distribution has been referred to as Rice distribution [47].

The problem of estimating pdf of global maximum in a sample of N maxima of a Gaussian process has been considered by Cartwright and Longuet-Higgins [3]. They have only determined expected value of the global maximum of Gaussian process for different values of N and ϵ . General expression for pdf of the global maximum is

complicated. Few assumptions are applied to obtain a simplified expression for pdf of the global maximum radius of Gaussian random cylinders. These assumptions are that number of maxima a Gaussian cylinder will have in each realization is equal to number of terms in the Fourier sum N , all of them are identically distributed and the distribution of each maximum is given by equation (2.4.2). It is also assumed that the angle between two consecutive maxima will be greater than the correlation angle such that all of these N maxima are independent. One of the maximum among all these maxima is a global maximum. The pdf of maximum among N i.i.d. random variables is given as [43],

$$f_{\mathbf{R}_M}(r) = N f_{\text{lmx}}(r) [F_{\text{lmx}}(r)]^{N-1} \quad (2.4.3)$$

where $F_{\text{lmx}}(r)$ is the cumulative distribution function of $f_{\text{lmx}}(r)$ and for the above mentioned pdf of local maxima, equation (2.4.2), it is given as

$$F_{\text{lmx}}(r) = \Phi\left(\frac{(r - r_d)}{\epsilon\sigma_p}\right) - \sqrt{1 - \epsilon^2} \Phi\left(\frac{(r - r_d)\sqrt{1 - \epsilon^2}}{\epsilon\sigma_p}\right) \exp\left\{-\frac{(r - r_d)^2}{2\sigma_p^2}\right\}. \quad (2.4.4)$$

It is important to note that the above equation does not depend on θ , hence the global maximum of radius $\mathbf{r}(\theta)$ is equally likely to occur at any angle, i.e., Θ_M is uniformly distributed between $[-\pi, \pi]$.

The assumption of having N maxima in each realization is very crude. N is the largest number of maxima of a Gaussian cylinder and it is not necessary that Gaussian cylinder will have N maxima in each realization. It is also not necessary that the angle between two consecutive maxima should be greater than the correlation angle. Hence these maxima are not necessarily independent of each other. Therefore, it is important to verify the simplified expression for pdf of global maximum radius of Gaussian cylinder. Verification of the expression (2.4.3) is done with the help

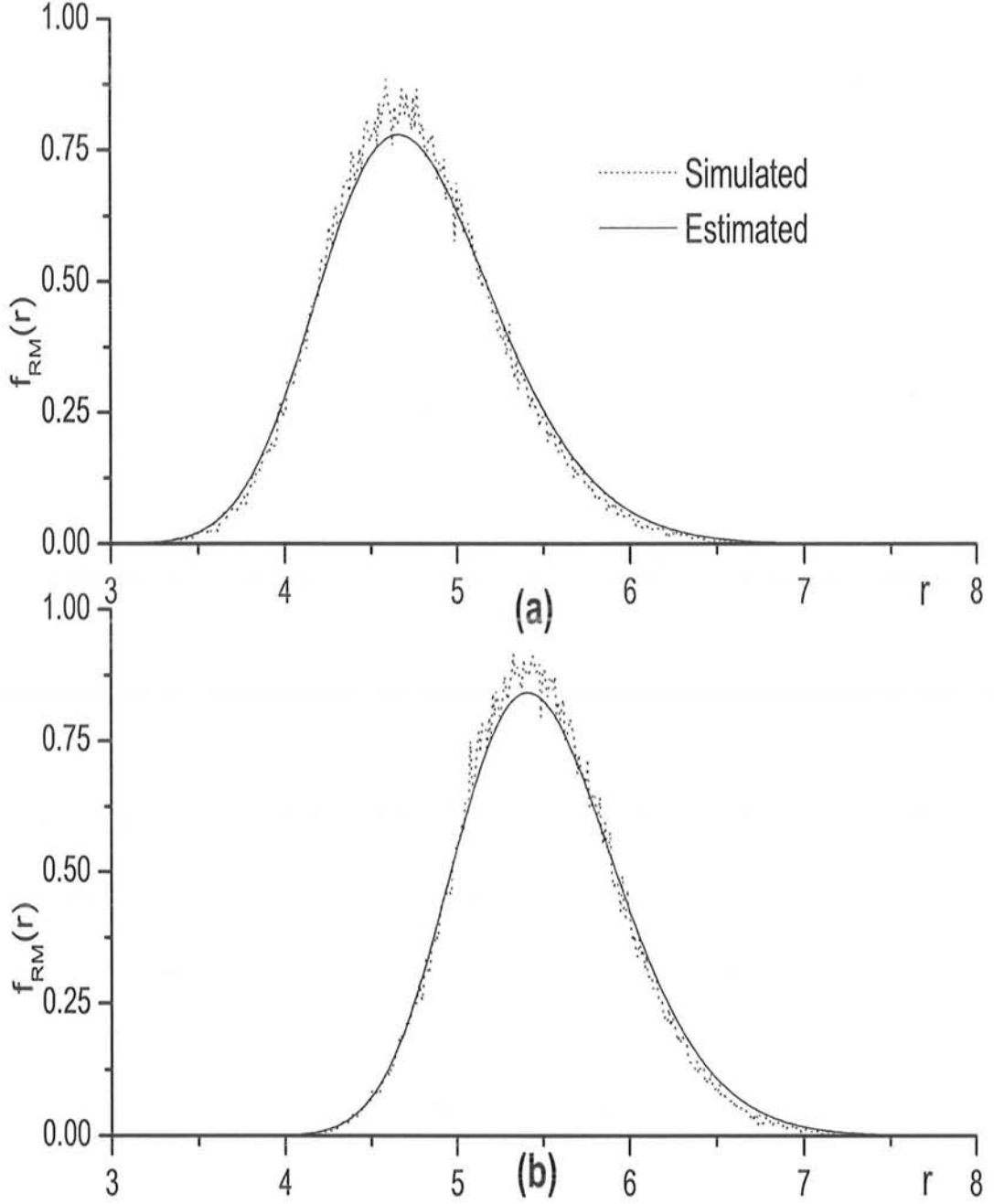


Figure 2.6: Pdf of global maximum radius of Gaussian cylinders, $f_{\mathbf{R}_M}(r)$. a) $r_d = 3\lambda$, $B = 1$ and $N = 5$ and b) $r_d = 4\lambda$, $B = 1$ and $N = 4$.

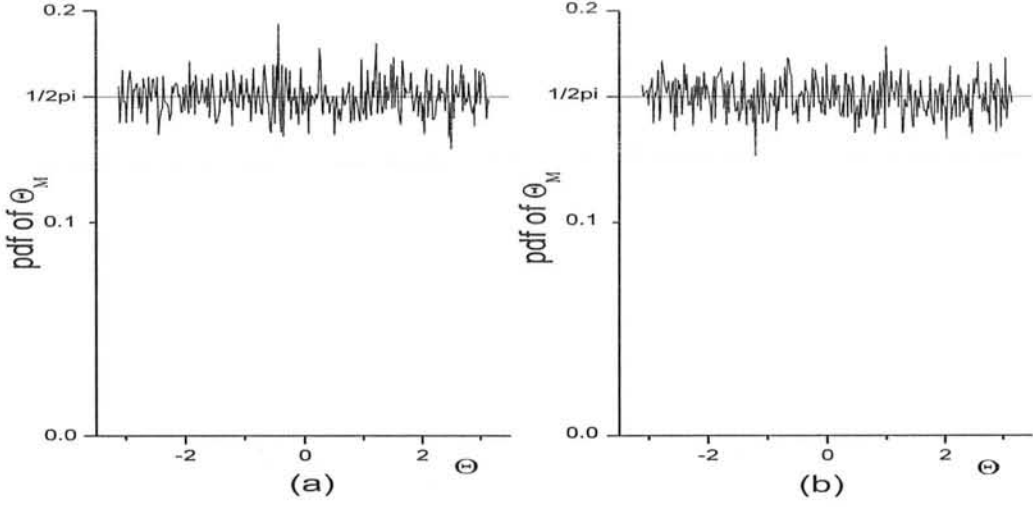


Figure 2.7: Pdf of angle at which maximum radius of Gaussian cylinders occurs, Θ_M . a) $r_d = 3\lambda$, $B = 1$ and $N = 5$ and b) $r_d = 4\lambda$, $B = 1$ and $N = 4$.

of numerical simulation. Hundred thousand Gaussian cylinders are generated and the global maximum radius R_M with corresponding angle, Θ_M , have been recorded for each cylinder. Recorded data is then processed to estimate the pdf of R_M and Θ_M . Figure 2.6 shows the pdfs of global maximum radius of two Gaussian cylinders having different input parameters. Dotted line in the figure is the pdf estimated from simulated data and solid line is the plot of equation (2.4.3). The two curves are in good agreement with each other for both of the graphs shown. Irrespective of the fact that the assumptions employed to derive equation (2.4.4) are very raw, close proximity of dotted and solid curves encourages one to use this simplified expression for determining an approximate pdf of maximum global radius of Gaussian cylinder.

Probability density function of the angle at which maximum global radius, Θ_M , occurs is also estimated from the simulated data and is shown in Figure 2.7. The estimated pdf is almost horizontal at an amplitude of $1/2\pi$, verifying the fact that

the angle Θ_M is uniformly distributed between $[-\pi, \pi]$. Uniform distribution of Θ_M between $[-\pi, \pi]$ signifies that \mathbf{R}_M is equally likely to occur at any angle.

2.5 Lateral Width

Lateral width of an object can be defined as its maximum projection on a plane. It is the width of a scatterer seen by the incident wave in the geometric optics limits hence the projection plane is taken to be normal to incident. Lateral width of a scatterer depends upon the direction of incidence. The lateral width of a circular cylinder is equal to its diameter, irrespective of the direction of incidence due to its symmetrical cross section. The diameter of a circular cylinder which can circumscribe a random cylinder cannot be said as lateral width of random cylinder. Optical theorem relates total power scattered by an object to its lateral width, therefore, it is an important geometrical parameter of a scatterer to study its scattering properties. Since the radius of random cylinder is random therefore its lateral width is also random. If statistical properties of the radius of random cylinder are stationary then statistics of its lateral width will be independent of the direction from which plane wave is made incident on random cylinder. A plane which is normal to the incident plane wave will be referred to as normal plane in this section.

Lateral width of a two dimensional object can also be defined as the minimum distance between two parallel planes such that the said object is confined by them. These parallel planes should be placed orthogonal to the normal plane. The distance between confining planes is maximum projection of the cylinder on the normal plane. Let a plane wave propagating along y -axis be incident on a random cylinder and the axis of cylinder is along z -axis then the confining planes are constant x planes.

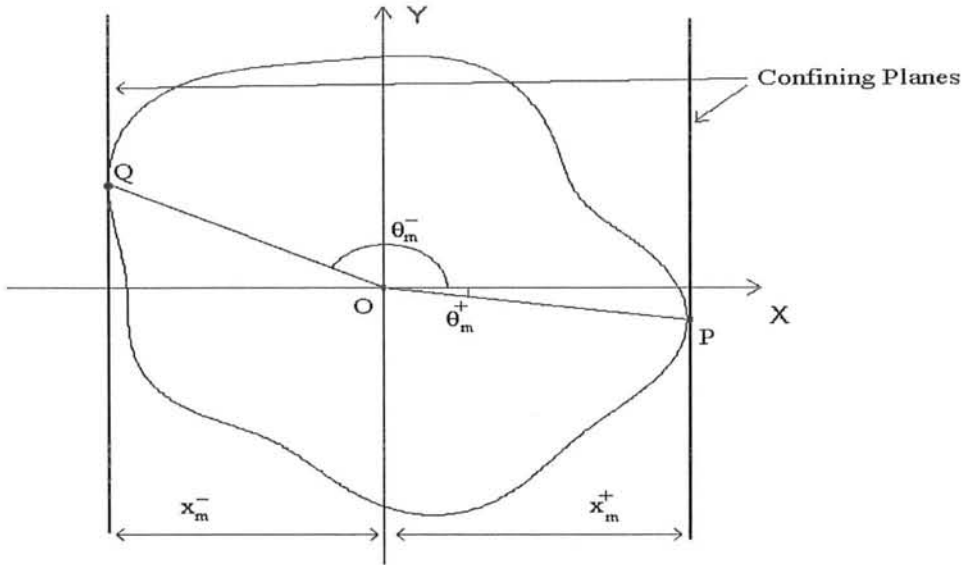


Figure 2.8: A random cylinder and its lateral width.

Confining planes are defined by equations $x = x_m^+$ and $x = x_m^-$ and any constant y plane is a normal plane, as shown in Figure 2.8. Points P and Q , in the figure, denote the points where the confining planes are tangent to the random cylinder and θ_m^+ & θ_m^- are the angles which position vectors P and Q make with positive x -axis, respectively. In terms of x_m^+ & x_m^- lateral width, l_w , of a cylindrical object can be written as

$$l_w = x_m^+ - x_m^- \quad (2.5.1)$$

Considering the fact that center of the cylindrical object is at origin, x_m^- is always negative. Thus lateral width can be written as

$$l_w = x_m^+ + |x_m^-| \quad (2.5.2)$$

Statistics of lateral width will now be investigated.

N	S. D. θ_m^+ (deg)	S. D. θ_m^- (deg)	Coefficient of Correlation
3	15.06888	15.08394	-0.202910
4	17.18016	17.28060	+0.089330
5	17.85338	17.89140	-0.097275
6	17.19116	17.17218	+0.002639
7	17.40207	17.32471	+0.001439
8	17.67735	17.65376	-0.005990
9	17.84554	17.72943	-0.000720
10	17.85338	17.89140	-0.000890

Table 2.2: Numerical estimate of standard deviations and correlation coefficient between θ_m^+ and θ_m^- , for different number of terms, N .

To investigate the statistics of lateral width first the correlation between \mathbf{x}_m^+ and \mathbf{x}_m^- is determined. It was earlier emphasized while modelling the random cylinder, in section(2.2), that random cylinder should be smooth, therefore, it is not very likely that any given realization of random cylinder is skewed or deformed in such a way that the angular separation between points P & Q , i.e., $\Delta\theta = |\theta_m^+ - \theta_m^-|$ becomes very small. The two points P and Q can therefore be considered uncorrelated if the angular separation $\Delta\theta$ is greater than $2\tau_1$, where $\tau_1 = \pi/(N+1)$ represents the angle where first zero of the correlation function in equation (2.1.7) occurs. To further demonstrate that the points P & Q are uncorrelated, the coefficient of correlation between the two angles is computed from simulated data and it is given in Table 2.2. It shows that the estimated correlation coefficient is of the order of 10^{-3} for $N > 5$. Hence, for $N > 5$ it is safe to assume that \mathbf{x}_m^+ and \mathbf{x}_m^- are uncorrelated with each other.

It has been shown that \mathbf{x}_m^+ and \mathbf{x}_m^- are uncorrelated with each other but to simplify the process to obtain pdf of lateral width it is further assumed that these two are

independent of each other. This is a crude approximation but will greatly facilitate to approximate the pdf of lateral width, which is otherwise difficult to determine. With the assumption that both \mathbf{x}_m^+ and \mathbf{x}_m^- are independent of each other, statistics of any one of these random variables can be determined independent of other. Hence the pdf of maximum projection of the radius on positive x -axis, \mathbf{x}_m^+ , is determined first.

Let $\mathbf{x}^+(\theta)$ be the projection of radius on positive x -axis. It can be written as

$$\mathbf{x}^+(\theta) = \mathbf{r}(\theta) \cos \theta \quad -\pi/2 < \theta < \pi/2, \quad (2.5.3)$$

where $\mathbf{r}(\theta)$ is random radius and for a fixed value of θ , $\cos \theta$ is a constant scaling factor. Since the radius of Gaussian cylinder is normally distributed, therefore, for a given value of θ , the pdf of \mathbf{x}^+ is also normal, given as,

$$f_{\mathbf{x}^+}(x) = \frac{1}{\sqrt{2\pi}\sigma_p \cos \theta} \exp\left\{-\frac{1}{2}\left[\frac{x - r_d \cos \theta}{\sigma_p \cos \theta}\right]^2\right\}. \quad (2.5.4)$$

The covariance between any two points of \mathbf{x}^+ can be determined using the statistics of radius \mathbf{r} and it is given as,

$$E[(\mathbf{x}_i^+ - r_d \cos \theta_i)(\mathbf{x}_j^+ - r_d \cos \theta_j)] = \cos \theta_i \cos \theta_j R_p(\cos \theta_i - \cos \theta_j) \quad (2.5.5)$$

where function $R_p(\cdot)$ is covariance of the auxiliary random process \mathbf{p} and is given by equation (2.1.7). The above relation shows that process \mathbf{x}^+ is a non stationary process as its covariance depends on individual values of θ_i and θ_j . Maximum of the process $\mathbf{x}^+(\theta)$ for $-\pi/2 < \theta < \pi/2$ is the maximum projection of radius on positive x -axis, given as,

$$\mathbf{x}_m^+ = \max_{-\pi/2 < \theta < \pi/2} [\mathbf{x}^+(\theta)]. \quad (2.5.6)$$

\mathbf{x}_m^+ is the displacement of confining plane on positive x -axis.

A system which determines maximum of an input is a non linear system. It has memory and its inverse system does not exist. These properties of $\max(\cdot)$ function makes it difficult to obtain statistical properties of its output from the statistics of its input. Non stationarity of the input process, \mathbf{x}^+ , further complicates the problem of determining statistical parameters of the output, \mathbf{x}_m^+ . Therefore, an analytical solution for determining the statistical properties of \mathbf{x}_m^+ is difficult and in this thesis numerical techniques are employed to estimate the statistics of \mathbf{x}_m^+ , from the statistics of the input process, \mathbf{x}^+ .

Cumulative distribution function CDF of maximum projected radius, $F_{\mathbf{x}_m^+}(x)$, is numerically estimated. Samples of the projected radius, \mathbf{x}^+ , are obtained first. Then the probability that all these samples are less than a certain number, x , is determined. The process \mathbf{x}^+ is a bandlimited process, therefore, according to the stochastic sampling theorem, it can be fully represented by its samples [44]. Stochastic sampling theorem states that if $\mathbf{f}(t)$ is a bandlimited process, then

$$\mathbf{f}(t + \tau) = \sum_{n=-\infty}^{\infty} \mathbf{f}(t + nT) \frac{\sin[\omega_o(\tau - nT)]}{\omega_o(\tau - nT)}, \quad (2.5.7)$$

for every t and τ , where ω_o is the maximum frequency of $\mathbf{f}(t)$ and $T = \pi/\omega_o$. Since $N + 1$ is the highest frequency component of \mathbf{x}^+ , therefore, the sampling interval of $\mathbf{x}^+(\theta)$ must be $\theta_s \leq \pi/(N + 1)$.

Let random variables, $\mathbf{x}_1^+, \mathbf{x}_2^+, \dots, \mathbf{x}_K^+$ be samples of process \mathbf{x}^+ and $\theta_1, \theta_2, \dots, \theta_K$ be their respective angles, then \mathbf{x}_m^+ can be written as,

$$\mathbf{x}_m^+ = \max(\mathbf{x}_1^+, \mathbf{x}_2^+, \dots, \mathbf{x}_K^+). \quad (2.5.8)$$

and its cumulative distribution function can be written as [43]

$$F_{\mathbf{x}_m^+}(x) = Pr(\mathbf{x}_i^+ \leq x_m^+, \forall i) = F_{\mathbf{x}^+}(x_m^+, x_m^+, \dots, x_m^+) \quad (2.5.9)$$

where $Pr(x)$ is probability of event x and $F_{\mathbf{x}^+}(\cdot)$ is joint CDF of all the samples. To evaluate the above expression, first the number of samples and their corresponding angles for a given N are determined. Mean value of each sample and covariances of all samples with each other are estimated. Finally their joint CDF, $F_{\mathbf{x}_m^+}(\cdot)$, is evaluated numerically. Numerical results thus obtained are numerically differentiated to obtain the pdf of \mathbf{x}_m^+ , i.e., $f_{\mathbf{x}_m^+}(x)$. Figure 2.9 shows the pdf of maximum projection of radius on positive x -axis, for two representative cylinders. Solid lines in the figure are the plots of numerically estimated pdf, whereas, dotted curves are estimates of pdfs obtained from simulated data. In both of the graphs, the solid and dotted curves are in good agreement with each other.

Using similar arguments, the pdf of maximum projection of radius on negative x -axis can be obtained. The only difference between the two pdfs is that domain of \mathbf{x}^- is negative, else it will be similar to the pdf obtained for \mathbf{x}^+ . If absolute value of the random variable, \mathbf{x}^- , is used as the argument of pdf of maximum projection on negative axis, then the pdf obtained will be identical to the pdf of maximum projection on positive axis, as all the properties of Gaussian cylinder are independent of azimuthal angle.

Lateral width of Gaussian cylinder is sum of \mathbf{x}_m^+ and $|\mathbf{x}_m^-|$, therefore, the pdf of lateral width will be equal to convolution of the pdfs of \mathbf{x}_m^+ and $|\mathbf{x}_m^-|$. Both \mathbf{x}_m^+ and $|\mathbf{x}_m^-|$ are identically distributed, hence the pdf of lateral width can be obtained by convolving the pdf of \mathbf{x}_m^+ with itself. The convolution of the two pdfs is done numerically. The pdf of lateral widths of two representative cylinders obtained using above procedure is shown in Figure 2.10. Dotted curve is the estimated pdf of lateral width obtained from simulated data and solid curve is their numerical estimates.

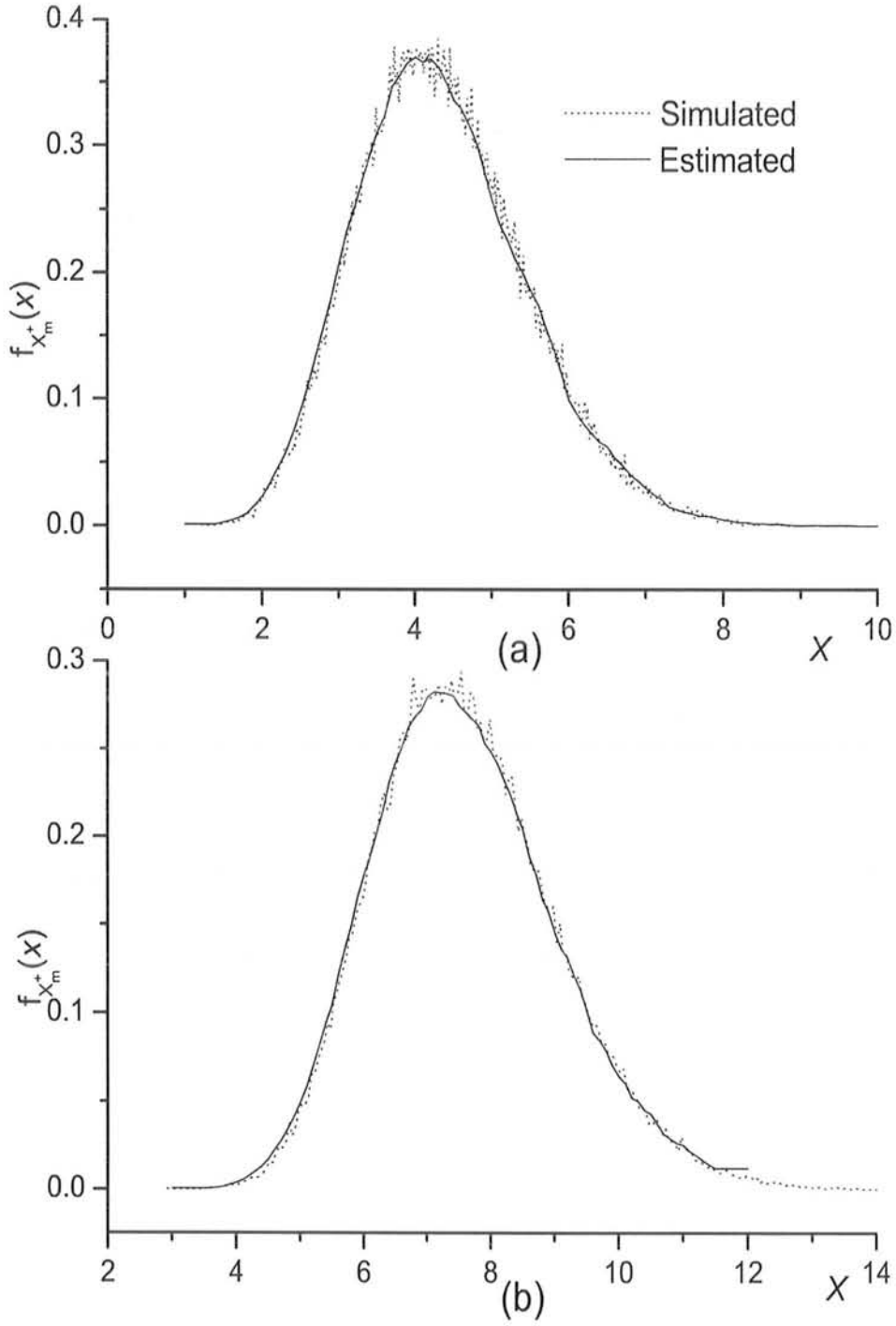


Figure 2.9: Pdf of x_m^+ , $f_{x_m^+}(x)$, of Gaussian cylinder. a) $r_d = 3\lambda$, $B = 1$, $N = 5$ and b) $r_d = 5\lambda$, $B = 1$, $N = 10$.

These curves tend to agree better as N increases, emphasizing the fact that statistics of x_m^+ and x_m^- become more and more independent with increase in N .

The angles, which the position vectors P and Q make with positive x -axis, directing towards the points where confining planes are tangent to random cylinder are random. Arguments leading to the conclusion that statistics of x_m^+ and x_m^- are independent of each other can be used to say that the statistics of these two angles are also independent and identically distributed. Probability distribution of θ_m^+ is obtained from the simulated data and is shown in Figure 2.11, for two representative random cylinders. Dotted line in the figure shows the estimated pdf from the simulated data and solid line shows a Gaussian fitted curve to the estimated pdf. It is apparent from the figure that the estimated pdf is not Gaussian. To further qualify this statement Shapiro–Wilk normality test is applied to the simulated data. The result showed that the data points are not normal at 0.05 level, i.e., the probability that the simulated data points have a normal distribution is less than 0.95. Estimated mean of θ_m^+ , determined from simulated data, is approximately 0 and their estimated standard deviation has been given in Table 2.2. Statistical properties of θ_m^+ are not probed further as they are not required for electromagnetic scattering.

In this chapter a stochastic process is defined with the help of finite Fourier series. It is analytically shown that the defined process is stationary. The probability distribution function and infinite order moments of the process are also obtained. Gaussian and Lognormal random cylinder models are defined with the help of this process. Average area and circumference due to rms differential length of both the cylinder models are obtained. Out of the two one model is chosen for the scattering problem. Statistics of geometrical parameters, such as maximum radius and lateral

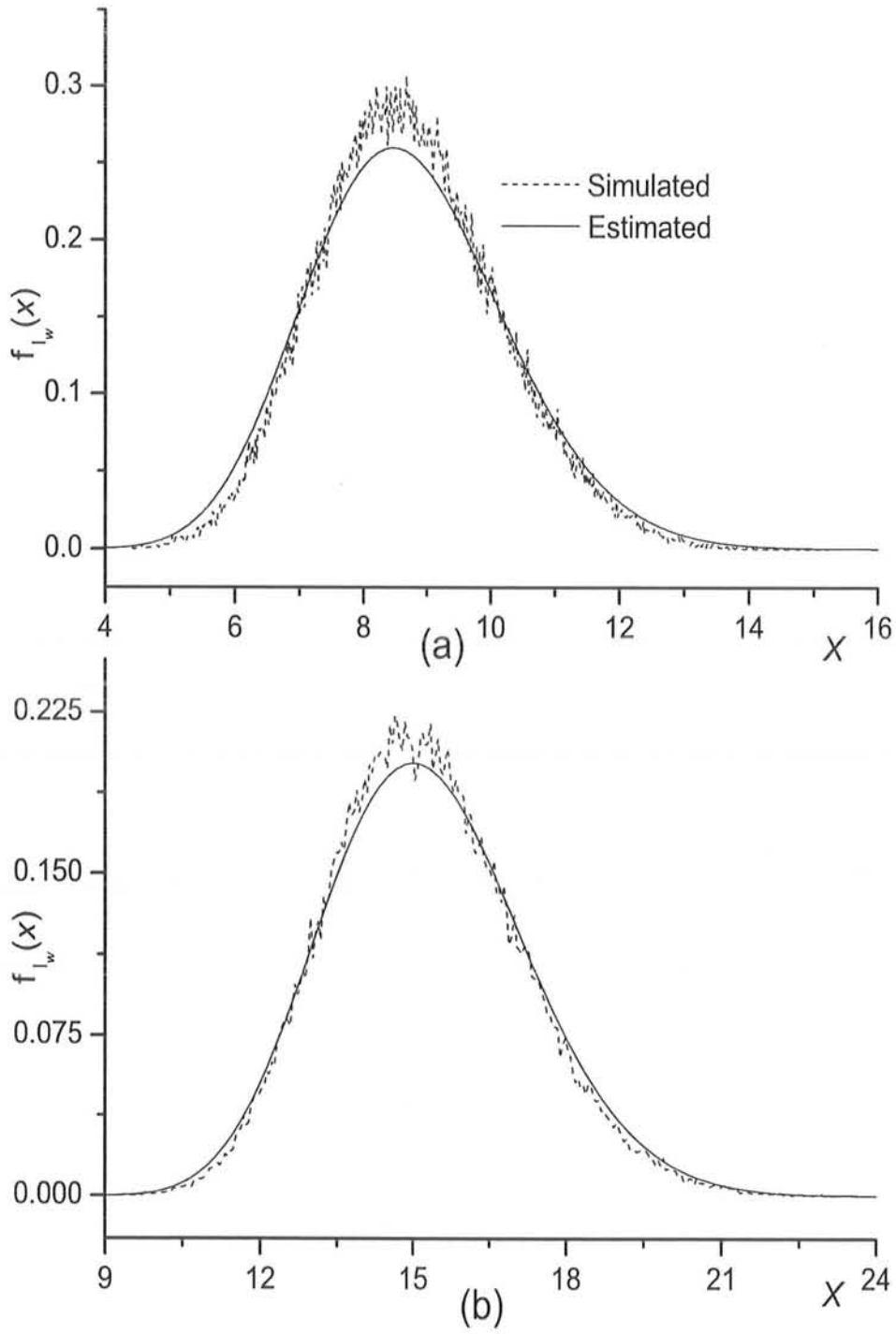


Figure 2.10: Pdf of l_w , $f_{l_w}(x)$, of Gaussian cylinder. a) $r_d = 3\lambda$, $B = 1$, $N = 5$ and b) $r_d = 5\lambda$, $B = 1$, $N = 10$.

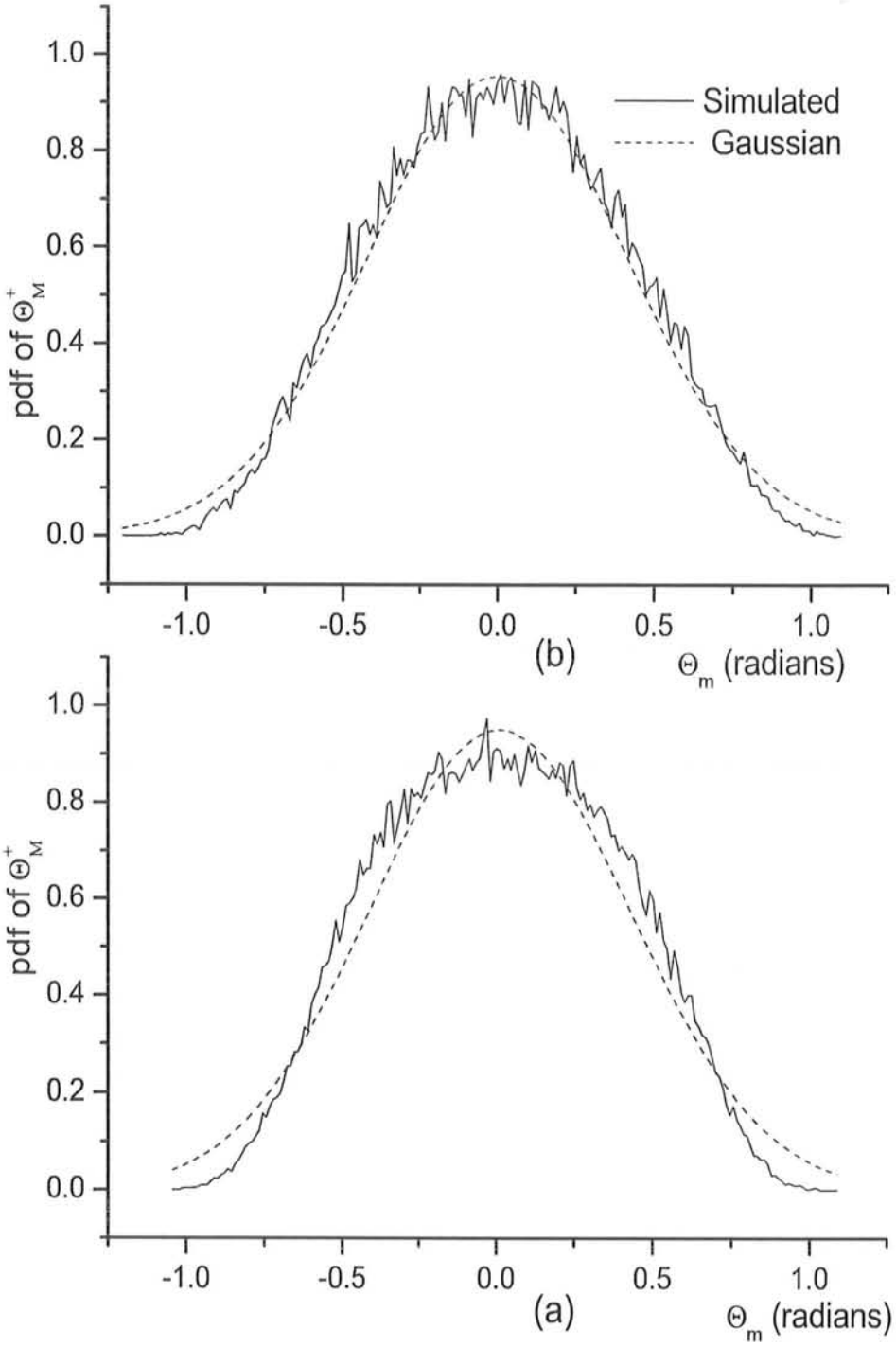


Figure 2.11: Probability density of θ_m^+ of Gaussian cylinder. a) $r_d = 3\lambda$, $B = 1$, $N = 5$ and b) $r_d = 3\lambda$, $B = 1$, $N = 10$.

width of the chosen model are also estimated. An estimate of probability distribution of these two parameters is obtained. All the analytical solutions are supported by simulated results.

Chapter 3

Scattering

Scattering of a plane wave has always been an interesting topic for researchers. Scattering problems largely depend upon shape of the scatterer, its constituent material and its surroundings. There exist many well established analytical as well as numerical methods to study scattering of electromagnetic field from objects of various shapes, materials and placed in different surroundings. Despite a rich history little work is found on electromagnetic scattering from random objects. Earlier work on scattering from random objects has been on scattering from one dimensional or two dimensional planar random surfaces. Scattering of light from heavenly particles also invited researchers towards the study of scattering from randomly shaped particles.

The problem of scattering from two dimensional cylindrical structure has been attempted earlier [35, 36, 34, 37, 38]. Almost all the earlier solutions for scattered field from random cylinder are approximately analytical, obtained with the help of perturbation theory. In the earlier work two different approaches have been used to obtain scattered field from random cylinders. In each case solutions for scattered field from random cylinder are verified by comparing the zeroth order solution, i.e., unperturbed solution with that of a circular cylinder. Ogura and Nakayama [35] as

well as Skaropoulos and Chrissoulidis [38] have also used energy consistency test, i.e., optical theorem test to verify their solutions.

Eftimiu [34] has obtained an approximate solution by employing the Green's function integral. The incident plane wave is expanded in terms of Bessel's function and the scattered field is expressed by unknown surface currents. To apply perturbation theory the exponential in the two dimensional free space far zone Green's function is written in terms of its power series for small variations of the cylindrical surface. The resultant scattered field is expressed in terms of Hankel function and a roughness parameter. Solution thus obtained is only valid for small values of roughness parameter. This method has been extended to obtain scattered field from a circular cylinder whose radius is random as well as for axially corrugated cylinders [34, 37]. A numerical solution for average scattered field from random circular cylinders has also been obtained by Atif [49].

Ogura et.al. [35, 36] while tackling a similar problem have obtained another approximate analytic solution for perturbed and unperturbed scattered fields from random cylindrical surface. The unperturbed scattered field according to their solution is the field scattered from a circular cylinder. The perturbed scattered field is written as a stochastic nonlinear functional of the Gaussian random surface and it is dealt with by expanding into a series of orthogonal Wiener-Hermite functionals. On applying the boundary conditions the series expansion is transformed into a set of recursive equations. This set of equations is then solved for small perturbation. Analytical results accurate to second order in surface roughness have been obtained. This work has been extended to obtain solutions accurate to fourth order in surface roughness for scattered field from random cylindrical surface by Skaropoulos and Chrissoulidis [38].

In this chapter free space scattering parameters of perfect electrically conducting(PEC) random cylinder are studied. The proposed solution for scattered field is not restricted for small randomness of the cylinders. The field scattered by a random cylinder is determined numerically using Method of Moments(MM) [50, 51]. Field scattered from an object of random cross section will be random hence statistical properties of scattering parameters are studied. These statistics are numerically estimated. Large number of samples are needed to better estimate the statistical properties of scattered field, thus time taken to determine one sample, i.e., scattered field from one random cylinder, becomes very important. A marginal reduction in processing time of one sample reduces total execution time by hours.

It is difficult to verify the reliability of numerically obtained scattered field because of the randomness of cylindrical surface. Hence reliability of the MM and the scattered field is ensured by three different procedures. First scattered field is obtained numerically from unperturbed cylinder, i.e., a circular cylinder and it is compared with the analytical solution. This step is useful for verifying the MM code. Secondly average value of scattered field from an ensemble of random cylinder obtained for different angles of observations is compared with the earlier documented results. Energy consistency test or optical theorem test is finally applied on few hundred thousand random cylinders. After ensuring the reliability of the numerically obtained scattered field, total scattering cross section of random cylinder is obtained from it for further analysis.

Average total scattering cross section of random cylinder is compared with the total scattering cross section of a strip and a circular cylinder. These comparisons are made to determine which canonical shape can serve as a better equivalent model for

random cylinders. Certain bounds have been obtained for the values of average total scattering cross section and average lateral width of random cylinder as well as for the radius of equivalent circular cylinder. Relation between the total scattering cross section of random cylinders and their lateral width is finally probed. Both quantities are random hence to observe their dependence on each other two dimensional scatter plots have been obtained. An estimate of the joint pdf of lateral width and total scattering cross section has also been obtained.

3.1 Scattered Field

The scattered field from random cylinders is obtained by MM. MM is applied to an integral equation relating the incident electric field to the unknown currents induced on the surface of perfectly conducting cylindrical scatterer. Application of MM helps solve these unknown surface currents. Details on application of MM are available in books [50, 51, 52]. In this section MM is given for the sake of completeness. This section also gives other details and approximations used while determining the scattered field from random cylinder, such as, weighting and testing functions, far field approximation of Green's function, number of segments into which the contour of integration is sampled, procedure to obtain the segments of random cylinder, etc.

The geometry of the problem is such that a perfectly electrically conducting random cylinder is considered to be placed in free space with its axis along z -axis. A linearly polarized plane wave having polarization parallel to z -axis, E_z^{inc} , is incident on the random cylinder. Let the plane wave be propagating along the direction θ_i , as shown in Figure 3.1. Electric field of the incident wave can be written as,

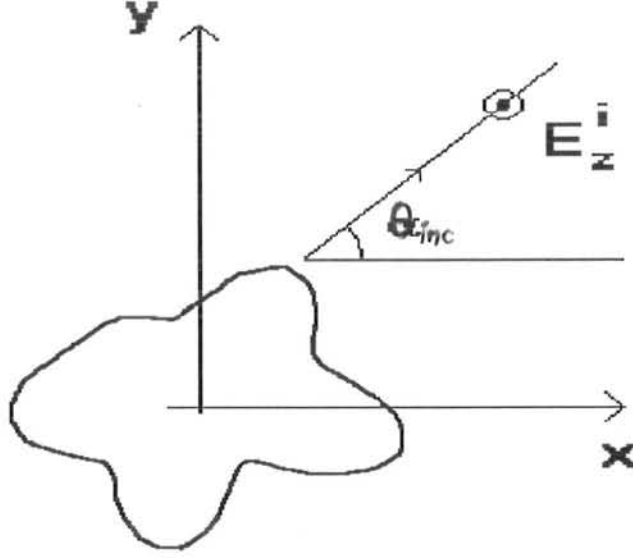


Figure 3.1: Random cylinder in free space.

$$E_z^{\text{inc}}(\mathbf{r}) = \exp\{i(\mathbf{k} \cdot \mathbf{r})\} \quad (3.1.1)$$

where \mathbf{k} is the wave vector and \mathbf{r} is the 2-D position vector in (x, y) coordinates. Time dependence of the plane wave is taken as $\exp(-i\omega t)$ and is suppressed throughout. Incident field interacts with random cylinder and produces currents on the surface of the cylinder. These induced surface currents re-radiate a field known as scattered field. Induced surface currents and scattered field both are numerically determined with the help of MM.

Let J_z denote the surface currents and E_z^{sc} represents the scattered field produced by these currents. Field produced by surface currents can be expressed in terms of two dimensional free space Green's function, $G(\mathbf{r}; \mathbf{r}')$, as

$$E_z^{\text{sc}}(\mathbf{r}) = \int_C J_z(\mathbf{r}') G(\mathbf{r}; \mathbf{r}') dl' \quad (3.1.2)$$

The two dimensional free space Green's function is given by Hankel function of zeroth order and first kind, as[52]

$$G(\mathbf{r}; \mathbf{r}') = -\frac{\omega\mu}{4} H_0^{(1)}(k|\mathbf{r} - \mathbf{r}'|) \quad (3.1.3)$$

where $k = 2\pi/\lambda$, is the magnitude of the wave vector \mathbf{k} . Boundary condition on the surface of cylinder is applied to obtain an expression between the incident and scattered field. On applying the boundary condition the above integral equation will become,

$$E_z^{\text{inc}}(\mathbf{r}) = - \int_{\mathcal{C}} J_z(\mathbf{r}') G(\mathbf{r}; \mathbf{r}') dl' \quad \text{at } \mathcal{C} \quad (3.1.4)$$

where \mathcal{C} is the surface of the random cylinder. The above integral equation is known as Electric Field Integral Equation(EFIE). EFIE is numerically solved to determine unknown currents J_z with the help of MM.

Surface of random cylinder has to be discretized into M segments to apply MM. Discretization of the surface also discretizes unknown surface currents. Discretized surface currents are expressed as,

$$J_z(\mathbf{r}') = \sum_{n=1}^M J_n \Pi_n(\mathbf{r}') \quad (3.1.5)$$

where J_n are unknown samples of currents and $\Pi_n(\mathbf{r}')$ are interpolating functions known as basis functions. Choice of basis functions depends on many factors which will be discussed later in this section. The above EFIE becomes a linear equation after discretization of the surface , i.e.,

$$E_z^{\text{inc}}(\mathbf{r}) = - \sum_{n=1}^M J_n \int_{\mathcal{C}} \Pi_n(\mathbf{r}') G(\mathbf{r}; \mathbf{r}') dl' \quad (3.1.6)$$

The above linear equation holds for every value of \mathbf{r} on \mathcal{C} . In general, infinite number of linear equations can be written from above equation.

In order to determine unknown coefficients J_n , only M linearly independent equations are needed. M linearly independent equations have been obtained by using a set of M orthonormal functions, $w_m(\mathbf{r})$, known as testing functions. These testing functions are then multiplied with above equation and the product is integrated over \mathcal{C} resulting in M linearly independent equations. These linearly independent equations can be expressed as matrix equation, as,

$$E_z^{\text{inc}}[m] = Z[m, n]J[n] \quad (3.1.7)$$

where,

$$\begin{aligned} E_z^{\text{inc}}[m] &= \int_{\mathcal{C}} E_z^{\text{inc}}(\mathbf{r})w_m(\mathbf{r})dl \\ Z[m, n] &= - \int_{\mathcal{C}} \int_{\mathcal{C}} w_m(\mathbf{r})\Pi_n(\mathbf{r}')G(\mathbf{r}; \mathbf{r}')dl'dl \end{aligned}$$

and $J[n]$ is a vector of unknown currents J_n . Matrix $Z[m, n]$ has units of impedance hence it is known as impedance matrix. After selection of suitable basis and testing functions, elements of $E_z^{\text{inc}}[m]$ and $Z[m, n]$ can be evaluated. Matrix $Z[m, n]$ is inverted and pre-multiplied on both sides to obtain the unknown currents $J[n]$.

Selection of basis and testing functions depends on many factors. Apart from accuracy another important factor to consider is the processing time because the process of determining scattered field has to be repeated for around half a million times for a single simulation. The processing time is reduced by choosing basis functions as non-overlapping pulse functions and testing functions as Dirac delta functions. Mathematically, they are given as,

$$\Pi_n(\mathbf{r}) = \begin{cases} 1 & \mathbf{r} \in \Delta C_n, \\ 0 & \text{otherwise.} \end{cases} \quad (3.1.8)$$

$$w_m(\mathbf{r}) = \delta(\mathbf{r} - \mathbf{r}_m) \quad (3.1.9)$$

where ΔC_n is the n^{th} segment and \mathbf{r}_m is the position vector to the center of m^{th} segment. With these choices of basis and test functions the elements of E_z^{inc} and Z become

$$E_z^{inc}[m] = \exp\{i(\mathbf{k} \cdot \mathbf{r}_m)\} \quad (3.1.10)$$

$$\begin{aligned} Z[m, n] &= - \int_{\Delta C_n} G(\mathbf{r}_m; \mathbf{r}') dl' \\ &= \frac{\omega\mu}{4} \int_{\Delta C_n} H_0^{(1)}(k|\mathbf{r}_m - \mathbf{r}'|) dl' \end{aligned} \quad (3.1.11)$$

The surface segment ΔC_n is small in length and Hankel function varies slowly over it. This fact is further exploited to reduce processing time.

If length of a segment is small the vector \mathbf{r}' will have small variation. Small variation in \mathbf{r}' produces small variation in argument of Hankel function. Therefore, Hankel function can be assumed constant over the segment and its value is determined at the center of segment, i.e., $H_0^{(1)}(k|\mathbf{r}_m - \mathbf{r}_n|)$. This approximation is valid for all values of n , except when $m = n$. At $m = n$ the Hankel function is singular as its argument becomes zero. If the position vector \mathbf{r}_n is made to point at any location other than the center of segment, the argument of Hankel function will never be zero and this singularity can be avoided. This approach introduces large error, because Hankel function varies rapidly near zero. Therefore, to keep the error low, integral in equation (3.1.11) is analytically evaluated for $m = n$. Hankel function is first approximated by its small argument approximation [53]

$$\lim_{kr \rightarrow 0} H_0^{(1)}(kr) \approx 1 + \frac{2i}{\pi} \ln\left(\frac{1.781kr}{4e}\right) \quad (3.1.12)$$

and then it is integrated over the segment [51]. The elements of impedance matrix

can thus be written as

$$Z[m, n] = \begin{cases} \frac{\omega\mu}{4} H_0^{(1)}(k|\mathbf{r}_m - \mathbf{r}_n|) \Delta l_n & m \neq n, \\ \frac{\omega\mu}{4} \Delta l_n \{1 + i \frac{2}{\pi} \ln(1.781k\Delta l_n/4e)\} & m = n. \end{cases} \quad (3.1.13)$$

where Δl_n is the length of n^{th} segment, ΔC_n .

Processing time is proportional to square of total number of segments, M . Reducing M will considerably reduce the processing time but will increase error. In this trade-off between error and processing time, the factor of error in the scattered field is more important than the processing time. Warnick [54, 55] estimated the rms error introduced by MM in induced currents as well as in scattered field, while studying scattering from circular cylinder. He estimated that error produced in surface current obtained by MM under similar assumptions as used in this thesis is

$$\frac{\|\Delta J\|_{RMS}}{\|J\|_{RMS}} \approx 0.7 \, n_\lambda^{-2} \quad (3.1.14)$$

and error in back scattering field amplitude is

$$\frac{\|\Delta S(0)\|_{RMS}}{\|S(0)\|_{RMS}} \approx 1.9 \, (ka)^{-1} \, n_\lambda^{-3} \quad (3.1.15)$$

where n_λ is number of segments per wavelength and a is radius of the cylinder. The above expressions show that errors in current and the scattering amplitude are approximately second and third order in n_λ^{-1} , respectively.

The error estimates given above are obtained for a circular cylinder, considering its segments to be of equal length. Segments of a random cylinder are obtained by uniformly sampling the central angle into M samples, i.e., the angle subtended by each segment is $\Delta\theta = 2\pi/M$. Single valuedness of radius of random cylinder helps to determine length of the segment, Δl_n , using cosine formula, given as,

$$\Delta l_n = \sqrt{r_{n1}^2 + r_{n2}^2 - 2r_{n1}r_{n2} \cos \Delta\theta} \quad (3.1.16)$$

where r_{n1} and r_{n2} are radii of the random cylinder at angles $\theta_n - \Delta\theta/2$ and $\theta_n + \Delta\theta/2$, respectively. Since r_{n1} and r_{n2} are random, therefore, Δl_n is also random hence above estimates of errors can not be directly applied.

The error introduced by MM is directly proportional to segment length [55]. Total number of segments M of a random cylinder is obtained by considering a circular cylinder having radius equal to average global maximum radius, section (2.4), i.e., $M = 2\pi n_\lambda E[\mathbf{R}_M]$. The length of each segment of average global maximum radius circular cylinder, i.e., $\Delta l_n = 1/n_\lambda$, is assumed to be equal to average maximum segment length of random cylinders. Therefore, with $2\pi n_\lambda E[\mathbf{R}_M]$ equiangular segment of a random cylinder average maximum segment length will be equal to $1/n_\lambda$ and the error introduced by MM will be proportional to it.

Besides the error produced by MM, randomness of cylinder is also an important factor for determining the value of M . Sampling error will be introduced if a rough surface, i.e., a surface having large number of small peaks, is sampled with small value of M . This situation can be avoided with Gaussian cylinder. Randomness of Gaussian cylinder is controlled by number of terms in the Fourier series. Final term in the Fourier series, i.e., $\cos(N\theta + \psi_N)$ introduces highest oscillation in the radius of Gaussian cylinder. According to Nyquist theorem, minimum number of samples needed to sample a function without aliasing is equal to twice the highest frequency of the function. Hence minimum number of samples needed to sample a random cylinder without aliasing is $2N$. This is a lower bound on the value M . Large values of N tend to make the surface of the random cylinder rough hence not very large values of N are taken. If the value of M is chosen according to above criteria, i.e., $M = 2\pi n_\lambda E[\mathbf{R}_M]$ then its value will generally be much larger than its lower bounding

value. In this thesis, the value of n_λ is chosen to be equal to 15, such that the average maximum segment length will be equal to $1/15$ wavelengths.

The currents induced on the surface of random cylinder can be determined once value of M is chosen. After determination of the surface currents, scattered field is evaluated with the help of integral equation, given by equation (3.1.2). Surface currents obtained above are approximate because the basis function used in equation (3.1.5) are pulse function. Using the same representation of surface currents, the integral equation will become a linear equation, written as,

$$E_z^{\text{sc}}(\mathbf{r}) = \sum_{n=1}^M J_n G(\mathbf{r}; \mathbf{r}_n) \Delta l_n \quad (3.1.17)$$

where $G(\mathbf{r}; \mathbf{r}_n)$ is free space Green's function, given by equation (3.1.3), $\mathbf{r}_n(x, y)$ is the position vector pointing to center of segment and $\mathbf{r}(x, y)$ is the observation point. Since scattered field in far zone is desirable, therefore, to save the computational time the Green's function is approximated for large argument[52], i.e.,

$$\lim_{k|\mathbf{r}-\mathbf{r}_n| \rightarrow \infty} G(\mathbf{r}; \mathbf{r}_n) \approx \frac{-\omega\mu}{4} \sqrt{\frac{2}{\pi k|\mathbf{r}-\mathbf{r}_n|}} \exp\{ik|\mathbf{r}-\mathbf{r}_n| - i\frac{\pi}{4}\}. \quad (3.1.18)$$

The above equation is true for every value of \mathbf{r} in the far zone.

Numerical values of far zone scattered field are obtained at some selected observation points, \mathbf{r} . If $|\mathbf{r}| \gg |\mathbf{r}_n|$, then distance between these two vectors can be approximated as

$$r = |\mathbf{r} - \mathbf{r}_n| \approx |\mathbf{r}| - |\mathbf{r}_n| \cos(\theta - \theta_n). \quad (3.1.19)$$

where, θ and θ_n are the angles which position vectors \mathbf{r} and \mathbf{r}_n make with the horizontal axis, respectively. Using zeroth order approximation of r for the magnitude and first order for the phase of scattered field, the Green's function for far zone scattered

field can be written as,

$$G(\mathbf{r}; \mathbf{r}_n) = -\frac{\omega\mu}{4} \sqrt{\frac{2}{\pi k|\mathbf{r}|}} \exp\{ik(|\mathbf{r}| - |\mathbf{r}_n| \cos(\theta - \theta_n)) - i\frac{\pi}{4}\} \quad (3.1.20)$$

Using the above approximated Green's function in equation (3.1.17), far zone scattered field at point \mathbf{r} is obtained. In cylindrical coordinates, far zone scattered field is usually expressed as a diverging cylindrical wave, i.e., $E_z^{\text{sc}}(\theta) = \xi(\theta)e^{ik\rho}/\sqrt{k\rho}$, where direction dependent $\xi(\theta)$ is known as the scattering amplitude.

The field scattered by random cylinder is random and it needs to be analyzed statistically. Only source of randomness in the scattered field is the random cylinder. If random cylinder is considered Gaussian, as modelled in last chapter, then the statistics of random cylinder are stationary with respect to angle. Stationarity of the cylinder statistics implies that statistics of field scattered will only depend on relative angle between the incidence and observation. An analytical solution for probability distribution of the scattered field is difficult to obtain, even if statistics of the radius are known. This is because scattered field is a complicated function of radius.

Mathematically, MM can be summarized to express scattered field E_z^{sc} in terms of the incident field E_z^{inc} , impedance matrix Z and 2-D Green's function G as,

$$E_z^{\text{sc}}(\mathbf{r}_l) = G(\mathbf{r}_l, \mathbf{r}_m)[\{Z(\mathbf{r}_m, \mathbf{r}_n)\}^{-1} E_z^{\text{inc}}(\mathbf{r}_n)] \Delta l_n \quad (3.1.21)$$

where $\mathbf{r}_m(\theta)$ and $\mathbf{r}_n(\theta)$ are position vectors pointing to various points on circumference of the random cylinder and $\mathbf{r}_l(\theta)$ is the far zone observation vector. According to equations (3.1.11) and (3.1.18) the two arguments (\mathbf{a}, \mathbf{b}) of Z and G matrices can be written as $|\mathbf{a} - \mathbf{b}|$. Analytical expression for the pdf of elements of these matrices is difficult to obtain, even if all the statistics of \mathbf{r} are known as these elements are complicated functions of \mathbf{r} . In principle, one may analytically determine the pdf of

each element of the impedance matrix Z but Z matrix needs to be inverted. During matrix inversion it is difficult to keep track of operations on each element of the matrix, especially when the matrix is large. Even the pdfs of each element of G , Z^{-1} and E_z^{inc} will not help to analytically determine the pdf of scattered field, as all of these are not independent. Due to these complications, all the statistical analysis of surface currents and/or scattered field are performed numerically.

Scattered field strongly depends upon the shape of scatterer hence field scattered by random cylinder is random and it is difficult to verify the solution obtained for surface currents as well as scattered field. First step towards verification of the above procedure and the Fortran code is to use a circular cylinder as bench mark scatterer. Surface currents and scattered field are obtained for circular cylinder by MM and compared with the analytic solutions [52]. Figure 3.2 shows the plots of induced surface currents and scattered field by a circular cylinder evaluated numerically and analytically for two different radii. The numerical curves shown in these plots are in very good agreement with their respective analytical curve, verifying the formulation as well as the code.

Random nature of scatterer inhibits the use of any pattern matching benchmarks to validate either the current induced or scattered field. Therefore, scattered field from random cylinder, determined by MM, is further tested for reliability by comparing it with results given by Eftimiou [34], Ogura & Nakayama [35] and Skaropoulos & Chrissoulidis [38]. They have obtained the average scattering amplitude and have given its comparison with scattering amplitude of mean radius circular cylinders. They have also employed optical theorem to validate their solutions and have referred to it as energy consistency test. In this thesis, both of these procedures are applied on

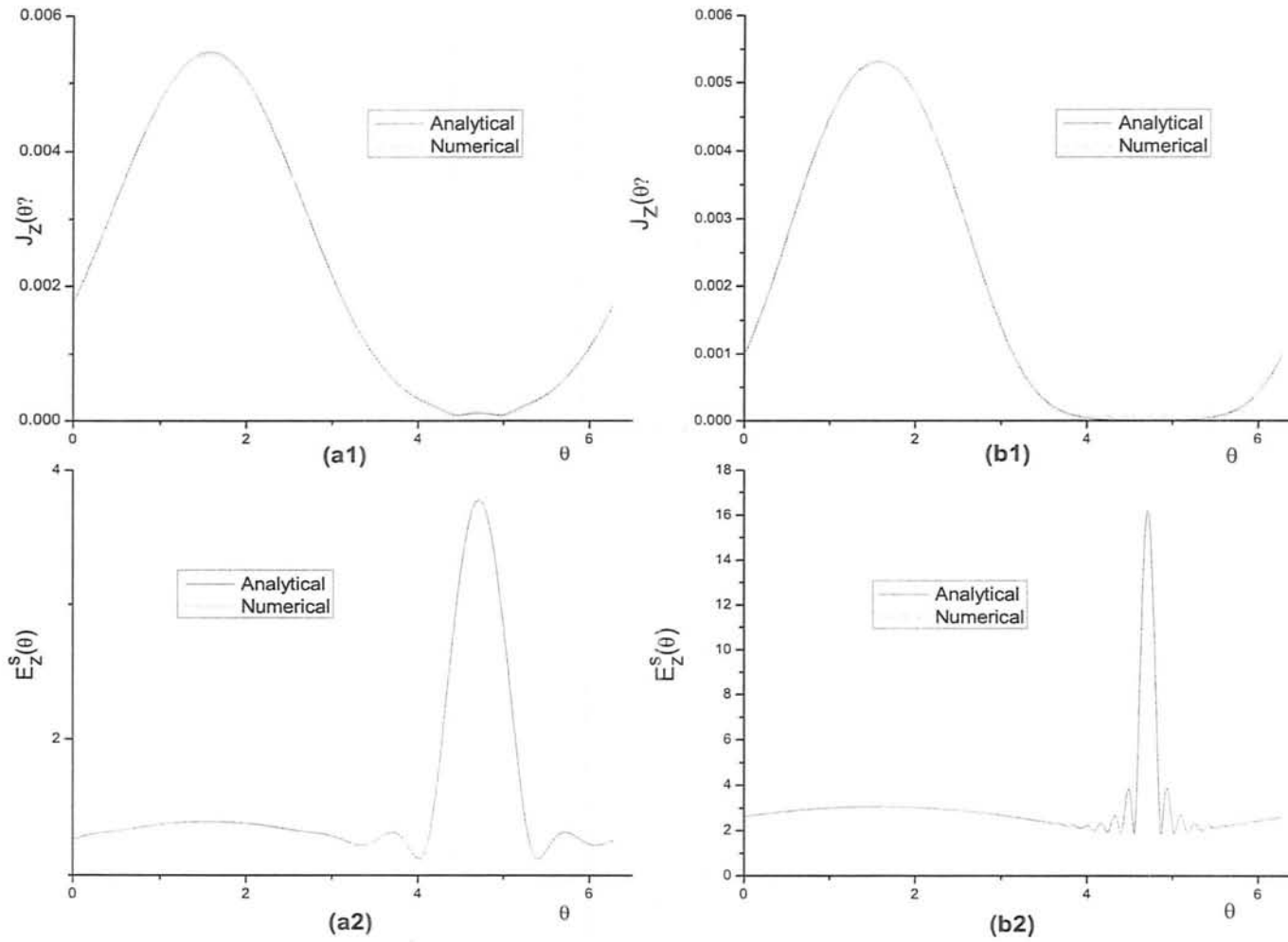


Figure 3.2: Induced surface currents and scattering amplitude for a circular cylinder of a) radius = 0.6λ and b) radius = 3λ ; 1) Induced current and 2) Scattered Field.

scattering amplitude obtained by MM to ensure reliability of the solution before any further analysis. In the next section the average or coherent part of the scattering amplitude is determined as first step to ensure reliability of the numerically obtained scattered field.

3.2 Coherent Scattering Amplitude

Scattering amplitude of random cylinder, $\xi(\theta)$, can be written as a sum of average and fluctuating scattering amplitudes,

$$\xi(\theta) = E[\xi(\theta)] + \xi_f(\theta) \quad (3.2.1)$$

where $E[\xi_f(\theta)] = 0$. Average and fluctuating parts of the scattering amplitude are referred to as coherent and incoherent parts of the scattering amplitude [31]. Angular distribution of the coherent scattering amplitude is obtained and compared with the earlier documented results to ensure reliability of the present solution. The ensemble average of scattering amplitude at each angle of observation is the coherent scattering amplitude.

If all the ensemble data is stored, to determine the ensemble average, with fine angular resolution, size of the output data file becomes too large to manage. Therefore, average of the scattering amplitude is estimated using a sequential mean estimator [44]. A sequential mean estimator updates its estimated mean value as soon as data from new sample points is available. It is expressed as

$$E[\xi(\theta)]_N = \frac{1}{N} \{ (N-1)E[\xi(\theta)]_{N-1} + \xi(\theta) \} \quad (3.2.2)$$

where $E[\cdot]_N$ is the average value due to N sample points. As soon as new sample data is generated it is properly incorporated to determine the new average value of

scattering amplitude. This average value at each observation angle is the only output of the estimator.

Absolute value of coherent scattering amplitude of few random cylinders, with same mean radius and different variance, has been obtained and is shown in Figure 3.3. The two plots, (i) and (ii), of the Figure show same data but on different scales. In plot(i) of the Figure, y -axis is on linear axis, whereas y -axis of the plot(ii) is on logarithmic scale. Linear plot is given to observe variations of the average scattering amplitude in the forward direction and due to low amplitude of the average scattering amplitude in the backward direction it is much more convenient to observe the effect of randomness in this region on logarithmic scale. Scattering amplitude of mean radius circular cylinder is also shown in the figure.

It is apparent from the figure that main lobe widths of coherent scattering amplitude of all random cylinders and mean radius circular cylinder are equal. It can be observed from the figure that main lobe amplitude of coherent scattering amplitude increases with increase in variance of the radius, i.e., higher the randomness of the ensemble higher is the scattering amplitude in forward direction. Whereas, away from forward region absolute value of coherent scattering amplitude is less than that of a mean radius circular cylinder. The side lobe amplitude decreases as randomness of the cylinders increases. The figure also shows that in back scattered region coherent scattering amplitude has erratic behaviour with very low amplitude. These plots show that as randomness increases the scattering amplitude behaves like noise with very low mean value in the back scattered region. The trend in these plots is similar to those obtained by Eftimiu [34], Ogura and Nakayama [35], Skaropoulos and Chrissoulidis [38] as well as Atif [49].

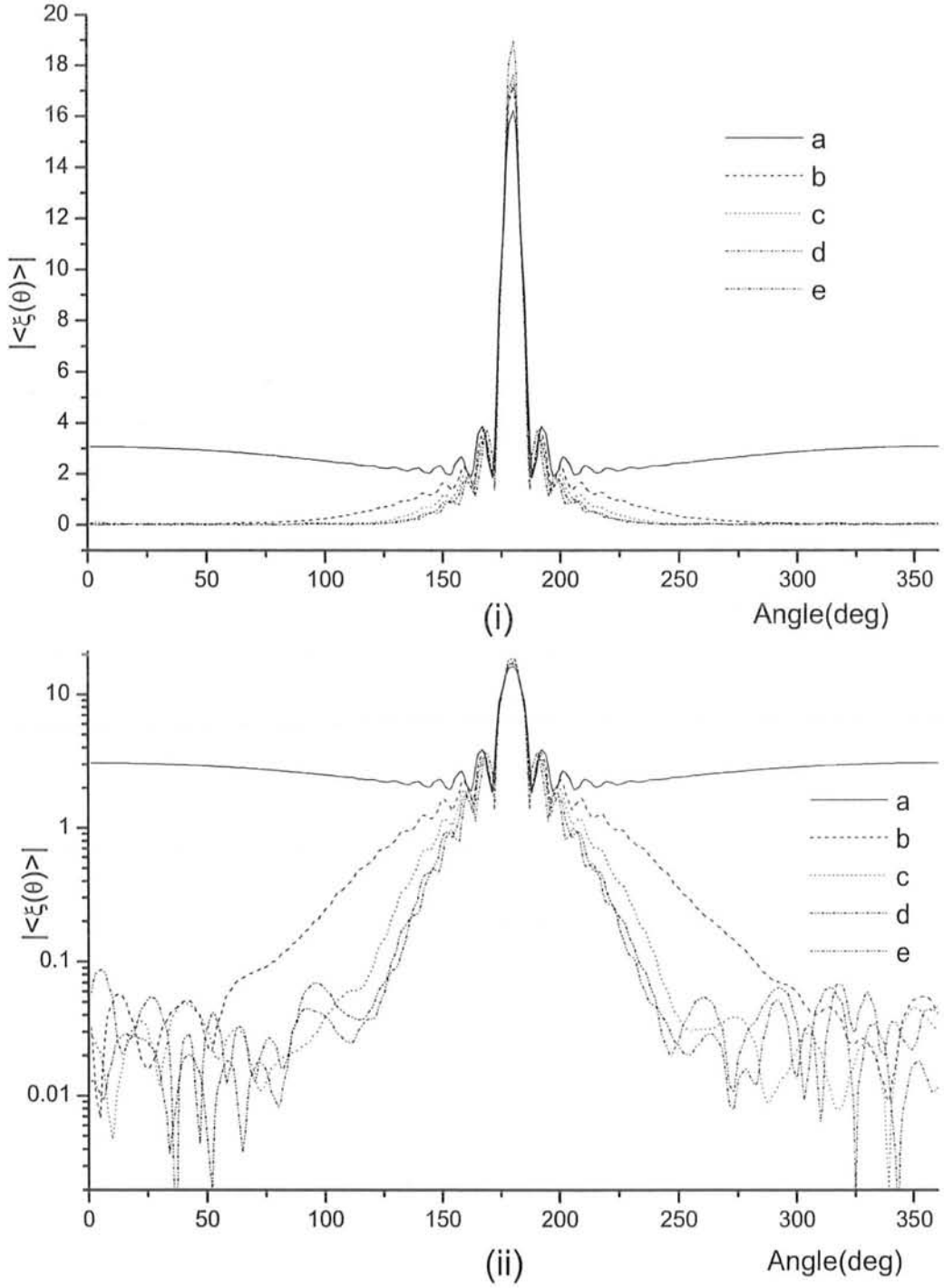


Figure 3.3: Coherent scattering amplitude of cylinders with $r_d = 3\lambda$; (a) Circular cylinder. (b) $B = 0.25$, $N = 10$. (c) $B = 0.5$, $N = 5$. (d) $B = 0.6$, $N = 5$ and (e) $B = 0.5$, $N = 10$.

A graphical comparison of the average scattering amplitude is made with the previously documented results. It is a visual comparison and is not very reliable. Optical theorem test has been considered as more reliable test to determine the accuracy of the scattered field [35] as it is an analytic test. In the next section reliability of the random scattered field obtained from MM is determined by applying optical theorem test.

3.3 Optical Theorem Test

Optical theorem, for two dimensional scatterers relates its total scattering cross section to imaginary part of its scattering amplitude in forward direction. Mathematically, optical theorem is given as [27],

$$\sigma_T = \frac{\sqrt{8\pi}}{k} \Im \left\{ \frac{\xi(\theta_{inc})}{\sqrt{i}} \right\} \quad (3.3.1)$$

where $\xi(\cdot)$ is the scattering amplitude, σ_T is total scattering cross section and operator $\Im(\cdot)$ denotes imaginary part of complex number. The above expression is an analytic expression and is valid for all perfectly electrically conducting two dimensional scatterers, irrespective of their cross section. It has been used by Ogura & Nakayama [35] and Skaropoulos & Chrissoulidis [38] to validate their solutions for scattered field. Usage of optical theorem to validate scattered field has been referred to as energy consistency test by them.

Total scattering cross section of a two dimensional scatterer is defined as the ratio of total scattered power per unit length to incident power per unit area. In general, time average power per unit area, S , is given as $\frac{1}{2} \Re\{\mathbf{E} \times \mathbf{H}^*\}$, where $\Re(\cdot)$ is real part and asterisk indicates complex conjugate of complex number. Without loss of

generality, the incident plane wave is assumed to be travelling along positive x -axis, i.e., $E_z^{\text{inc}} = \exp(ikx)$. The incident power per unit area is therefore given as,

$$S^{\text{inc}} = -\frac{1}{2} \Re\{E_z^{\text{inc}}(-H_y^{\text{inc}*})\} = \frac{1}{2\eta} \quad (3.3.2)$$

where η is free space impedance. Far zone electric and magnetic field components of scattered field from a cylindrical structure can be expressed as $\mathbf{E}^{\text{sc}} = \xi(\theta)\{e^{ik\rho}/\sqrt{k\rho}\}\hat{\theta}$ and $\mathbf{H}^{\text{sc}} = -ik\xi(\theta)\{e^{ik\rho}/\sqrt{k\rho}\}\hat{\phi}$ where $\xi(\theta)$ is the scattering amplitude. The time average total power scattered from a cylindrical surface per unit length can thus be written as

$$\begin{aligned} P^{\text{sc}} &= \frac{1}{2} \int_0^{2\pi} \lim_{\rho \rightarrow \infty} \Re\{\mathbf{E}^{\text{sc}} \times \mathbf{H}^{\text{sc}*}\} \rho d\theta \\ &= \frac{1}{2k\eta} \int_0^{2\pi} |\xi(\theta)|^2 d\theta \end{aligned} \quad (3.3.3)$$

Using the above two equations total scattering cross section for two dimensional scatterers can be expressed as

$$\sigma_T = \frac{P^{\text{sc}}}{S^{\text{inc}}} = \frac{1}{k} \int_0^{2\pi} |\xi(\theta)|^2 d\theta \quad (3.3.4)$$

Integrand in above equation, $|\xi(\theta)|^2$, has been defined as differential scattering cross section [35, 38] or Bistatic Radar Cross Section (RCS). The above equation shows that total scattering cross section is a function of scattering amplitude in all directions. Optical theorem, equation (3.3.1), relates total scattering cross section to imaginary part of scattering amplitude in forward direction, therefore, optical theorem can be used to validate the field scattered by random cylinders.

To check the reliability of the scattered field with the help of optical theorem left and right hand sides of the equation (3.3.1) are determined from the scattered field of each random cylinder and then the difference between these two is determined. For

convenience, let the quantity on right hand side of equation (3.3.1) be referred to as $\tilde{\sigma}_T$, i.e.,

$$\tilde{\sigma}_T = \frac{\sqrt{8\pi}}{k} \Im \left\{ \frac{\xi(\theta_{inc})}{\sqrt{i}} \right\} \quad (3.3.5)$$

and in this section the symbol σ_T will be a quantity obtained using equation (3.3.4). The integral in equation (3.3.4) is solved with the help of Simpson's method of numerical integration. Since scattering amplitude and total scattering width are random, therefore, both σ_T and $\tilde{\sigma}_T$ are random variables.

One needs to prove that random variables σ_T and $\tilde{\sigma}_T$ are statistically equal in order to show that the scattered field obtained with the help of MM satisfies optical theorem. Ogura and Nakayama [35] have used only the mean values of σ_T and $\tilde{\sigma}_T$ to show that the scattered field obtained by them satisfies the optical theorem. They termed the expression relating ensemble averages of σ_T and $\tilde{\sigma}_T$ as extended optical theorem. Mathematically, the extended optical theorem is given as

$$\frac{1}{k} \int_0^{2\pi} E [|\xi(\theta)|^2] d\theta = \frac{\sqrt{8\pi}}{k} \Im \left\{ \frac{E [\xi(\theta_i)]}{\sqrt{i}} \right\}. \quad (3.3.6)$$

Referring to above equation as extended optical theorem, Ogura & Nakayama have called the ensemble average of total scattering cross section as total scattering cross section.

To show that the scattered field obtained by moments method satisfies the optical theorem average as well as standard deviation of $e_\sigma = \sigma_T - \tilde{\sigma}_T$ are estimated, in this thesis. Since optical theorem is independent of scatterer's lateral width and only the difference of σ_T and $\tilde{\sigma}_T$ is used to show that it holds, therefore, it is not important that the ensemble for optical theorem test should consist of random cylinders having similar input statistics. Several hundred thousand random cylinders of mean radius

varying between 0.5λ to 3λ and different input statistics have been generated. Total scattering cross section, σ_T , is determined with the help of equation (3.3.4) and equation (3.3.5) is used to evaluate $\tilde{\sigma}_T$. The difference between σ_T and $\tilde{\sigma}_T$, i.e., e_σ and statistics of e_σ are then estimated. It is observed that mean value of e_σ is nearly equal to zero with standard deviation of the order of 10^{-6} . The maximum value of absolute difference is of the order of 10^{-4} . Hence according to the Chebyshev inequality it can be concluded that the two random variables σ_T and $\tilde{\sigma}_T$ are equal with probability one and the scattered field obtained by using MM does satisfy optical theorem. These statistics also show that MM can be used reliably to determine the field scattered even from physically large random cylinders, whereas the scattered field obtained by earlier methods [35, 38] used to solve a similar problem shows deviation from the optical theorem test as the size of the cylinder increases.

Total scattering cross section of random cylinders is used to verify the solution for scattered field. After having successfully passed the optical theorem test, total scattering cross section is further analyzed. According to the definition of total scattering cross section, equation (3.3.4), absolute value operator eliminates the phase component of scattering amplitude and its angular dependence is integrated out. Hence total scattering cross section is a real valued random outcome of a chance experiment, making it easier to analyze.

3.4 Total Scattering Cross Section

Total scattering cross section σ_T is a function of scattering amplitude of a scatterer and is a useful electromagnetic quantity. For two dimensional scatterers, it is the power intercepted by the scatterer per unit length from the incident field. The total

intercepted power is scattered and for imperfectly conducting scatterers some power is also absorbed. It depends upon cross sectional shape and lateral width of a scatterer. Its dependence upon cross sectional shape and lateral width is so complicated that analytical expressions, either exact or approximate, are available only for very few canonical scattering shapes [1]. This complication is due to the fact that total scattering cross section is obtained only after determination of the scattered field.

Papas [56, 57] has determined approximate analytic expressions relating the total scattering cross section of a circular cylinder and a flat strip at normal incidence to their lateral width. Papas showed that the ratio of σ_T and twice lateral width decreases monotonically for circular cylinder. This ratio has damped oscillatory behaviour for a flat strip, at low frequencies. In high frequency limit, the ratio approaches unity for both of these scatterers, as shown in the Figure 3.4. Plots, shown in Figure 3.4, have been obtained numerically by first determining the scattering amplitude in forward direction with the help of MM and then employing optical theorem, equation (3.3.1). These plots deviate a little from those obtained by Papas but they are in good agreement with those given by Bowman et.al. [1]. The deviation is due to the fact that Papas has approximated the solution to obtain simplified analytic expressions for σ_T of both circular cylinder and strip.

It is apparent from Figure 3.4 that σ_T of a scatterer depends on lateral width as well as the cross sectional shape of the scatterer. These graphs also show that for a given lateral width, total scattering cross section of a strip, σ_T^{st} , is always less than that of a circular cylinder, σ_T^{cc} . The dependence of σ_T on cross sectional shape is more pronounced when the lateral width of scatterer is small or comparable to wavelength of the incident plane wave. It can be observed from the figure that if the lateral

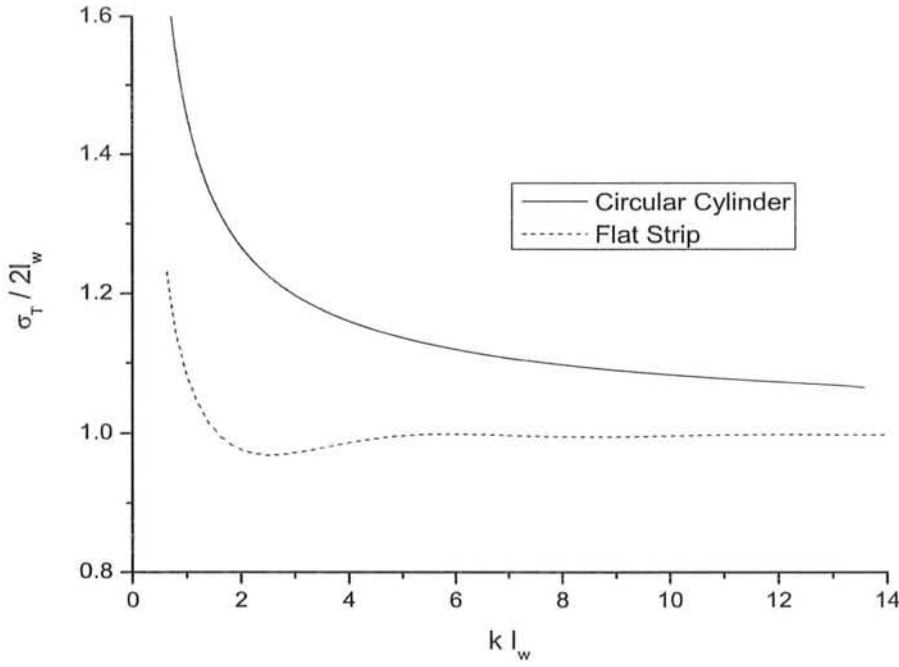


Figure 3.4: Normalized Total Scattering cross section of a circular cylinder and flat strip.

width of circular cylinder or strip is large compared to the incident wavelength, then its total scattering cross section is approximately twice of lateral width.

Total scattering cross section of a random cylinder is a random variable as field scattered from it is random. Since it is difficult to determine the statistics of scattered field from the statistics of radius of random cylinder, hence predicting anything about total scattering cross section is even more difficult. It has been shown that total scattering cross section is closely associated with scatterer's lateral width but effect of shape cannot be neglected. There could be infinitely many random cylinders having different cross sectional shape but same lateral width. Since total scattering cross section depends both on cross sectional shape and lateral width therefore total

scattering cross section of random cylinders is a multivalued function of lateral width. Analytically it is difficult to determine the statistics of total scattering cross section of random cylinders, even if the statistics of lateral width are known. The statistics of total scattering cross section are therefore estimated numerically.

As stated earlier, total scattering cross section of a scatterer depends on both the cross sectional shape and the lateral width. Lateral width is a scalar quantity compared to cross sectional shape which is a plane curve, hence it is easier to observe the behaviour of total scattering cross section as a function of lateral width, i.e., σ_T vs \mathbf{l}_w . It is thus desired to relate an electromagnetic quantity, i.e., total scattering cross section to a purely geometric quantity, i.e., lateral width. Let random variable σ_T^{rc} denote total scattering cross section and random variable \mathbf{l}_w denote the lateral width of a random cylinder. To estimate statistical properties of σ_T^{rc} , ensembles of random cylinders have been generated with different input statistics. Each ensemble consists of fifty thousand random cylinders. Total scattering cross section, σ_T^{rc} , together with lateral width \mathbf{l}_w of each random cylinder were recorded for further statistical analysis.

Roughly speaking random cylinders can vary from thin to thick. Among regular shaped cylindrical structures a strip is the thinnest and a circular cylinder is the thickest. Therefore to develop an insight into the scattering characteristics of random cylinder, the average total scattering cross section, $E[\sigma_T^{\text{rc}}]$, is compared with total scattering cross section of a flat strip σ_T^{st} and a circular cylinder σ_T^{cc} . Average total scattering cross section of random cylinders is numerically estimated for each ensemble from the stored data. A numerically estimated average value is a random quantity by itself with some distribution which depends upon the estimator. Complete specification of a reference scatterer requires that its shape and dimensions both

should be specified. Therefore, width of strip and radius of circular cylinder need to be specified for completely defining the comparative canonical shape.

It has been observed in Figure 3.4 that, at least for electrically large cylindrical scatterers, total scattering cross section of a scatterer has simple relation to its lateral width. Therefore, it is reasonable that the width of a comparative strip be taken equal to average lateral width, $E[l_w]$. As far as the radius of the comparative circular cylinder is concerned there are two options. Since average radius of a random cylinder r_d is always less than the radius of a circular cylinder completely bounding the random cylinder, hence one candidate for comparative circular cylinder is the one which has the radius equal to r_d . The other obvious option is to keep the diameter of the comparative cylinder equal to average lateral width, $E[l_w]$. The geometrical parameters r_d , N , σ_p^2 and $E[l_w]$ of some representative ensembles are recorded along with $E[\sigma_T^{rc}]$, σ_T^{st} , $\sigma_T^{cc}|_{r=r_d}$ and $\sigma_T^{cc}|_{\text{Dia}=E[l_w]}$ in Table 3.1.

It can be observed from the values in the Table 3.1 that estimated average total scattering cross section, $E[\sigma_T^{rc}]$, for all these ensembles is greater than total scattering cross sections of the comparative flat strips, $\sigma_T^{st}|_{w=E[l_w]}$. Table 3.1 further shows that estimate of $E[\sigma_T^{rc}]$ is also greater than total scattering cross section of circular cylinder having radius equal to mean radius of random cylinder, $\sigma_T^{cc}|_{r=r_d}$. It can be inferred from these observation that the two quantities, i.e., $\sigma_T^{st}|_{w=E[l_w]}$ and $\sigma_T^{cc}|_{r=r_d}$ can serve as the lower bounding values of average total scattering cross section of an ensemble in probabilistic sense, i.e., the probability of these events tends to one. The estimated values of average total scattering cross section $E[\sigma_T^{rc}]$, in the Table 3.1, are less than total scattering cross section of circular cylinder of diameter equal to lateral width, $\sigma_T^{cc}|_{\text{Dia}=E[l_w]}$ for all ensembles. Thus it can be said with probability tending to one

r_d (λ)	N	σ_p^2	$E[\mathbf{l}_w]$ (λ)	$E[\sigma_T^{\text{rc}}]$	σ_T^{st} $w = E[\mathbf{l}_w]$	σ_T^{cc} Dia = $2r_d$	σ_T^{cc} Dia = $E[\mathbf{l}_w]$
0.7	5	0.00833	1.49551	3.44419	2.98656	3.31846	3.48856
0.7	6	0.36000	2.09577	4.55788	4.19144	3.31846	4.79576
1.0	5	0.00833	2.07797	4.68476	4.15184	4.58632	4.75429
1.0	6	0.01000	2.10970	4.71861	4.21140	4.58632	4.81649
1.0	7	0.01167	2.14247	4.75541	4.27094	4.58632	4.87961
1.0	8	0.01333	2.17148	4.79035	4.33049	4.58632	4.96341
1.0	9	0.01500	2.20109	4.82847	4.38989	4.58632	5.00484
1.0	6	0.25000	2.83801	6.05676	5.65138	4.58632	6.29811
1.5	8	0.01333	3.14802	6.83428	6.23074	6.67175	6.91947
1.5	10	0.01667	3.20482	6.90102	6.41000	6.67175	7.08669
1.5	6	0.04000	3.25467	7.03502	6.51000	6.67175	7.21080
2.0	8	0.01333	4.12841	8.87549	8.25048	8.74024	9.02847
2.5	8	0.01333	5.11351	10.91587	10.21054	10.79971	11.04399

Table 3.1: A comparison of average total scattering cross section with total scattering cross section of a flat strip of width $E[\mathbf{l}_w]$ and circular cylinders having diameters equal to $2r_d$ and $E[\mathbf{l}_w]$.

that $\sigma_T^{cc}|_{\text{Dia}=E[l_w]}$ is an upper bound on the estimate of average total scattering cross section of an ensemble. These observations can be summarized as

$$\sigma_T^{st}|_{w=E[l_w]} \leq E[\sigma_T^{rc}] \leq \sigma_T^{cc}|_{\text{Dia}=E[l_w]} \quad (3.4.1)$$

$$\sigma_T^{cc}|_{r=r_d} \leq E[\sigma_T^{rc}] \leq \sigma_T^{cc}|_{\text{Dia}=E[l_w]} \quad (3.4.2)$$

The above inequalities show that estimate of average total scattering cross section of an ensemble is bounded in probabilistic sense, i.e., with probability tending to one the average total scattering cross section is bounded.

According to the above inequalities there are two candidates for lower bound on the value of average total scattering cross section, i.e., $\sigma_T^{st}|_{w=E[l_w]}$ and $\sigma_T^{cc}|_{r=r_d}$. Which of these two defines a tighter bound? Since these two quantities are candidates for lower bounding value hence maximum of the two will define a tighter bound. If input parameters of the ensemble are known then its mean radius is known and in principle average lateral width of the ensemble can also be determined. The total scattering cross section of both circular cylinder with radius equal to mean radius, $\sigma_T^{cc}|_{r=r_d}$ and a strip of width equal to lateral width $\sigma_T^{st}|_{w=E[l_w]}$ can thus be obtained. Larger of the two values will be a better lower bound. From data in the Table 3.1 one can observe that if the variance of ensemble is small then total scattering cross section of a circular cylinder with radius equal to mean radius can be a better bound and for large variance total scattering cross section of a strip promises to be a better bound. It can also be observed from the Table 3.1 that for different ensembles of a given mean radius, r_d , the value of average total scattering cross section $E[\sigma_T^{rc}]$ increases with increase in variance of the ensemble. Hence it appears that the average value of total scattering cross section $E[\sigma_T^{rc}]$ is closely related to average lateral width $E[l_w]$ rather than mean radius r_d .

Jaggard and Papas [40] have shown that certain bounds on capacitance of conducting cylinders of arbitrary shape can be determined in terms of its area and perimeter. It has been shown by them that the capacitance of arbitrarily shaped cylindrical structure is bounded in between the capacitances of a circular cylinder and a strip. This relation is developed due to the fact that a circle has minimum perimeter to area ratio whereas for a strip this ratio is infinite. These two shapes are therefore called bounding structures by them. Data in Table 3.1 shows that similar bound may exist for average total scattering cross section of random cylinders. The total scattering cross section of a circular cylinder having diameter equal to average lateral width, $\sigma_T^{cc}|_{\text{Dia}=E[l_w]}$, defines an upper bound for average total scattering cross section and total scattering cross section of a strip with width equal to average lateral width $\sigma_T^{st}|_{w=E[l_w]}$, is a lower limiting value of average total scattering cross section of random cylinders. Hence total scattering cross sections of a circular cylinder and a strip serve as two bounding structures for average total scattering cross section of random cylinders, if lateral width of all is same.

Determining either the scattered field or any other associated scattering parameter of random cylinders is generally a very complicated problem. In this section, despite all the complexities involved due to randomness of the cylinders it has been shown that the average total scattering cross section of random cylinders can possibly be bounded. The bounding values are defined in terms of the total scattering cross section of a circular cylinder and that of a strip, which are easier to obtain as compared to that of random cylinders. The only issue is to determine average lateral width of random cylinders. This can be obtained from the input parameters of the ensemble either with the help of analysis given in section (2.5) or numerically by generating

cylinders. Therefore, an insight into the average total scattering cross section can be developed using these bounds without actually solving for scattered field from random cylinder. In the next section an equivalent circular cylinder is used to approximate the average total scattering cross section of random cylinder and bounds on its radius are obtained.

3.5 Equivalent Radius

The concept of equivalent radius has been used to approximate the characteristics of a non circular cylinder with the help of calculations performed on an equivalent circular cylinder in various fields such as electromagnetics, acoustics and fluid dynamics [58, 41, 42, 59]. An equivalent cylinder is defined as a circular cylinder such that certain parameter of a non circular cylinder is invariant. Radius of the equivalent circular cylinder is called the equivalent radius. In the case of capacitance of a non circular cylinder with respect to a cylinder at infinity it has been shown that the equivalent radius is bounded by isoperimetric inequalities. The bounds of these isoperimetric inequalities are completely described by knowledge of non circular cylinder's cross sectional area and perimeter length [40].

Intuitively, it can be said that the equivalent circle must lie between the circles which geometrically bound the scatterer, i.e., equivalent circular cylinder must lie in between inscribed and circumscribed circles. This bounding region can further be reduced if the cross sectional area and perimeter length of the scatterer is known. Jaggard and Papas [40] have shown that for a cross section of area A and perimeter

length l , the two bounding radii can be defined as

$$r_{\text{in}} = \sqrt{A/\pi} \quad (3.5.1)$$

$$r_{\text{out}} = \frac{l}{2\pi} \quad (3.5.2)$$

such that the expression bounding the equivalent radius is given as

$$\sqrt{A/\pi} \leq r_{\text{eq}} \leq \frac{l}{2\pi} \quad (3.5.3)$$

In the above equation, equality holds only for a circular cylinder. The bounding limits become widely spaced when the cross section has fewer axes of symmetry or is markedly different from a circle.

In this section, it is of interest to show whether such bounds exist for the equivalent radius of random cylinders. Equivalent radius of an ensemble of random cylinders is taken to be the radius of a circular cylinder whose total scattering cross section is equal to the average total scattering cross section of the ensemble. It will be denoted by r_{eq} . As mentioned earlier, in section 2.2, that the radius of the Gaussian cylinder cannot be less than $r_d - NB$ and it cannot be greater than $r_d + NB$. Hence, circles of radii $r_d - NB$ and $r_d + NB$ are inscribed and circumscribed circles of an ensemble, respectively. Equivalent radius of Gaussian cylinder, therefore, must lie between $r_d \pm NB$. Can the bounding region for random cylinders be narrowed by using isoperimetric inequality, such as one described by equation (3.5.3)?

The answer to above question is arrived at by using average values of area and perimeter length of an ensemble. The two bounding radii for an isoperimetric inequality are taken to be equivalent area radius and equivalent circumferential radius. An equivalent area radius r_{ea} is the radius of a circular cylinder having area equal to average area of random cylinder. Similarly, an equivalent circumferential radius r_{ec} is

the radius of a circular cylinder having circumference equal to circumference due to rms differential length of random cylinder. The equivalent area and circumferential radii for Gaussian cylinders have been given in section 2.2 as,

$$r_{ea} = \sqrt{r_d^2 + \sigma_P^2} \quad (3.5.4)$$

$$r_{ec} = \sqrt{r_d^2 + \sigma_P^2 \left(1 + \frac{(N+1)(2N+1)}{6}\right)} \quad (3.5.5)$$

From the expressions above, it can be observed that $r_{ea} < r_{ec}$ and both these radii are equal only when $\sigma_P^2 = 0$, i.e., the cross section is circular. Equivalent area radius can likely serve as lower bound and equivalent circumferential radius as upper bound of an isoperimetric inequality, if it exists.

The perimeter of certain non convex or star like shapes can become very large and at times corresponding r_{ec} can become greater than the radius of circumscribed circle. In such cases the radius of circumscribed circle can be used as an upper bound of the equivalent radius. Therefore, if the equivalent circumferential radius of Gaussian cylinder r_{ec} is greater than its circumscribed radius $r_d + NB$, then circumscribed radius should be used as upper bounding value. The bounding region for equivalent radius will therefore be $[r_{ea}, \min\{r_{ec}, (r_d + NB)\}]$. Since $r_{ea} \geq r_d$, therefore, if an isoperimetric inequality exists, then the bounded region will be reduced by more than half of the region defined by inscribed and circumscribed radii, i.e., $[(r_d - NB), (r_d + NB)]$.

If the equivalent radius, r_{eq} , of an ensemble is greater than equivalent area radius r_{ea} and less than equivalent circumferential radius r_{ec} , then it can be said that an isoperimetric inequality similar to that for capacitance exists. Equivalent radii of different ensembles of random cylinders have been obtained numerically because it is difficult to obtain radius for a given total scattering cross section of a circular cylinder

from the analytic expression, given by Bowman [1]. Hence a lookup table approach is adopted to obtain equivalent radii. In this approach total scattering cross sections of circular cylinders having radii between 0.5λ to 5λ with an increment of 0.001λ are obtained using MM and are recorded. This method will work because the total scattering cross section of circular cylinder is a monotonically increasing function of radius and the two quantities have one to one correspondence. Therefore, given a value of average total scattering cross section $E[\sigma_T^{\text{rc}}]$, equivalent radius can be readily determined.

The equivalent radius r_{eq} together with $E[\sigma_T^{\text{rc}}]$, $E[\mathbf{l}_w]$, r_{ea} , r_{ec} and other input parameters of an ensemble are tabulated in Table 3.2. Mean radius of the tabulated samples has been varied from 0.7λ to 2.5λ . Only few ensembles with mean radius greater than 1λ are generated because the variation in total scattering cross section due to difference in shape of a scatterer nearly diminishes for electrically large scatterers and also because the time required for simulation of such an ensemble was in days with available computing resources. The effect of variance on equivalent radius is probed by generating ensembles of different variance keeping the mean radius constant. Since the equivalent circumferential length also depends on N , therefore its effect is highlighted by generating some ensembles having different values of N but same values of mean radius and variance. The equivalent circumferential radius is not greater than the circumscribed circle's radius, $r_d + NB$ for any ensemble in the Table, hence circumscribed radius is not given.

It can be observed from the Table 3.2 that the value of equivalent radius, r_{eq} is greater than the equivalent area radius, r_{ea} and it is less than the equivalent circumferential radius r_{ec} , irrespective of input parameters of the Gaussian cylinder. The

r_d	N	σ_p^2	$E[\sigma_T^{\text{rc}}]$	$E[\mathbf{l}_w]/2$	r_{ea}	r_{ec}	r_{eq}	r_{ee}
0.7	5	0.00833	3.44419	0.74775	0.70593	0.76811	0.7310	0.73702
0.7	6	0.36000	4.55788	1.04789	0.92195	2.51197	0.9945	1.71696
1.0	5	0.00833	4.68476	1.03899	1.00416	1.04881	1.0250	1.02648
1.0	6	0.01000	4.71861	1.05485	1.00499	1.07781	1.0330	1.04140
1.0	7	0.01167	4.75541	1.07124	1.00582	1.11580	1.0420	1.06081
1.0	8	0.01333	4.79035	1.08574	1.00664	1.16333	1.0500	1.08499
1.0	9	0.01500	4.82847	1.10055	1.00747	1.22066	1.0590	1.11406
1.0	15	0.01502	4.89915	1.13571	1.00748	1.50210	1.0760	1.25479
1.0	10	0.01667	4.86689	1.11598	1.00830	1.28776	1.0685	1.14803
1.0	11	0.01833	4.90157	1.13061	1.00913	1.36443	1.0765	1.18678
1.0	5	0.01875	4.78823	1.07349	1.00933	1.10680	1.0495	1.05806
1.0	12	0.02000	4.94203	1.14530	1.00995	1.45029	1.0865	1.23012
1.0	13	0.02167	4.97809	1.15757	1.01078	1.54488	1.0950	1.27783
1.0	15	0.02500	5.06071	1.18488	1.01242	1.75831	1.1145	1.38537
1.0	7	0.02625	4.92245	1.12412	1.01304	1.24549	1.0815	1.12927
1.0	5	0.03333	4.92133	1.11277	1.01653	1.18322	1.0815	1.09987
1.0	9	0.03375	5.06115	1.17149	1.01673	1.45000	1.1150	1.23337
1.0	11	0.04125	5.19802	1.21627	1.02042	1.71428	1.1475	1.36735
1.0	7	0.04667	5.12833	1.18220	1.02307	1.40712	1.1310	1.21510
1.0	13	0.04875	5.33343	1.25813	1.02408	2.02978	1.1800	1.52693
1.0	9	0.06000	5.33222	1.24571	1.02956	1.72047	1.1795	1.37501
1.0	5	0.07500	5.23546	1.19802	1.03682	1.37840	1.1565	1.20761
1.0	14	0.09333	5.81035	1.38631	1.04563	2.80357	1.2940	1.92460
1.0	15	0.10000	5.90492	1.41321	1.04881	3.06050	1.3170	2.05465
1.0	7	0.10500	5.57265	1.29881	1.05119	1.79025	1.2370	1.42072
1.0	11	0.16500	6.17803	1.47128	1.07935	2.95888	1.3825	2.01912
1.0	13	0.19500	6.43767	1.54286	1.09316	3.67151	1.4450	2.38234
1.0	5	0.20833	5.81659	1.34692	1.09924	1.87083	1.2955	1.48504
1.0	15	0.22500	6.67571	1.60761	1.10680	4.45253	1.5020	2.77966
1.0	9	0.24000	6.34427	1.50476	1.11355	2.97321	1.4225	2.04338
1.0	11	0.29333	6.65712	1.59150	1.13725	3.84534	1.4975	2.49130
1.0	15	0.40000	7.16017	1.72856	1.18322	5.87083	1.6190	3.52702
1.0	11	0.45833	6.92455	1.65759	1.20761	4.74781	1.5620	2.97771
1.0	15	0.62500	7.38730	1.78437	1.27475	7.30011	1.6740	4.28743
1.5	8	0.01333	6.83428	1.57401	1.50444	1.61348	1.5405	1.55896
1.5	10	0.01667	6.90102	1.60241	1.50555	1.70538	1.5565	1.60546
1.5	6	0.04000	7.03502	1.62734	1.51327	1.70196	1.5890	1.60762
2.0	8	0.01333	8.87549	2.06420	2.00333	2.08646	2.0345	2.04490
2.5	8	0.01333	10.9159	2.55675	2.50267	2.56970	2.5305	2.53618

Table 3.2: Different equivalent radii of random cylinders.

average total scattering cross section is numerically estimated hence it is random and so is the corresponding equivalent radius. Thus the equivalent area radius is the lower bound and equivalent circumferential radius is upper bound for equivalent radius of random Gaussian cylinder in probabilistic sense. It can therefore be said that the probability of equivalent radius of Gaussian cylinder bounded by an isoperimetric inequality tends to one. The above observations can be summarized as

$$\text{Prob}\{r_{\text{ea}} \leq r_{\text{eq}} \leq r_{\text{ec}}\} \rightarrow 1 \quad (3.5.6)$$

The above inequality is the same as the one given for capacitance of arbitrarily shaped cylinders by Jaggard and Papas [40].

Another important observation that can be made from the data in Table 3.2 is that the half of estimated average lateral width, i.e., $E[\mathbf{l}_w]/2$ of an ensemble is also greater than equivalent area radius r_{ea} and less than equivalent circumferential radius r_{ec} , that is

$$r_{\text{ea}} \leq \frac{E[\mathbf{l}_w]}{2} \leq r_{\text{ec}} \quad (3.5.7)$$

Due to random nature of the estimated lateral width, the above expression is true in the probabilistic sense, i.e., half of average lateral width is also bounded within the same bounds as that of equivalent radius with probability tending to one. Lateral width is a geometrical parameter and it is random for random cylinders. An approximate pdf of lateral width \mathbf{l}_w has been obtained in section 2.5. In principle, the average value of lateral width can be obtained from the pdf but calculations involved to determine the approximate pdf are complicated. Therefore, evaluation of average value of lateral width by using the approximated pdf is not easy. If not much accuracy is desired, an estimate of the value of average lateral width can be obtained

from these two simple bounding values, i.e., r_{ea} and r_{ec} .

An approximation to find the radius of an equivalent PEC circular cylinder which possesses the same capacitance with respect to a cylinder at infinity as does a metallic cylinder with arbitrary cross section is given by Jaggard [60]. He asserted that the arithmetic mean of the two bounding radii, i.e., equivalent area and equivalent circumferential radii, is a good approximation for equivalent radius. On the basis of total scattering cross section as the invariant parameter, does this approximation valid for random cylinders as well? To answer this question, value of the arithmetic average of equivalent area radius and equivalent circumferential radius is obtained and defined as approximate equivalent radius, r_{ee} .

The approximate equivalent radius is shown in column labelled r_{ee} of the Table 3.2. Values in column r_{ee} are compared with the values of equivalent radius shown in column r_{eq} . It is observed from Table 3.2 that the two values are close to each other if the variance and number of terms N is small. These values deviate markedly from each other when the variance of random cylinder is large, especially when number of terms is also large. It is also interesting to note, from the Table 3.2, that the value of approximate equivalent radius is always greater than the corresponding value of equivalent radius r_{eq} . This shows that the upper bound of equivalent radius, i.e., equivalent circumferential radius has large values and approximate equivalent radius can serve as another upper bound for equivalent radius. This observation is consistent with earlier observation, section 2.2, that an increase in variance σ_p^2 of the random cylinder increases its circumferential radius, tracing lots of crest and troughs.

How good a strip serve as an equivalent model for determining average total scattering cross section of random cylinder compared to a circular cylinder? An

equivalent strip is an infinitesimally thin strip whose total scattering cross section is equal to the average total scattering cross section of random cylinder. The width of equivalent strip will be referred to as equivalent width and it will be denoted by w_{eq} . Equivalent width and equivalent diameter, $2r_{eq}$, are then compared with the average lateral width of random cylinders. A better equivalent model will be the one whose equivalent length will be closer to the average lateral width.

Equivalent width of a flat strip is determined numerically, using similar method as used to determine equivalent radius. Total scattering cross sections of flat strips of width ranging between 0.5λ to 5λ , with an increment size of 0.01λ , are obtained using MM and are recorded, to make a lookup table. The equivalent width, w_{eq} , can thus readily be obtained from the table. It is determined that which of these two equivalent lengths, i.e., equivalent radius and equivalent width is closer to the average lateral width to show which canonical cross sectional shape serves as a better model. Proximity of average lateral width from the two equivalent lengths is determined by evaluating absolute relative differences of average lateral width from the two equivalent length, i.e., $|E[l_w] - 2r_{eq}|/E[l_w]$ and $|E[l_w] - w_{eq}|/E[l_w]$. Minimum of the two differences will determine which equivalent length is closer to average lateral width and which canonical cross sectional shape serves as a better model.

The absolute relative differences of average lateral width and the two equivalent lengths together with actual values of average lateral width, equivalent diameter and equivalent width are tabulated in Table 3.3. The Table also shows input parameters and average values of total scattering cross section of different ensembles of random cylinders. It can be seen from the Table 3.3 that circular cylinder is a better equivalent model as the values of equivalent diameter, $2r_{eq}$, are closer to average lateral

r_d	σ_p^2	$E[\sigma_T^{\text{rc}}]$	$E[\mathbf{l}_w]$	$2r_{\text{eq}}$	$\frac{E[\mathbf{l}_w] - 2r_{\text{eq}}}{E[\mathbf{l}_w]}$	w_{eq}	$\frac{E[\mathbf{l}_w] - w_{\text{eq}}}{E[\mathbf{l}_w]}$
0.7	0.00833	3.44419	1.49551	1.462	0.02240	1.725	0.1535
0.7	0.36000	4.55788	2.09577	1.989	0.05095	2.280	0.0879
1.0	0.00833	4.68476	2.07797	2.050	0.01346	2.350	0.1309
1.0	0.01000	4.71861	2.10970	2.066	0.02070	2.365	0.1210
1.0	0.01167	4.75541	2.14247	2.084	0.02729	2.385	0.1132
1.0	0.01333	4.79035	2.17148	2.100	0.03291	2.400	0.1052
1.0	0.01500	4.82847	2.20109	2.118	0.03775	2.420	0.0995
1.0	0.25000	6.05676	2.83801	2.707	0.04616	3.030	0.0676
1.5	0.01333	6.83428	3.14802	3.081	0.02129	3.420	0.0864
1.5	0.01667	6.90102	3.20482	3.113	0.02865	3.460	0.0796
1.5	0.04000	7.03502	3.25467	3.178	0.02355	3.520	0.0815
2.0	0.01333	8.87549	4.12841	4.069	0.01439	4.440	0.0755
2.5	0.01333	10.91587	5.11351	5.061	0.01027	5.460	0.0678

Table 3.3: A comparison of average lateral width of random cylinder with twice equivalent radius and equivalent width.

width, $E[\mathbf{l}_w]$, than the values of equivalent width, w_{eq} . Although difference between equivalent diameter and $E[\mathbf{l}_w]$ increases when the variance, σ_p^2 , of an ensemble increases but as far as the ensembles given in Table, this difference is less than the difference between equivalent width and $E[\mathbf{l}_w]$. Thus, even for quite large variance of an ensemble, a circle is a better equivalent model to determine average total scattering cross section of random cylinders than a strip. The Table further shows that value of absolute relative difference becomes small for both equivalent shapes when average value of \mathbf{l}_w is large. This shows that as far as total scattering cross section is concerned the distinction between cross sectional shape of a scatterer decreases if its lateral width is large compared to wavelength of the incident wave.

In the above analysis, it has been shown that equivalent radius, r_{eq} , and half of average lateral width, $E[\mathbf{l}_w]/2$, both are bounded within equivalent area radius, r_{ea} and equivalent circumferential radius, r_{ec} . Average lateral width is a geometric

parameter but it is difficult to obtain. Whereas the two bounding radii are simple to determine from the input parameters. It has also been shown that if the variance σ_p^2 of random cylinder is small, average of the two bounding radii, r_{ee} , provides good approximate value of equivalent radius. Once the equivalent radius or lateral width is approximately determined average total scattering cross section of random cylinders can be easily approximated. Finally it is shown that for a given average lateral width a circular cylinder of diameter equal to $E[l_w]$ is a better equivalent model than a strip to determine average total scattering cross section, if the variance σ_p^2 is not very large. Hence approximations to estimate average lateral width and average total scattering cross section are obtained in terms of very simple to determine parameters. How does the cross sectional shape affect the total scattering cross section of random cylinders? In the next section the effect of cross sectional shape is probed by obtaining scatter plots between lateral width and total scattering cross section.

3.6 Scatter Diagram

In the previous section average total scattering cross section of random cylinder has been compared with total scattering cross sections of a cylinder and a strip. The dependence of average total scattering cross section on the average lateral width of random cylinders has also been studied. These studies were focused mainly around the dependence of total scattering cross section on average lateral width of random cylinders. In case of scatterers like a circular cylinder and strip, the lateral width completely specifies their cross sectional shape. Whereas it is difficult to say anything about cross sectional shape of a random cylinder from its lateral width. Random cylinders of different cross sectional shapes can have same lateral width and average

lateral width of random cylinder gives very little insight into the cross sectional shape of random cylinder. Therefore, analysis in previous section does not reveal much insight on the dependence of total scattering cross section on cross sectional shape of random cylinders.

In this section, the total scattering cross section of random cylinder is studied to probe the effects of random cross sectional shape on it. Cross sectional shape of a two dimensional scatterer is a plane curve. In general, a function of ρ and θ is needed to define cross sectional shape completely. On the other hand, total scattering cross section is a scalar quantity. Hence cross sectional shape and total scattering cross section do not have one to one correspondence and it is difficult to analytically analyze them together. Another complication is that the cross sectional shape of random cylinder is random. Total scattering cross section of a regular shaped scatterer is customarily shown against its lateral width. In such cases a given value of lateral width uniquely defines the scatterer, which is not true in case of random cylinders.

A simple way to probe into the effect of cross sectional shape of random cylinder on total scattering cross section is to draw a two dimensional scatter diagram. The scatter diagram shows relationship between total scattering cross section and lateral width. Each outcome of a realization, i.e., l_w and σ_T^{rc} , defines an ordered pair which is plotted as a single point on the plot. The two dimensional scatter plots are obtained for some ensembles of random cylinders and are shown in Figure 3.5 and Figure 3.6. Each ensemble consists of fifty thousand random cylinders. The scatter diagrams shown in Figure 3.5 are of ensembles having different mean radius, r_d . The variance in radius, σ_p^2 , of all these ensembles is the same. All the ensembles of Figure 3.6 have

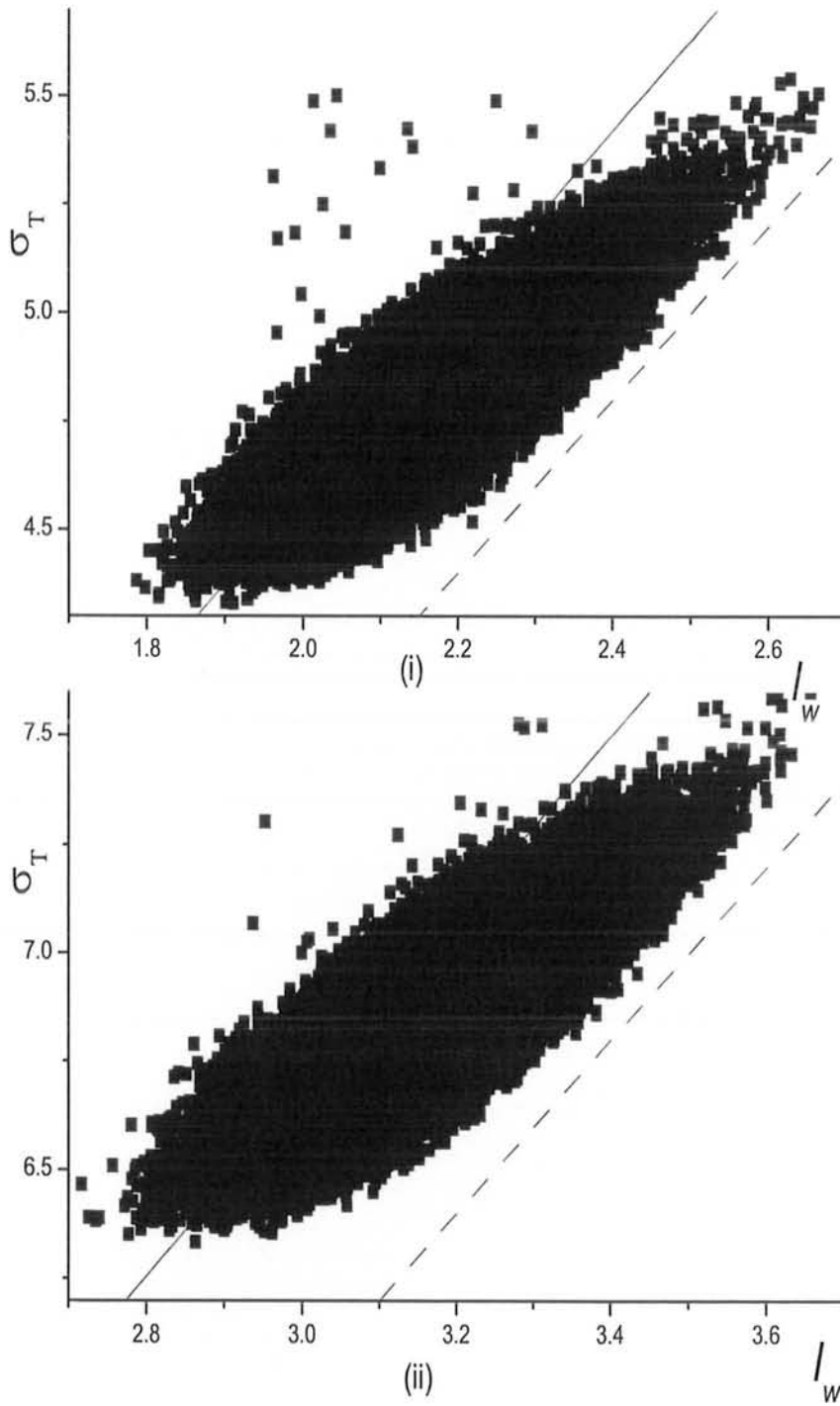


Figure 3.5: Scattered plot of σ_T^{tc} vs l_w for $\sigma_p^2 = 0.01333$ and mean radius = (i) 1.0λ and (ii) 1.5λ .

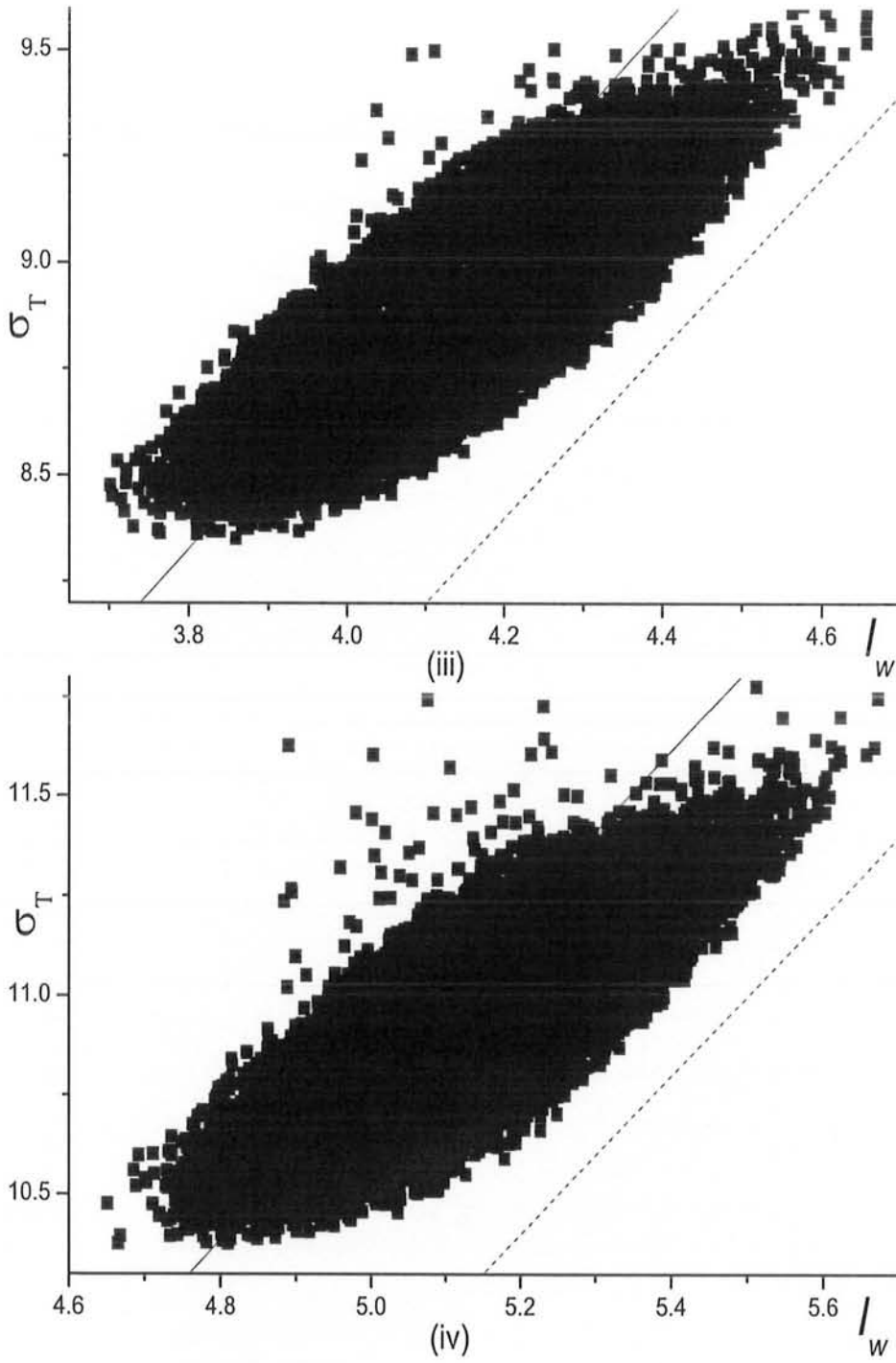


Figure 3.5: Scattered plot of σ_T^{rc} vs l_w for $\sigma_p^2 = 0.01333$ and mean radius = (iii) 2.0λ and (iv) 2.5λ .

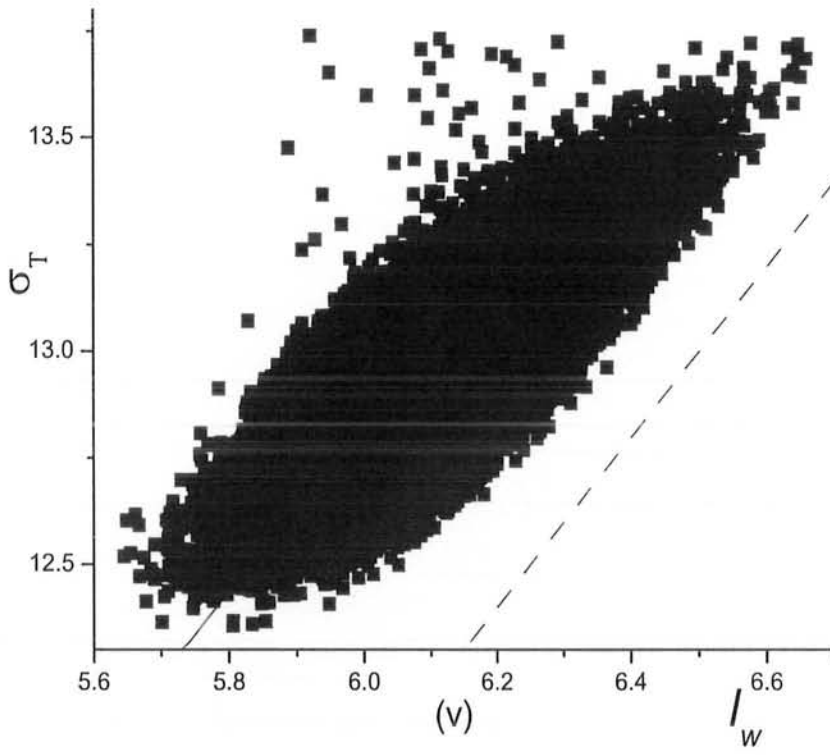


Figure 3.5: Scattered plot of σ_T^{rc} vs l_w for $\sigma_p^2 = 0.01333$ and mean radius = 3.0λ .

same mean radius but their variances are different. Continuous line on each diagram marks the total scattering cross section of circular cylinder with diameter equal to lateral width. A dotted line marking $\sigma_T^{\text{rc}} = 2l_w$ is also shown on each plot.

It can be observed that the distribution pattern of sample points in all the plots of Figures 3.5 and 3.6, is quite similar, i.e., scatter points of all the ensembles are similarly distributed irrespective of the value of mean radius and variance, σ_p^2 . The pattern of sample points on the scatter plot reveals that total scattering cross section of random cylinder is highly correlated with its lateral width. To further analyze and quantify the above observation statistics of total scattering cross section and lateral width together with their correlation coefficient are estimated. An approximate pdf of lateral width has been obtained in section 2.5, but its evaluation is complicated. Therefore, in absence of any statistical insight to the total scattering cross section of random cylinder and complication in determining the pdf of lateral width, these statistics are estimated from the data numerically. These numerically obtained estimates are tabulated in Table 3.4. The column labelled $\rho_{\sigma l_w}$ of the Table 3.4 shows the coefficient of correlation between σ_T^{rc} and l_w . The entries in this column show that correlation between these two quantities is very high.

From the plots in Figures 3.5 and 3.6, it is observed that majority of the sample points lie in region between solid line and dotted line. This shows that total scattering cross section of majority of the random cylinders is less than that of a circular cylinder and greater than twice their lateral width. It can also be observed from these plots that as the lateral width increases, more and more sample points lie below the solid line. It has been determined from the data points that the number of points above the solid line in each plot is less than twenty percent of the total points. The scatter

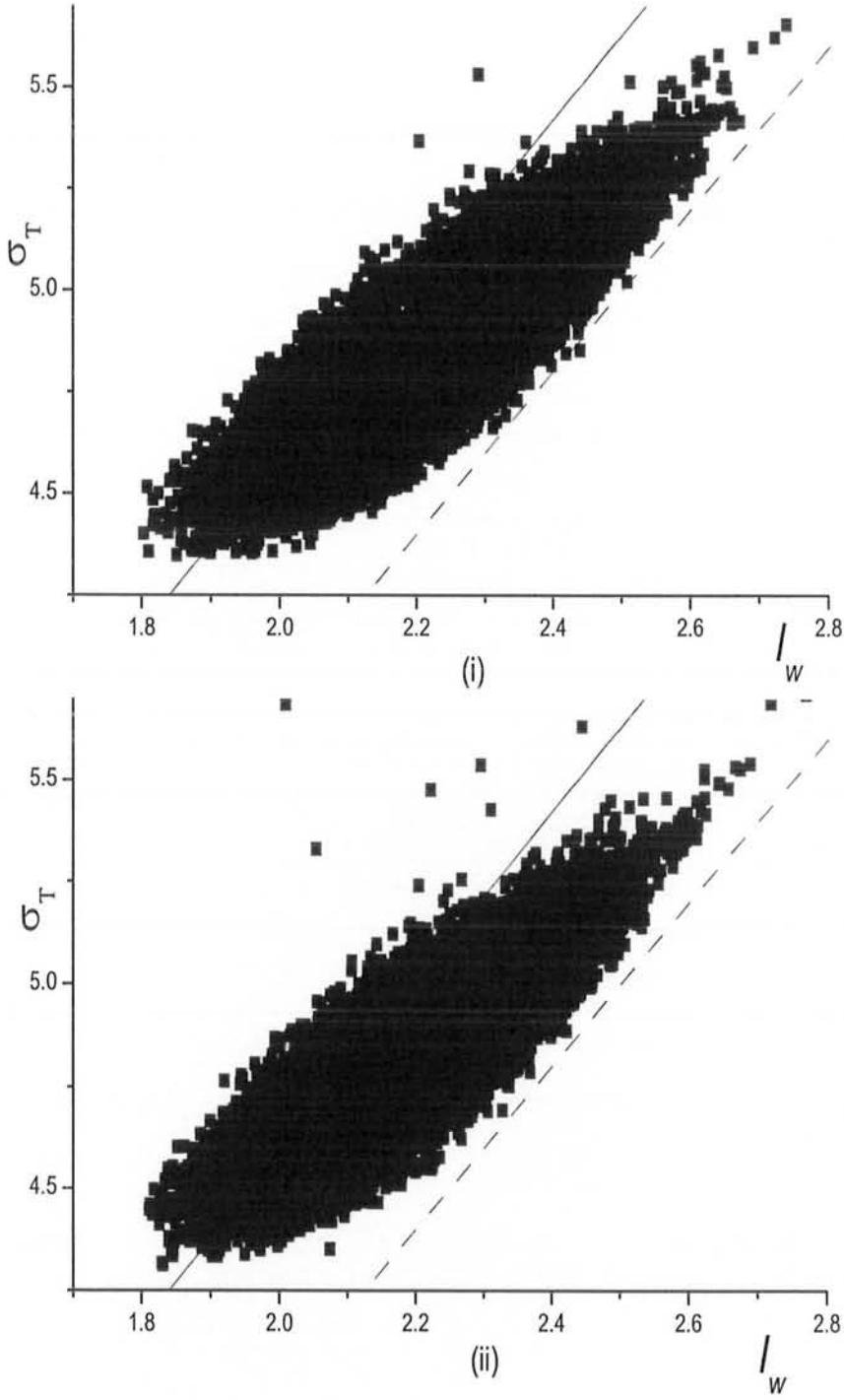


Figure 3.6: Scattered plot of σ_T^{rc} vs l_w for mean radius 1.0λ and $\sigma_p^2 =$ (i) 0.01500 and (ii) 0.01333.

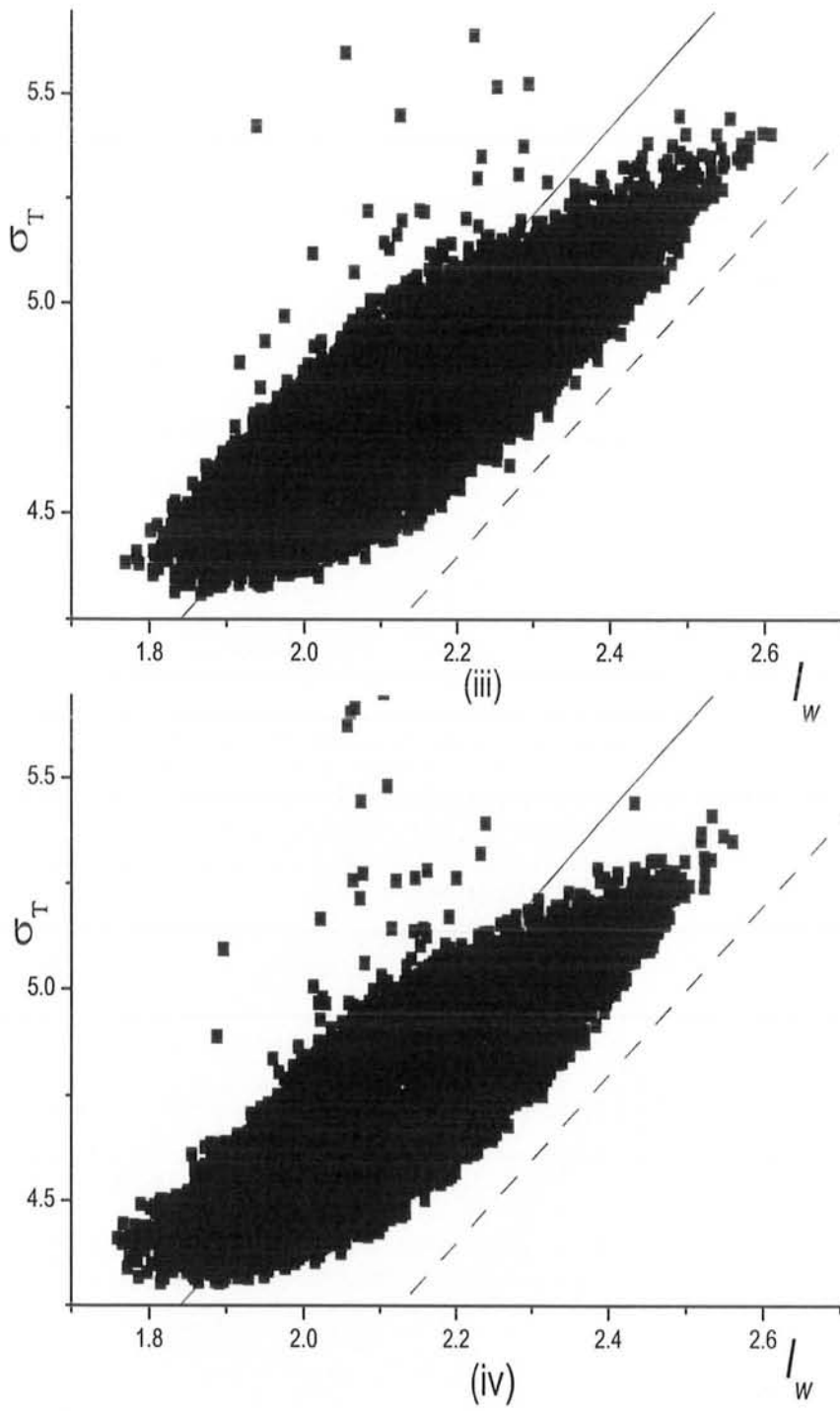


Figure 3.6: Scattered plot of σ_T^{rc} vs l_w for mean radius 1.0λ and $\sigma_p^2 =$ (iii) 0.01167 and (iv) 0.01000.

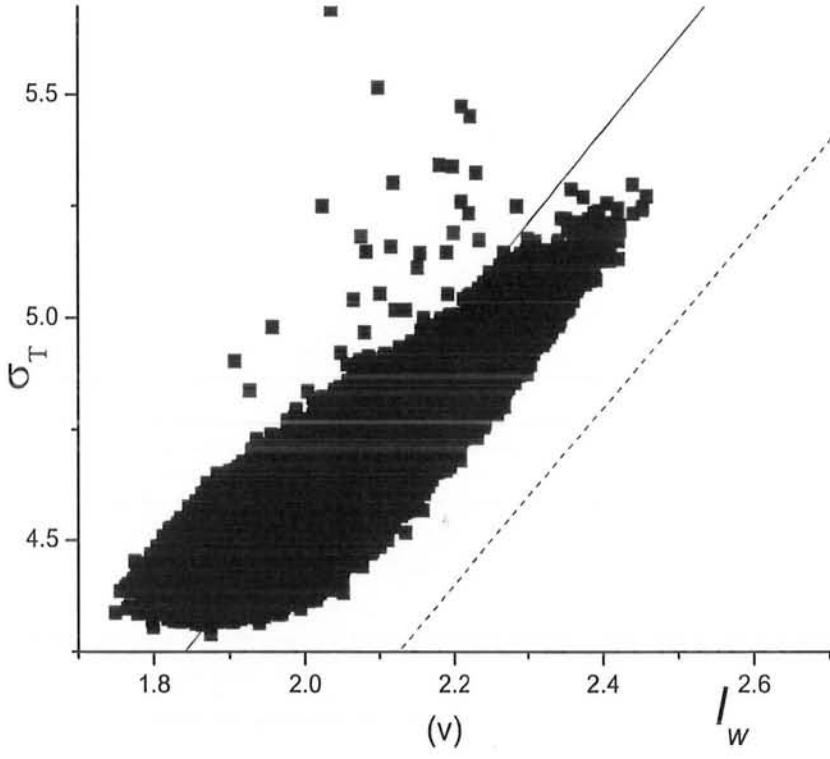


Figure 3.6: Scattered plot of σ_T^{rc} vs l_w for mean radius 1.0λ and $\sigma_p^2 = 0.00833$.

Plot	r_d	σ_p^2	$E[\mathbf{l}_w]$	S.D. (\mathbf{l}_w)	$E[\sigma_T^{\text{rc}}]$	S.D. (σ_T^{rc})	$\rho(\sigma_T^{\text{rc}}, \mathbf{l}_w)$
Figure 3.5							
(i)	1.0	0.01333	2.17148	0.11560	4.79035	0.16408	0.83680
(ii)	1.5	0.01333	3.14802	0.12244	6.83428	0.17096	0.82275
(iii)	2.0	0.01333	4.12841	0.12844	8.87549	0.17865	0.80455
(iv)	2.5	0.01333	5.11351	0.13232	10.9159	0.18271	0.78980
(v)	3.0	0.01333	6.10158	0.13570	12.95304	0.19040	0.78302
Figure 3.6							
(i)	1.0	0.01500	2.20109	0.12007	4.82847	0.17054	0.84533
(ii)	1.0	0.01333	2.17148	0.11560	4.79035	0.16408	0.83680
(iii)	1.0	0.01167	2.14247	0.11182	4.75541	0.15958	0.83589
(iv)	1.0	0.01000	2.10970	0.10798	4.71861	0.15449	0.82516
(v)	1.0	0.00833	2.07797	0.10192	4.68476	0.14866	0.88569

Table 3.4: Values of mean, standard deviation and covariance coefficient of lateral width and total scattering cross section.

plots in Figure 3.5 show that as mean radius of random cylinder increases the distance between sample points and dotted line increases. Whereas from the plots of Figure 3.6, one can observe that an increase in the variance σ_p^2 of an ensemble decreases the distance between its sample points and dotted line.

A measure of randomness in the cross sectional shape of random cylinder can be given in terms of equivalent radii ratio(EQRR), defined in section (2.2). EQRR depends on both the mean radius and variance σ_p^2 of random cylinder. Equivalent radii ratio signifies deviation in cross sectional shape from a circular cylinder. EQRR of a circular cylinder is one, which is lower bounding value of this ratio. There exists no upper bound on the value of EQRR. Larger the deviation of cross sectional shape from a circle higher will be the EQRR. Hence, variation of convex cross sectional shapes from a circle increases EQRR and instead of analyzing the scatter plots for variations in mean radius and σ_p^2 separately, these plots can be analyzed in light of this ratio. In Figure 3.5, EQRR varies due to variation in mean radius, r_d and in

Diagram	r_d	N	σ_p^2	r_{ea}	r_{ec}	EQRR
Figure 3.5						
(i)	1.0	8	0.01333	1.00664	1.16333	1.15565
(ii)	1.5	8	0.01333	1.50444	1.61348	1.07248
(iii)	2.0	8	0.01333	2.00333	2.08646	1.04150
(iv)	2.5	8	0.01333	2.50267	2.56970	1.02678
(v)	3.0	8	0.01333	3.00222	3.05832	1.01869
Figure 3.6						
(i)	1.0	9	0.01500	1.00747	1.22066	1.21160
(ii)	1.0	8	0.01333	1.00664	1.16333	1.15565
(iii)	1.0	7	0.01167	1.00582	1.11580	1.10934
(iv)	1.0	6	0.01000	1.00499	1.07781	1.07246
(v)	1.0	5	0.00833	1.00416	1.04881	1.04447

Table 3.5: Equivalent radii ratio of those random cylinders whose scatter plots are given in Figures 3.5 and 3.6.

Figure 3.6 it changes due to change in variance, σ_p^2 . The values of EQRR of all these ensembles together with other parameters are tabulated in Table 3.5. The EQRR is maximum in plot (i) of both the figures and it subsequently decreases to minimum value for plot (v). One can observe from the graphs in both figures that as EQRR increases the distance between dotted line and scattered points decreases.

Total scattering cross section of a strip is always less than that of a circular cylinder and its value is slightly less than twice the lateral width of strip, when the lateral width is comparable or greater than wavelength of incident wave. Decrease in the distance between scatter points and dotted line with increase in EQRR shows that such random cylinders have been generated whose total scattering cross section is closer to that of a strip rather than that of a circular cylinder. An increase in EQRR is a measure of deformation in shape from a circle. If the cross sectional shape of random cylinder is modelled by an equivalent convex cross sectional shaped cylinder on the basis of total scattering cross section then an increase in EQRR points that the

equivalent shape will be flatter than a circle. Decrease in distance between scatter point and dotted line also hints in the same direction. Therefore, as long as total scattering cross section is the parameter of interest, with an increase in EQRR more and more random cylinders are generated which appear flatter to incident plane wave.

To support above conclusion that equivalent convex cross sectional shape of random cylinders appears flatter to the incident plane wave as EQRR increases, two dimensional scatter diagrams of ensembles with large EQRR are obtained. Figure 3.7 show scatter diagrams of two ensembles with large EQRR. It can be observed from these plots that sample points touch dotted line and few sample points even cross the dotted line, i.e., the total scattering cross section of few random cylinders is less than twice their lateral width. Equivalent convex cross sectional shape of such random cylinders, on the basis of total scattering cross section, can said to be closer to a strip rather than to a cylinder. Thus the equivalent convex cross sectional shape becomes flatter and flatter as EQRR of the ensemble increases.

It has been shown in this section that the coefficient of correlation of the two random variables σ_T^{rc} and l_w is high for almost all of the ensembles irrespective of their input statistics. The probability that total scattering cross section of random cylinder is less than that of a circular cylinder whose diameter is equal to lateral width has been observed to be very high. This probability increases when lateral width is greater than mean diameter. It has also been observed that the equivalent convex cross sectional shape of random cylinder becomes flatter and flatter with increase in EQRR of the ensemble. Regularity in the distribution of scatter points invites one to investigate joint probability distribution of total scattering cross section and lateral width.

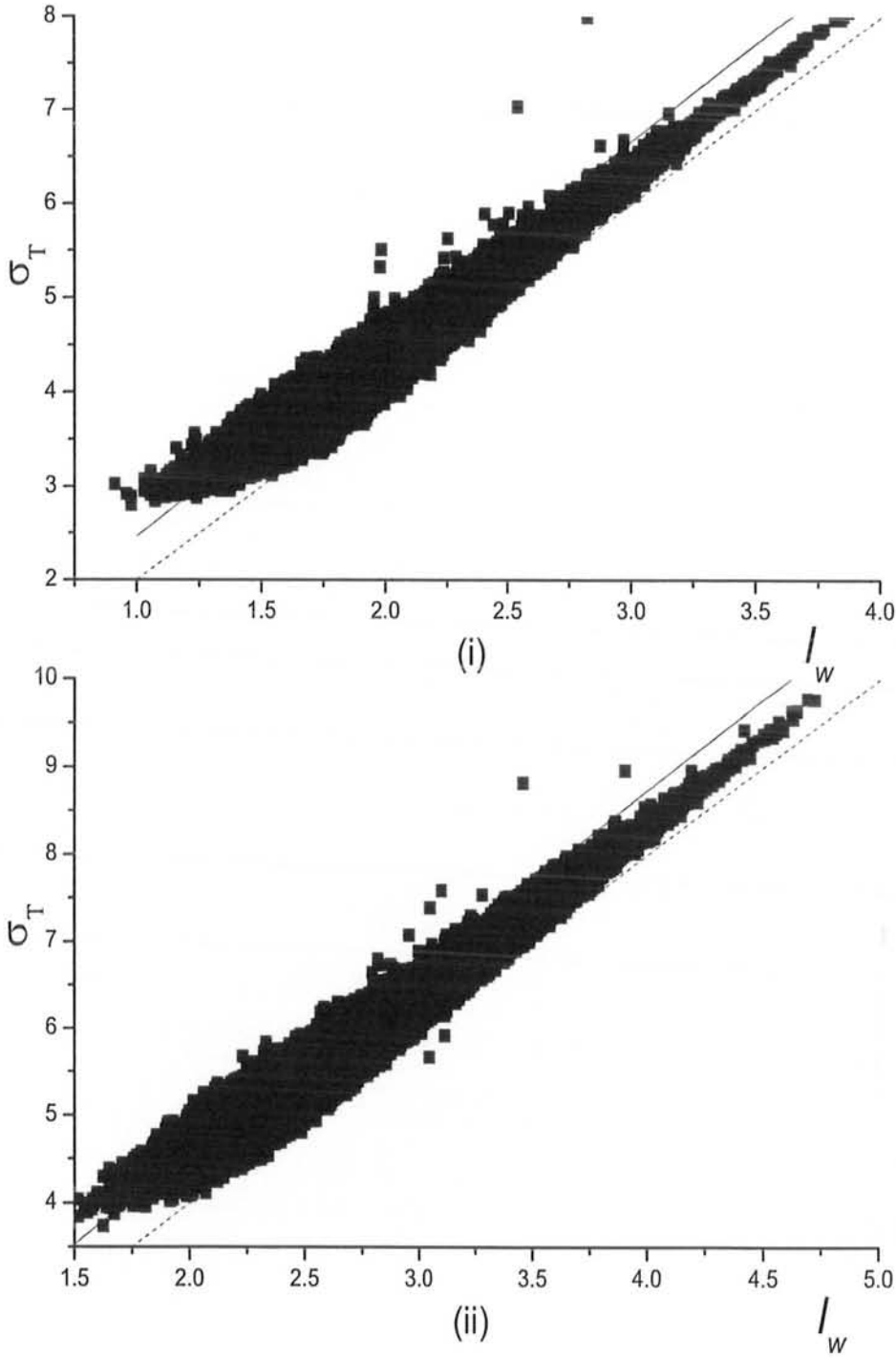


Figure 3.7: Scattered plot of σ_T^{rc} vs l_w of random cylinder with high equivalent radii ratio(EQRR). (i) EQRR = 2.72462, $\sigma_p^2 = 0.36$. (ii) EQRR = 2.00832, $\sigma_p^2 = 0.25$.

3.7 Joint Probability Density Function

In this section, an estimate of the joint probability density function of total scattering cross section, σ_T^{rc} , and lateral width, l_w , is obtained and an attempt is made to approximate it with any well known distribution. Relative frequency of the sample points is numerically obtained to estimate their joint probability density function. Total plot area is divided into small uniform rectangles such that the area of all these rectangles is equal. Number of sample points lying in each rectangle is counted. The count is normalized by the product of total number of sample points in the ensemble and area of the rectangle. This normalized relative frequency of sample points is an estimate of joint probability density function of σ_T^{rc} and l_w , $f_{\sigma l_w}(\sigma_T^{\text{rc}}, l_w)$.

Procedure of estimating the joint density from data points is implemented using Fortran programming language. Input to the Fortran code is a data file containing total number of sample points in an ensemble, lateral width and total scattering cross section. The file is first sorted in ascending order of lateral width. Output of the code is another data file which contains normalized count of points in each rectangle and coordinates of the midpoint of corresponding rectangle. Contour plots are generated to graphically represent the estimated joint pdf from these output files. These estimates of joint probability density from numerical data for some of the representative ensembles are shown in Figure 3.8.

The contour plots, shown in Figure 3.8, reveal that the density of sample points varies smoothly. The pattern of the contours shows that the density of the sample points is low at the edges and high near the center. Peak values of these plots lie close to the mean value of both random variables, σ_T^{rc} and l_w . The contours of these plots appear similar to a bivariate Gaussian contours. In order to determine that

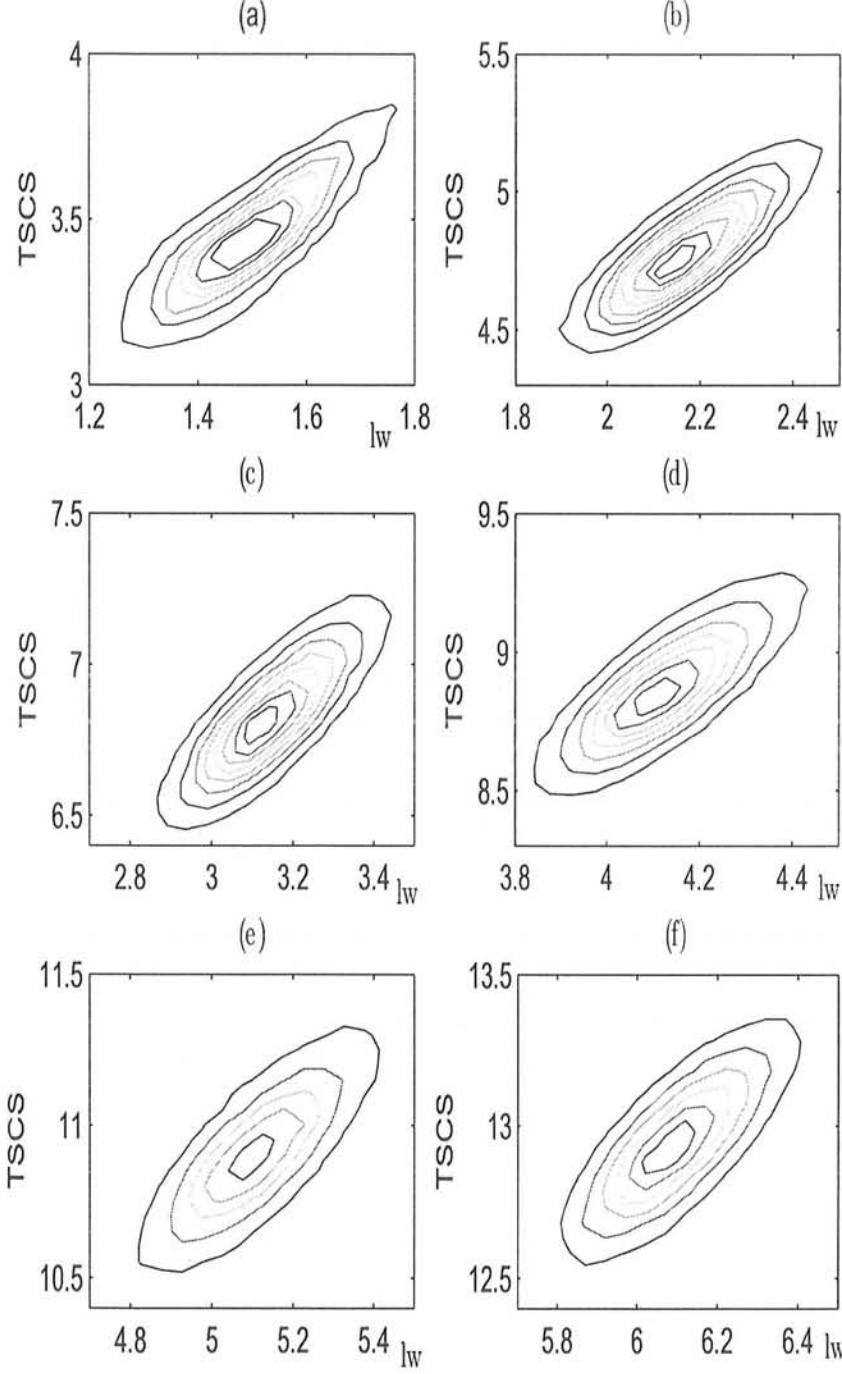


Figure 3.8: Contour plot of estimate of $f_{\sigma l}(\sigma_T^{\text{rc}}, \mathbf{l}_w)$. \mathbf{l}_w and σ_T^{rc} are represented along x and y -axis, respectively. $\sigma_p^2 =$ (a) 0.008333. (b,c,d,e,f) 0.01333 and $r_d =$ (b) 1.0λ . (c) 1.5λ . (d) 2.0λ . (e) 2.5λ . (f) 3.0λ .

how close these estimated joint pdfs are to a bivariate Gaussian distribution contour plots of bivariate Gaussian distribution are obtained. For comparison between the two distributions, the bivariate Gaussian must have same statistical parameters as that of the ensembles in Figure 3.8.

A bivariate Gaussian probability density function is mathematically given as[43]

$$f_{\sigma \mathbf{l}_w}(\sigma_T^{\text{rc}}, \mathbf{l}_w) = \frac{1}{2\pi\sigma_{rc}\sigma_{\mathbf{l}_w}\sqrt{1-\rho_{\sigma_T^{\text{rc}}\mathbf{l}_w}^2}} \exp \left[-\frac{1}{2(1-\rho_{\sigma_T^{\text{rc}}\mathbf{l}_w}^2)} \right. \quad (3.7.1)$$

$$\left. \left\{ \frac{(r-r_d)^2}{\sigma_{\mathbf{l}_w}^2} - \frac{2\rho_{\sigma_T^{\text{rc}}\mathbf{l}_w}(r-r_d)(\sigma_T^{\text{rc}} - E[\sigma_T^{\text{rc}}])}{\sigma_{\mathbf{l}_w}\sigma_{rc}} + \frac{(\sigma_T^{\text{rc}} - E[\sigma_T^{\text{rc}}])^2}{\sigma_{rc}^2} \right\} \right]$$

where $\sigma_{\mathbf{l}_w}^2$ and σ_{rc}^2 are variances of \mathbf{l}_w and σ_T^{rc} . The symbol $\rho_{\sigma_T^{\text{rc}}\mathbf{l}_w}$ in the above equation stands for the correlation coefficient between σ_T^{rc} and \mathbf{l}_w . Parameters required to evaluate above pdf, i.e., average values, variances and correlation coefficient of the two variables have been numerically estimated and are given in Table 3.4. The bivariate normal probability density is obtained with the help of a numerical routine named *BNRDF*. The routine *BNRDF* is given in standard IMSL library and it returns cumulative probability of bivariate normal random variables. The Fortran code evaluates bivariate probability density function, $f_{X,Y}(x,y)$, from its cumulative distribution, $F_{X,Y}(x,y)$, using the following relationship

$$f_{X,Y}(x,y) = \frac{\partial^2}{\partial x \partial y} F_{X,Y}(x,y)$$

$$= \frac{1}{\Delta x \Delta y} \{ F_{X,Y}(x + \Delta x, y + \Delta y) - F_{X,Y}(x + \Delta x, y) - F_{X,Y}(x, y + \Delta y) + F_{X,Y}(x, y) \} \quad (3.7.2)$$

where $\Delta x \Delta y$ is the area of small rectangular region in which the joint probability is determined. Since the resultant distribution has to be compared with the estimated distribution hence the area of the rectangular region is kept equal to the area used

while estimating the distribution from sample points. The output file of the code contains joint probability density of two random variables and coordinates of midpoint of the corresponding rectangular region.

Contour plots of bivariate Gaussian pdf for each ensemble of random cylinders are obtained from the output data file and are shown in Figure 3.9. The plots in Figure 3.9 show trends noticeably similar with corresponding plots in Figure 3.8. Although both the contour plots of an ensemble tend to agree visually but both of these are approximate plots, one is an estimate of pdf and other is obtained from estimated parameters. Since both the densities are approximate hence the difference between the two densities cannot be taken as error. As a figure of merit of comparison between the two densities the rms value of difference between the two densities is determined. The rms value of the difference per bin is observed to be of the order of 10^{-3} , for all the ensembles. These low values of rms difference per bin and graphical agreement of contour plots show that the joint pdf of σ_T^{rc} and \mathbf{l}_w , $f_{\sigma l}(\sigma_T^{\text{rc}}, \mathbf{l}_w)$, crudely resembles with a bivariate normal pdf. These plots are based on simulated data and there is no analytical or numerical insight to determine any constituent parameters of joint probability density of σ_T^{rc} and \mathbf{l}_w or to show that the two random variables are jointly Gaussian. Therefore, in absence of any other information, it is safe to assume that the joint pdf of σ_T^{rc} and \mathbf{l}_w is approximately a bivariate Gaussian distribution.

3.8 Summary

In this chapter, scattered field from random cylinders is obtained with the help of Method of Moment. Pulse and Dirac delta functions are used as basis and testing

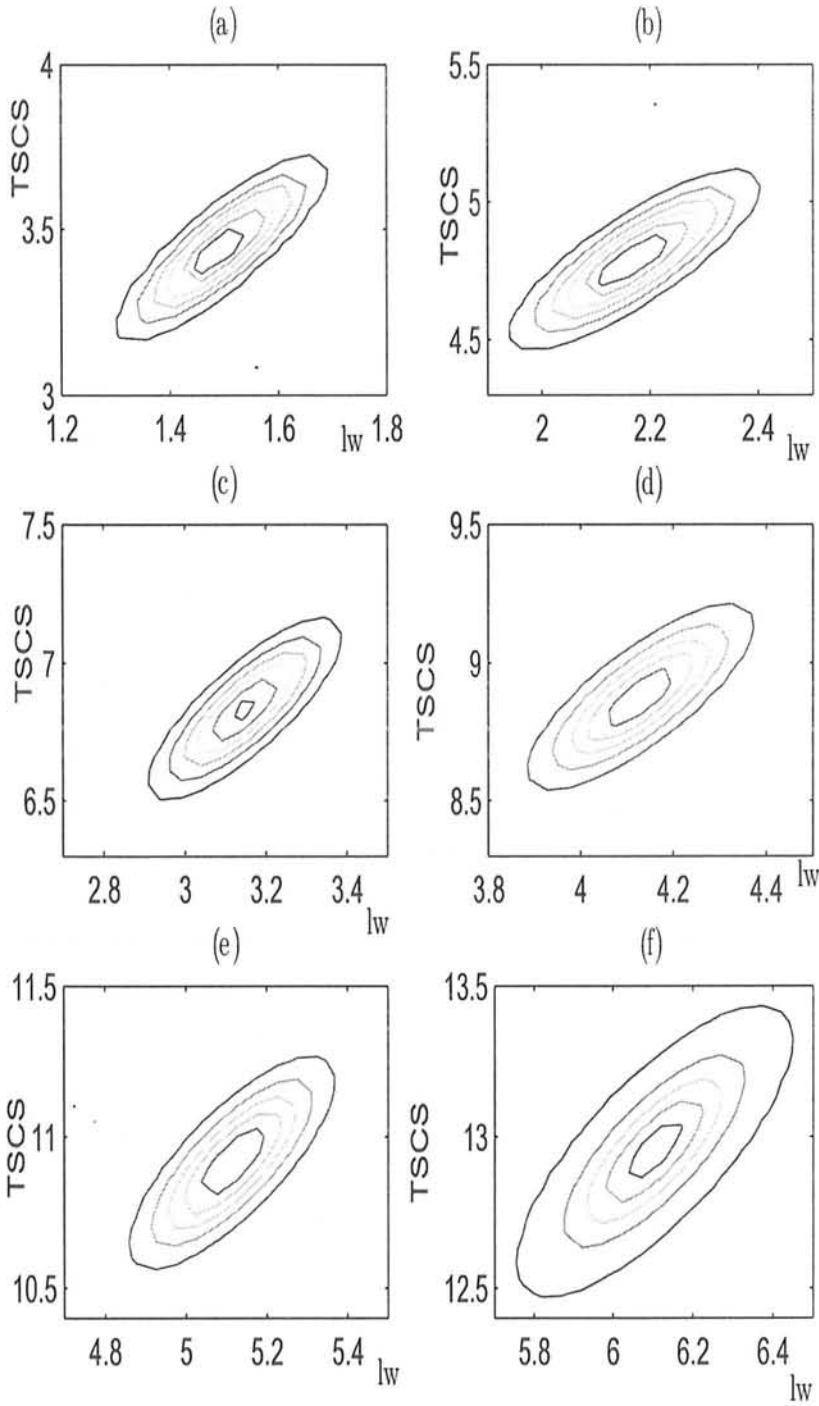


Figure 3.9: Contour plots of Bivariate Gaussian pdf for parameters; $\sigma_p^2 =$ (a) 0.008333. (b,c,d,e,f) 0.01333 and $r_d =$ (b) 1.0λ . (c) 1.5λ . (d) 2.0λ . (e) 2.5λ . (f) 3.0λ .

functions, respectively. Average of the numerically obtained scattered field is determined and is compared with the earlier reported works. Optical theorem is also used to verify the numerically obtained scattered field. Total scattering cross section is determined from the scattered field to apply the optical theorem. It has been shown that total scattering cross section satisfies the optical theorem with an average relative error of the order of 10^{-4} . It has been further found that total scattering cross section is more closely associated with lateral width of a random cylinder than its mean radius.

Average total scattering cross section of random cylinder is shown to be bounded between that of a circular cylinder and a strip. The lateral widths of these bounding structures are equal to average lateral width of random cylinders. Total scattering cross section of mean radius circular cylinder is also found to be always less than average total scattering cross section of random cylinder. Thus there are two possible lower bounds on the average total scattering cross section. Tightness of the lower bound depends upon variance of the ensemble. These bounds are in accordance with similar bounds obtained for conductance of arbitrarily shaped cylinders.

Radius of equivalent circular cylinder and width of equivalent strip are also determined in this chapter. The equivalence is determined on the basis of average total scattering cross section of random cylinder as invariant quantity. Radius of equivalent circular cylinder has been found to be closer to average lateral width than width of equivalent strip. It is observed that both the equivalent radius and half of average lateral width are also within same bounds. Their bounding values can be obtained from mean area and circumference due to rms differential length. With the help of these observations the average total scattering cross section of random cylinders can

be approximated without solving electromagnetic scattering problem. First obtain an approximate value of lateral width from its bounding values and then using average lateral width average total scattering cross section can be approximated from total scattering cross section of a strip and circular cylinder.

Finally, in this chapter, two dimensional scatter plots are obtained between total scattering cross section and lateral width of random cylinders. These plots show that both these quantities are highly correlated with each other and randomness of the ensemble has little effect on it. An estimate of joint probability density of the two variables is obtained. Mean, variance and covariance of the two random variables are also estimated from the simulated data for each ensemble. The estimated joint pdf is compared visually with bivariate Gaussian distribution. RMS value of the difference between two joint pdfs is also obtained. It is found that two joint pdfs agree closely with each but this comparison is not conclusive enough to conclude for sure that joint probability density of lateral width and total scattering cross section is Gaussian.

Chapter 4

Equivalent Elliptic Cylinder

A circular cylinder has been largely used to model non circular cylindrical structures [58, 41, 42, 59]. The circular cylinder is said to be an equivalent cylinder when a given property of the two cylinders is equal. Advantage of using circular cross section as equivalent cross section is that analytic expression for most of the scattering parameters of a circular cylinder are available in literature. Limitation of using circular equivalent cylinder is that it has only one parameter, i.e., its radius. This limitation becomes prominent when total scattering cross section of non circular cylinder is taken as invariant parameter to determine a circular equivalent. This is because total scattering cross section of a scatterer is closely related to its lateral width.

Total scattering cross section of a circular cylinder has one to one relationship with its radius, section 3.4, such that given a value of either of these parameters fix the value of other one. On the other hand, the total scattering cross section and lateral width of random cylinder are jointly distributed for random cylinder and each of these variables has a marginal distribution. Therefore, if total scattering cross section is considered as the invariant parameter, an equivalent structure with at least two parameters is considered as a better candidate for an equivalent structure of

random cylinders.

An elliptic cylinder is a close two dimensional convex structure with variable curvature. An elliptical cylinder is smooth and has two parameters, i.e., major and minor axes. Major and minor axes of an ellipse are maximum and minimum lengths of an ellipse, respectively. It has been observed in previous chapter that an equivalent convex cross section for average cross section of random cylinders should be flatter than a circle and thicker than a strip. The observation that for a given lateral width, the average total scattering cross section of random cylinder is less than that of a circular cylinder and greater than that of a flat strip also motivates one to use an elliptic equivalent model instead of circular equivalent. Can an elliptical cylinder be considered as a better equivalent model than a circular cylinder, when total scattering cross section is the invariant parameter?

Before answering the above question, the demerits of using an elliptical equivalent for random cylinders are discussed. One disadvantage of using elliptical equivalent model can be that two parameters of random cylinder, i.e., average lateral width and average total scattering cross section are needed to determine it while only average total scattering cross section is needed to determine an equivalent circular cylinder. Lateral width is a purely geometrical quantity and can be easily determined once the scatterer and direction of incidence is known. As far as random cylinders are concerned, average lateral width can be approximated from its input parameters, as discussed in previous chapter. Another counter argument that can be raised against using elliptic equivalent model is that two lengths are needed to be determined whereas for circular equivalent cylinder only its radius is needed. One of the two lengths needed to define an equivalent elliptic cross section will be kept equal to

average lateral width of the ensemble. Hence only one length needs to be determined to completely define an equivalent elliptic cylinder.

In this chapter an attempt has been made to model the average cross section of random cylinder by an equivalent cylinder of elliptical cross section. The equivalence between the two cylinders is determined on the basis of total scattering cross section. Length of one of the two axes of equivalent elliptical cylinder is taken equal to the average lateral width of random cylinders and length of other axis is determined such that total scattering cross section of equivalent cylinder is equal to average total scattering cross section of random cylinders. Total scattering cross section of an elliptical cylinder is obtained first. With the help of total scattering cross section an equivalent elliptic cylinder is determined. Finally an approximation is developed to determine the equivalent elliptical cylinder directly from the geometrical parameters of the random cylinder.

4.1 Total Scattering Cross Section

Since the scattering properties of the elliptical cylinder have to be compared with those of random cylinders hence it is assumed that the elliptical cylinder is placed in conditions similar to random cylinder, i.e., a PEC elliptical cylinder placed in free space with origin at its center and z -axis as cylindrical axis. It is also assumed that major axis of elliptical cylinder is along $y = 0$ line. A plane wave travelling along positive y -axis having \mathbf{E} field vector along z -axis is made incident on the elliptic cylinder such that major axis of elliptical cylinder is orthogonal to direction of incidence. The incident wave can be written as $E_z^{\text{inc}} = \exp\{-i(ky)\}$, where k is the wave number of the incident wave. Let E_z^{sc} be the scattered field and σ_T^{ec} be the total

scattering cross section of elliptical cylinder.

An elliptic cylinder if represented in elliptic cylindrical coordinates (u, v, z) helps to solve the boundary value problem for two dimensional wave equation by separation of variables. An analytical solution of total scattering cross section of an elliptical cylinder is given in terms of Mathieu functions by Bowman [1]. Arguments of these functions are in terms of elliptical cylindrical coordinates (u, v) . The analytic solution for total scattering cross section is given in the form of an infinite series. A numerical solution to obtain total scattering cross section of an elliptical cylinder using MM is also obtained. The results obtained by MM are compared with the previously documented analytical results [1]. Optical theorem is used to further verify the numerical solution. Analytical expression for total scattering cross section is given first.

4.1.1 Analytical Solution

An elliptical cylinder can be represented in elliptical cylindrical coordinates (u, v, z) . The range of values these coordinates can take are $0 \leq u < \infty$, $0 \leq v < 2\pi$ and $-\infty < z < \infty$. Coordinates (u, v) are closely related with coordinates (ρ, ϕ) of circular cylindrical coordinate system and z coordinate in both these systems is identical. Similar to circular cylindrical coordinates, in which surface $\rho = \text{constant}$ represents a hollow circular cylinder, constant value of u represents an elliptical cylinder in elliptic cylindrical coordinates.

Let $u = u_1$ defines an elliptical cylinder, which scatters the incident wave. Its interfocal distance is d with its major and minor axes given as $d \cosh u_1$ and $d \sinh u_1$, respectively, as shown in Figure 4.1. The analytic solution of total scattering cross section of PEC elliptical cylinder, under the condition mentioned above, is given by

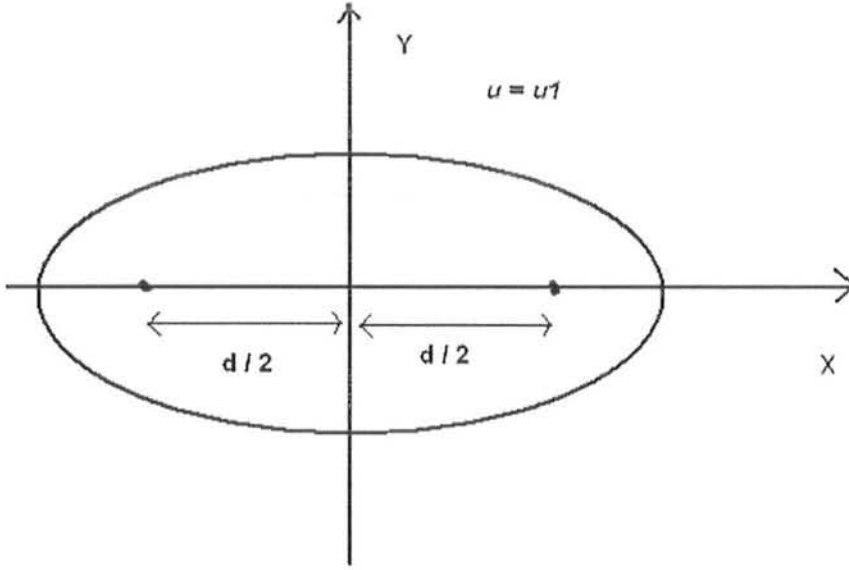


Figure 4.1: Elliptic cylindrical geometry.

Bowman [1], as

$$\sigma_T^{ec} = \frac{8\pi}{k} \sum_{m=0}^{\infty} \left[\frac{1}{N_{2m}^{(e)}} \left| \frac{Re_{2m}^{(1)}(kd/2, \cosh u_1)}{Re_{2m}^{(3)}(kd/2, \cosh u_1)} Se_{2m}(kd/2, 0) \right|^2 + \frac{1}{N_{2m+1}^{(o)}} \left| \frac{Ro_{2m+1}^{(1)}(kd/2, \cosh u_1)}{Ro_{2m+1}^{(3)}(kd/2, \cosh u_1)} So_{2m+1}(kd/2, 0) \right|^2 \right] \quad (4.1.1)$$

where $R(e, o)_m^{(j)}$ are even and odd radical Mathieu functions of j^{th} kind, symbols $S(e, o)_m$ are the corresponding even and odd angular functions and $m \geq 0$ is an integer. The definition and notation used for Mathieu function are same as given by Stratton [61]. The quantities $N_m^{(e), (o)}$ are given as [61]

$$N_m^{(e), (o)} = \int_0^{2\pi} [S(e, o)_m(kd/2, \cos v)]^2 dv \quad (4.1.2)$$

These are the normalization coefficients of Mathieu function.

Little is available in the literature about the rate of convergence of series representing exact solution for the total scattering cross section but it is likely that the

series converges at least as rapidly as the corresponding eigenfunction series for circular cylinder of diameter equal to major axis of ellipse, i.e., $d \cosh u_1$ [1]. Therefore, number of terms for the solution of total scattering cross section of elliptic cylinder, m , should be either equal to or greater than $3kd \cosh u_1$. Once the value of m is chosen total scattering cross section of elliptical cylinder can be determined. A numerical approach to determine total scattering cross section of an elliptical cylinder is given in the next section.

4.1.2 Numerical Solution

A numerical solution to determine total scattering cross section of an ellipse with the help of MM is given in this section. It is convenient to use cartesian coordinates for the usage of MM. Standard form of equation for an ellipse in cartesian coordinates is given as

$$\frac{x^2}{a^2} + \frac{y^2}{b^2} = 1 \quad (4.1.3)$$

where $\pm a$ and $\pm b$ are x and y intercepts, respectively. Let the length of major axis be denoted by L_M and l_m denotes the length of minor axis of the elliptical cross section. In the given configuration major axis is assumed to be along x -axis and it is equal to the distance between x -intercepts, i.e., $L_M = 2a$. Minor axis is therefore along y -axis and is equal to the distance between y -intercepts, i.e., $l_m = 2b$.

Transformation from elliptical cylindrical coordinates to cartesian coordinates for an elliptic cylinder with major axis along x -axis is given as

$$x = \frac{d}{2} \cosh u \cos v \quad (4.1.4)$$

$$y = \frac{d}{2} \sinh u \sin v \quad (4.1.5)$$

One advantage of representing an ellipse in cartesian coordinates is that the length of minor axis can be increased beyond major axis without changing any of the formulation whereas in elliptical coordinates the whole ellipse has to be rotated by $\pi/2$ to achieve such configuration. Another advantage of representing an elliptical cylinder in cartesian coordinates is that the length of any of its axes can be changed without affecting the other.

Moments Method formulation has been thoroughly explained in previous chapter. Basis and weighting functions needed to apply MM are also chosen to be same as used for random cylinders, given in section 3.1. The Green's function needed to determine induced currents and scattered field, for two dimensional scatterer, is a Hankel function. Argument of Hankel function is distance between two sample points. Since delta functions are used as testing and weighting functions therefore the argument of Hankel function is distance between center of two segments. This distance is obtained by using the distance formula in cartesian coordinates. Length of each elliptic segment is also required by MM. It is obtained with the help of cosine formula, equation (3.1.16). The cosine formula needs length of two position vectors pointing at end points of the segments. Length of any position vector \mathbf{r}_p pointing to any point on the elliptic cross section is given as

$$r_p = \frac{ab}{\sqrt{a^2 \sin^2 \theta_p + b^2 \cos^2 \theta_p}} \quad (4.1.6)$$

where θ_p is the angle that position vector \mathbf{r}_p makes with positive x -axis.

Total number of segments, M , in which an ellipse has to be divided to apply MM, is another input parameter required for code. It is difficult to divide an elliptic cross section into segments of equal length as its curvature is not constant. Therefore, segments are obtained by dividing the central angle equally into total number of

segments, such that central angle of each segment is same, i.e., $\Delta\theta = 2\pi/M$. Number of segments per unit wavelength, n_λ is used as input to the code. Total number of segments from given segment density is determined by considering a circular cylinder of radius equal to major axis and is given as $M = 2\pi L_M n_\lambda$. Length of largest segment of elliptic cross section, according to this formulation for M , will be equal to $1/n_\lambda$. An analysis of error introduced by MM for circular cylinder shows that error is proportional to the segment length [55]. Generalizing the same error analysis for an elliptic cylinder it can be deduced that maximum error introduced in the scattered field by MM will be proportional to segment of length $1/n_\lambda$.

Keeping all the other parameters same as those given in section 3.1 the scattered field for an elliptical cylinder placed in free space can be obtained. MM code is verified for equal values of both the axes such that the resultant cylindrical structure is a circular cylinder. Induced surface currents and scattered field in each direction are compared with those of a circular cylinder. The scattered field from an elliptic cylinder obtained by MM is also verified using optical theorem test. The results are considered reliable after qualifying the two tests. Total scattering cross section of elliptical cylinder is a by product of optical theorem test.

4.2 Equivalent Elliptical Cylinder

It has been inferred that the cross sectional shape of equivalent cylinder has to be flatter than a circle, section 3.6. Therefore, in this section, a cylinder with elliptical cross section is considered as an equivalent model. An equivalent elliptical cylinder will be one whose lateral width and total scattering cross section are equal to average lateral width and average total scattering cross section of random cylinders. Since

the cross sectional shape has to be flatter than a circle hence major axis of elliptical cylinder is considered lying in a plane normal to the incident plane wave. In this configuration the length of major axis, L_M , is the lateral width of elliptical cylinder. To be an equivalent cylinder the value of L_M has to be equal to average lateral width, $E[l_w]$, of an ensemble of random cylinders.

Length of minor axis is determined such that total scattering cross section of elliptical cylinder, σ_T^{ec} , is equal to average total scattering cross section of random cylinders, $E[\sigma_T^{rc}]$. In this thesis numerical iterative method is used to determine the length of minor axis, l_m . In this method σ_T^{ec} is determined for different elliptical cylinders with $L_M = E[l_w]$ and different values of l_m . The initial value of l_m is taken equal to L_M and it is subsequently decreased by a given decrement size until σ_T^{ec} of the resulting elliptic cylinder is approximately equal to $E[\sigma_T^{rc}]$. Decrement size used for l_m in this thesis is 10^{-4} . The difference in total scattering cross sections of equivalent elliptic cylinder and average random cylinder with above mentioned decrement size is observed to be of the order of 10^{-3} .

Values of minor axis of equivalent elliptic cylinder l_m are obtained for different ensembles of random cylinders and are tabulated in Table 4.1. The Table 4.1 shows input parameters of different ensembles together with average values of lateral width and total scattering cross section of the ensemble. The table also shows length of minor axis and total scattering cross section of the equivalent elliptic cylinder. It can be observed from these values that length of minor axis varies with variation in the value of variance σ_p^2 and number of terms N . From the table it can also be noticed that the flatness of equivalent elliptic cylinder decreases when values of σ_p^2 or N increases. This observation is consistent with earlier observations that the flatness

r_d	N	σ_p^2	$L_M = E[\mathbf{l}_w]$	l_m	$E[\sigma_T^{rc}]$	σ_T^{ec}
0.7	5	0.00833	1.49551	1.22360	3.44419	3.44418
0.7	6	0.36000	2.09577	1.11440	4.55788	4.55791
1.0	5	0.00833	2.07797	1.79180	4.68476	4.68477
1.0	6	0.01000	2.10970	1.67360	4.71861	4.71859
1.0	7	0.01167	2.14247	1.56040	4.75541	4.75542
1.0	8	0.01333	2.17148	1.47140	4.79035	4.79035
1.0	9	0.01500	2.20109	1.39160	4.82847	4.82846
1.0	15	0.01502	2.27142	1.12922	4.89915	4.89916
1.0	10	0.01667	2.23196	1.30876	4.86689	4.86694
1.0	11	0.01833	2.26122	1.21877	4.90157	4.90158
1.0	5	0.01875	2.14698	1.65117	4.78823	4.79166
1.0	12	0.02000	2.29060	1.15237	4.94203	4.94204
1.0	13	0.02167	2.31514	1.10638	4.97809	4.97809
1.0	15	0.02500	2.36976	1.01338	5.06071	5.06072
1.0	7	0.02625	2.24824	1.41098	4.92245	4.92245
1.0	5	0.03333	2.22554	1.59638	4.92133	4.92136
1.0	9	0.03375	2.34298	1.22518	5.06115	5.06116
1.0	11	0.04125	2.43254	1.07359	5.19802	5.19803
1.0	7	0.04667	2.36440	1.33399	5.12833	5.12834
1.0	13	0.04875	2.51626	0.96379	5.33343	5.33343
1.0	9	0.06000	2.49142	1.15579	5.33222	5.33225
1.0	5	0.07500	2.39604	1.53699	5.23546	5.23547
1.0	14	0.09333	2.77262	0.86659	5.81035	5.81038
1.0	15	0.10000	2.82642	0.82279	5.90492	5.90492
1.0	7	0.10500	2.59762	1.30240	5.57265	5.57266
1.0	11	0.16500	2.94256	1.00940	6.17803	6.17805
1.0	13	0.19500	3.08572	0.91920	6.43767	6.43771
1.0	5	0.20833	2.69384	1.53764	5.81659	5.89106
1.0	15	0.22500	3.21522	0.84864	6.67571	6.67572
1.0	9	0.24000	3.00952	1.16364	6.34427	6.34432
1.0	11	0.29333	3.18300	1.04184	6.65712	6.65713
1.0	15	0.40000	3.45712	0.88244	7.16017	7.16021
1.0	11	0.45833	3.31518	1.06884	6.92455	6.97182
1.0	15	0.62500	3.56874	0.91384	7.38730	7.38733
1.0	6	0.25000	2.83801	1.37140	6.05676	6.05676
1.5	8	0.01333	3.14802	2.28840	6.83428	6.83427
1.5	10	0.01667	3.20482	2.03900	6.90102	6.90103
1.5	6	0.04000	3.25467	2.25500	7.03502	7.03502
2.0	8	0.01333	4.12841	3.18280	8.87549	8.87548
2.5	8	0.01333	5.11351	4.13040	10.91587	10.91587

Table 4.1: Major and Minor axis of an equivalent elliptic cylinder having $\sigma_T^{ec} \approx E[\sigma_T^{rc}]$.

of equivalent convex cross section should decrease with increase in randomness.

Eccentricity of an ellipse is a parameter used to determine the flatness of an ellipse. It is represented by β and is given as

$$\beta = \frac{\sqrt{L_M^2 - l_m^2}}{L_M} \quad (4.2.1)$$

Its value varies between 0 and 1, with $\beta = 0$ representing a circle and $\beta = 1$ a strip. Eccentricity of equivalent elliptic cylinder is obtained using the values given in Table 4.1. Eccentricity of equivalent cylinder will provide a measure of its flatness. The eccentricity of equivalent elliptic cylinder together with the input parameters of the ensembles are tabulated in Table 4.2. Eccentricity of equivalent elliptic cylinder is compared with another of its parameter which provides a measure of deformation in shape from circular, i.e., equivalent radii ratio.

Equivalent radii ratio(EQRR) of random cylinders is compared with EQRR as well as eccentricity of equivalent elliptic cylinder to investigate whether any of the two parameters of equivalent elliptic cylinder are related to EQRR of random cylinders. Equivalent area and equivalent circumference radii both are needed to determine EQRR of an elliptical cylinder. The equivalent area radius, r_{ea}^e , of an ellipse is radius of a circle which has same area as that of an ellipse and is given as

$$r_{ea}^e = \frac{1}{2} \sqrt{L_M l_m} \quad (4.2.2)$$

where the area of an ellipse is $\pi L_M l_m / 4$. Similarly equivalent circumferential radius, r_{ec}^e , is radius of a circle whose circumference is equal to perimeter of an ellipse. The perimeter of an ellipse can be written as [62]

$$P_{\text{ell}} = 2L_M \int_0^{\pi/2} \left[1 - \frac{L_M^2 - l_m^2}{L_M^2} \cos^2 \theta \right]^{1/2} d\theta \quad (4.2.3)$$

The integral in above expression is complete elliptic integral and has been tabulated in reference books. Therefore, perimeter of the equivalent ellipse can be readily determined. Equivalent circumferential radius can thus be written as

$$r_{ec}^e = \frac{P_{\text{ell}}}{2\pi} \quad (4.2.4)$$

Columns labelled EQRR(Ell) and EQRR(RC) in the Table 4.2 show the values of equivalent radii ratio of equivalent elliptic cylinder and that of random cylinder, respectively. Equivalent radii ratio of random cylinder is given by equation (2.2.12).

It can be readily noticed from the Table 4.2, that equivalent radii ratio of equivalent elliptic cylinder increases with increase in its eccentricity. Equivalent radii ratio of random cylinder also increases with increase in eccentricity but it is difficult to relate the increase in its value with that of equivalent elliptic cylinder. Values of EQRR(RC) are very large when variance σ_p^2 of the ensemble is large. Comparison of the two equivalent radii ratios shows that the value of EQRR(RC) is always greater than EQRR(Ell). It is because of the fact that an elliptical cylinder has convex curvature whereas cross sectional shape of random cylinder does have non convex curvature. Hence perimeter of equivalent elliptical cylinder is less than that of a random cylinder and so is the equivalent radii ratio. Comparison of the two equivalent radii ratios is therefore of little help and no correspondence between the two could be established.

The values of L_M and l_m , in the Table 4.1, are thoroughly analyzed to determine any relation between the two or with any other parameter of the ensemble. Since relevant data of large number of ensemble with mean radius equal to 1λ is given, Table 4.1, hence to probe the effect of randomness, i.e., σ_p^2 and N on the values of L_M and l_m , the data of ensembles with mean radius 1λ is closely examined. It is

r_d	N	σ_p^2	$L_M = E[l_w]$	l_m	Eccen(β)	EQRR(Ell)	EQRR(RC)
1.0	5	0.00833	2.07797	1.79180	0.50643	1.00412	1.04445
0.7	5	0.00833	1.49551	1.22360	0.57496	1.00755	1.08806
2.5	8	0.01333	5.11351	4.13040	0.58954	1.00855	1.02678
1.0	6	0.01000	2.10970	1.67360	0.60885	1.01006	1.07246
2.0	8	0.01333	4.12841	3.18280	0.63689	1.01269	1.04149
1.0	5	0.01875	2.14698	1.65117	0.63917	1.01293	1.09656
1.0	7	0.01167	2.14247	1.56040	0.68524	1.01885	1.10937
1.5	8	0.01333	3.14802	2.28840	0.68671	1.01908	1.07247
1.0	5	0.03333	2.22554	1.59638	0.69676	1.02071	1.16396
1.5	6	0.04000	3.25467	2.25500	0.72108	1.02526	1.12469
1.0	8	0.01333	2.17148	1.47140	0.73543	1.02842	1.15561
1.0	5	0.07500	2.39604	1.53699	0.76715	1.03700	1.32945
1.5	10	0.01667	3.20482	2.03900	0.77150	1.03838	1.13276
1.0	9	0.01500	2.20109	1.39160	0.77478	1.03946	1.21160
1.0	7	0.02625	2.24824	1.41098	0.77854	1.04074	1.22946
1.0	10	0.01667	2.23196	1.30876	0.81004	1.05351	1.27721
1.0	5	0.20833	2.69384	1.53764	0.82109	1.05905	1.70192
1.0	7	0.04667	2.36440	1.33399	0.82564	1.06153	1.37542
1.0	11	0.01833	2.26122	1.21877	0.84231	1.07178	1.35204
0.7	6	0.36000	2.09577	1.11440	0.84691	1.07497	2.72462
1.0	9	0.03375	2.34298	1.22518	0.85238	1.07900	1.42613
1.0	12	0.02000	2.29060	1.15237	0.86424	1.08873	1.43600
1.0	7	0.10500	2.59762	1.30240	0.86523	1.08961	1.70307
1.0	15	0.01502	2.27142	1.12922	0.86767	1.09184	1.49107
1.0	6	0.25000	2.83801	1.37140	0.87550	1.09948	2.00832
1.0	13	0.02167	2.31514	1.10638	0.87842	1.10255	1.52848
1.0	9	0.06000	2.49142	1.15579	0.88588	1.11099	1.67106
1.0	11	0.04125	2.43254	1.07359	0.89734	1.12594	1.67998
1.0	15	0.02500	2.36976	1.01338	0.90395	1.13590	1.73674
1.0	9	0.24000	3.00952	1.16364	0.92223	1.17025	2.67002
1.0	13	0.04875	2.51626	0.96379	0.92374	1.17366	1.98204
1.0	11	0.16500	2.94256	1.00940	0.93932	1.21621	2.74135
1.0	11	0.29333	3.18300	1.04184	0.94492	1.23577	3.38126
1.0	11	0.45833	3.31518	1.06884	0.94660	1.24226	3.93155
1.0	14	0.09333	2.77262	0.86659	0.94990	1.25587	2.68120
1.0	13	0.19500	3.08572	0.91920	0.95460	1.27771	3.35862
1.0	15	0.10000	2.82642	0.82279	0.95669	1.28850	2.91807
1.0	15	0.22500	3.21522	0.84864	0.96454	1.33683	4.02289
1.0	15	0.62500	3.56874	0.91384	0.96666	1.35257	5.72668
1.0	15	0.40000	3.45712	0.88244	0.96687	1.35424	4.96176

Table 4.2: Table showing eccentricity and equivalent radii ratio of an equivalent elliptic cylinder with equivalent radii ratio of random cylinders.

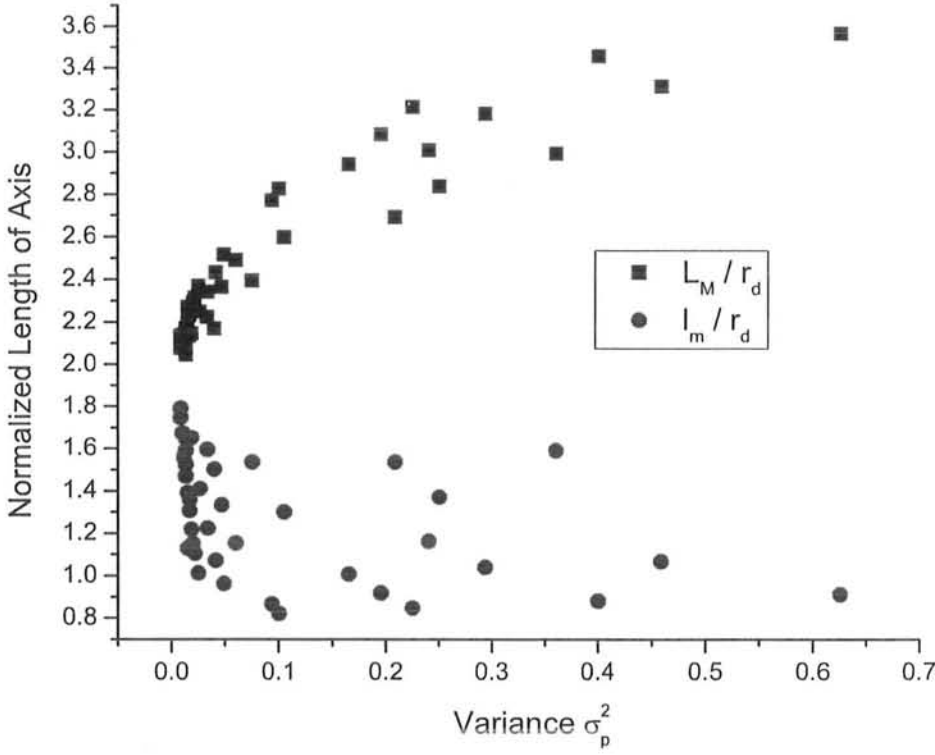


Figure 4.2: Scatter plot of major axis, L_M and minor axis l_m of equivalent elliptical cylinder versus the variance σ_p^2 of random cylinders. ■ Major axis. • Minor axis.

separated and is sorted in ascending order of variance σ_p^2 . With few anomalies, it is observed that as variance increases length of major axis increases and length of minor axis decreases. A scatter plot of L_M and l_m versus the variance σ_p^2 is drawn to highlight this observation and is given in Figure 4.2. Another observation that can be made from this data is that when the value of L_M increases corresponding value of l_m decreases. Is there any relation between the two?

Considering that the value of l_m decreases with increase in value of L_M , proportionality between the two is probed and product of the two lengths is taken. The

r_d	N	σ_p^2	$L_M = E[\mathbf{l}_w]$	l_m	$L_M l_m$	$L_M l_m / \pi$	r_{es}	$r_d - r_{es}$
0.7	5	0.00833	1.49551	1.22360	1.82991	0.58248	0.76320	-0.0632
0.7	6	0.36000	2.09577	1.11440	2.33553	0.74342	0.86222	-0.16222
1.0	5	0.00833	2.07797	1.79180	3.72331	1.18517	1.08865	-0.08865
1.0	6	0.01000	2.10970	1.67360	3.53079	1.12389	1.06014	-0.06014
1.0	7	0.01167	2.14247	1.56040	3.34311	1.06415	1.03157	-0.03157
1.0	8	0.01333	2.17148	1.47140	3.19512	1.01704	1.00848	-0.00848
1.0	9	0.01500	2.20109	1.39160	3.06304	0.97499	0.98742	0.01258
1.0	15	0.01502	2.27142	1.12922	2.56493	0.81644	0.90357	0.09643
1.0	10	0.01667	2.23196	1.30876	2.92110	0.92981	0.96427	0.03573
1.0	11	0.01833	2.26122	1.21877	2.75591	0.87723	0.93661	0.06339
1.0	5	0.01875	2.14698	1.65117	3.54503	1.12842	1.06227	-0.06227
1.0	12	0.02000	2.29060	1.15237	2.63962	0.84022	0.91663	0.08337
1.0	13	0.02167	2.31514	1.10638	2.56142	0.81533	0.90295	0.09705
1.0	15	0.02500	2.36976	1.01338	2.40147	0.76441	0.87431	0.12569
1.0	7	0.02625	2.24824	1.41098	3.17222	1.00975	1.00486	-0.00486
1.0	5	0.03333	2.22554	1.59638	3.55281	1.13089	1.06343	-0.06343
1.0	9	0.03375	2.34298	1.22518	2.87057	0.91373	0.95589	0.04411
1.0	11	0.04125	2.43254	1.07359	2.61155	0.83128	0.91175	0.08825
1.0	7	0.04667	2.36440	1.33399	3.15409	1.00398	1.00199	-0.00199
1.0	13	0.04875	2.51626	0.96379	2.42515	0.77195	0.87861	0.12139
1.0	9	0.06000	2.49142	1.15579	2.87956	0.91659	0.95739	0.04261
1.0	5	0.07500	2.39604	1.53699	3.68269	1.17224	1.08270	-0.0827
1.0	14	0.09333	2.77262	0.86659	2.40272	0.76481	0.87453	0.12547
1.0	15	0.10000	2.82642	0.82279	2.32555	0.74025	0.86038	0.13962
1.0	7	0.10500	2.59762	1.30240	3.38314	1.07689	1.03773	-0.03773
1.0	11	0.16500	2.94256	1.00940	2.97022	0.94545	0.97234	0.02766
1.0	13	0.19500	3.08572	0.91920	2.83639	0.90285	0.95019	0.04981
1.0	5	0.20833	2.69384	1.53764	4.14216	1.31849	1.14825	-0.14825
1.0	15	0.22500	3.21522	0.84864	2.72856	0.86853	0.93195	0.06805
1.0	9	0.24000	3.00952	1.16364	3.50200	1.11472	1.05580	-0.0558
1.0	6	0.25000	2.83801	1.37140	3.89205	1.23888	1.11305	-0.11305
1.0	11	0.29333	3.18300	1.04184	3.31618	1.05557	1.02741	-0.02741
1.0	15	0.40000	3.45712	0.88244	3.05070	0.97107	0.98543	0.01457
1.0	11	0.45833	3.31518	1.06884	3.54340	1.12790	1.06203	-0.06203
1.0	15	0.62500	3.56874	0.91384	3.26126	1.03809	1.01887	-0.01887
1.5	8	0.01333	3.14802	2.28840	7.20393	2.29308	1.51429	-0.01429
1.5	10	0.01667	3.20482	2.03900	6.53463	2.08004	1.44223	0.05777
1.5	6	0.04000	3.25467	2.25500	7.33928	2.33617	1.52845	-0.02845
2.0	8	0.01333	4.12841	3.18280	13.1399	4.18256	2.04513	-0.04513
2.5	8	0.01333	5.11351	4.13040	21.1208	6.72297	2.59287	-0.09287

Table 4.3: Estimate of mean radius r_d from L_M and l_m axis of equivalent ellipse.

product of L_M and l_m is tabulated in column labelled $L_M l_m$ of Table 4.3. Statistics of the values in this column show that their mean value is 3.08933 and standard deviation is 0.47268. This shows that the mean value of the product $L_M l_m$ is around 3 and it does not vary much with variance σ_p^2 . Are the two axes of equivalent elliptical cylinder proportional? To probe further the product of lengths L_M and l_m of equivalent elliptic cylinders of other ensembles is obtained. These values cluster around 3, 7, 13 and 21 for ensembles of mean radius 1λ , 1.5λ , 2λ and 2.5λ , respectively, as shown in the Table 4.3. This observation suggests that the product $L_M l_m$ can be considered constant for a given mean radius irrespective of the variance σ_p^2 .

How does the proportionality constant relate to mean radius of an ensemble? It is the product of two lengths, L_M and l_m , which appears to be constant for a given mean radius. Units of the product will be of area. The product is therefore compared with cross sectional area of mean radius circular cylinder. The values of the product, $L_M l_m$, of ensembles with mean radius 1λ is near π . The product is normalized by dividing it with π . The resultant values are shown in column labelled $L_M l_m / \pi$ of Table 4.3. These values are nearly equal to one for ensembles of mean radius 1λ . Whereas for other ensembles it appears that no linear relation exists between the normalized product and mean radius. Does any non linear relation exist between these two quantities? A nonlinear operation, i.e., square root is applied on the normalized product. The resultant values are found to be very close to mean radius of respective ensembles. These values are tabulated in column labelled r_{es} of Table 4.3. To show how close these values are to mean radius, difference of the two quantities, i.e., $r_d - r_{es}$ is analyzed. Mean value of the difference comes out to be 0.0005038 and its standard deviation is 0.07736. Maximum and minimum values of

the difference are 0.13962 and -0.16222, respectively. These statistics show that r_{es} is in good approximation of r_d .

The above operations and the resulting conclusion can be summarized as

$$r_{es} = \sqrt{\frac{L_M l_m}{\pi}} \approx r_d \quad (4.2.5)$$

Rearranging the above relation, it can be written as

$$L_M l_m = \pi r_{es}^2 \approx \pi r_d^2 \quad (4.2.6)$$

The above expression shows that the area of mean radius circular cylinder is approximately equal to the product $L_M l_m$. The product $L_M l_m$ can be considered as cross sectional area of a rectangular cylinder, having lengths equal to L_M and l_m , such that it encloses the equivalent elliptical cylinder. This area will be referred to as effective area in this thesis. It cannot be concluded from this expression that a rectangular shape is a better equivalent shape for random cylinders. This expression does not hint anything about the average cross sectional shape of random cylinders.

The above expression is summarized by concluding that the area of mean radius circular cylinder, if expanded into a rectangular region with one of its lengths equal to average lateral width of the ensemble, then the average total scattering cross section of ensemble should be equal to total scattering cross section of an ellipse whose axes are equal to lengths of the rectangular region. If the input statistics of an ensemble are known then area of mean radius circular cylinder and average value of lateral width can be determined. Knowing these two quantities l_m can be determined using above expression. An equivalent elliptical cylinder can be generated and total scattering cross section of equivalent ellipse can thus be obtained. This total scattering cross section will be approximately equal to the average total scattering cross section of an

ensemble of random cylinders. This expression does not hold for a circular cylinder, i.e., it becomes invalid if there is no randomness. This is because in the absence of any randomness on circular cylinder one can't have an equivalent ellipse and it will be meaningless to say that the area of mean radius circular cylinder is elongated into an ellipse. The effectiveness of this conclusion is tested in the next section.

4.3 Prediction of Total Scattering Cross Section.

The hypothesis developed in the previous section, to approximate the minor axis of an equivalent elliptical cylinder is tested in this section. This hypothesis has been developed using the ensemble averaged values of radius and lateral width of random cylinders. In this section, it is of interest to test the hypothesis for an individual random cylinder. According to the hypothesis, minor axis of equivalent elliptical cylinder can be predicted with the help of mean radius and lateral width of the random cylinder. Few random cylinders are generated with different input statistics. Mean radius and lateral width of each random cylinder is recorded. Total scattering cross section of each random cylinder is also determined and recorded. Minor axis of the equivalent elliptical cylinders are approximated with the help of equivalent area and lateral width of respective random cylinder. Total scattering cross section of approximated equivalent elliptical cylinder is determined. A comparison between the total scattering cross section of random cylinder and that of its approximated equivalent elliptical cylinder is made as a test of hypothesis.

Random cylinders are generated with different input statistics. The mean radius of these representative random cylinders varies from 0.7λ to 2.5λ . A set of five random

cylinders is generated for each set of input statistics. Lateral width and total scattering cross section are determined numerically and are tabulated. Equivalent area is determined using mean radius and it is used to obtain dimensions of an elliptical cylinder for each random cylinder. Keeping major axis of the elliptical cylinder equal to lateral width of random cylinder, length of minor axis of the elliptical cylinder is approximated with the help of equivalent area hypothesis given by expression (4.2.6). Total scattering cross section of the resultant elliptical cylinder is obtained numerically and is denoted by σ_T^{ecp} . Table 4.4 and Table 4.5 show the predicted values of total scattering cross section, σ_T^{ecp} , along with the input parameters as well as lateral width and total scattering cross section of few representative random cylinders. The length of minor axis of the elliptical cylinder and percentage of relative error between total scattering cross sections of random cylinder and corresponding approximate equivalent elliptical cylinder, $|\sigma_T^{rc} - \sigma_T^{ecp}| \times 100 / \sigma_T^{rc}$, is also shown in these tables.

Table 4.4 shows the relevant data of few samples of random cylinders whose variance is same and their mean radius varies between 0.7λ to 2.5λ . Columns labelled $L_M = l_w$ and σ_T^{rc} have values of lateral width and total scattering cross section of sample random cylinders. The minor axis of elliptical cylinder obtained using expression (4.2.6) is shown in column labelled l_m of the table. The total scattering cross section of the approximated equivalent elliptical cylinder is given in column labelled σ_T^{ecp} . This is the predicted value of total scattering cross section of the random cylinder. Percentage of absolute relative error between the actual and predicted values of the total scattering cross section is shown in the last column of the table. It can be observed that the relative error between the actual and predicted values of total scattering cross section of random cylinders is small. The maximum absolute relative

r_d	N	σ_p^2	$L_M = l_w$	σ_T^{rc}	l_m	σ_T^{ecp}	Rel Error(%)
0.7	5	0.00833	1.53030	3.45580	1.00594	3.44435	0.33138
0.7	5	0.00833	1.38039	3.09484	1.11517	3.19566	3.25781
0.7	5	0.00833	1.40905	3.20283	1.09250	3.24234	1.23357
0.7	5	0.00833	1.66199	3.64408	0.92623	3.67077	0.73264
0.7	5	0.00833	1.58084	3.54868	0.97377	3.53048	0.51284
1.0	5	0.00833	2.07822	4.68101	1.51168	4.61974	1.30901
1.0	5	0.00833	1.93518	4.46374	1.62341	4.37417	2.00670
1.0	5	0.00833	1.86644	4.51721	1.68320	4.25847	5.72780
1.0	5	0.00833	1.86241	4.44376	1.68684	4.25174	4.32101
1.0	5	0.00833	1.99972	4.64064	1.57101	4.48422	3.37076
1.5	5	0.00833	3.08246	6.74703	2.29317	6.70787	0.58043
1.5	5	0.00833	3.13249	6.93210	2.25654	6.79806	1.93360
1.5	5	0.00833	3.20769	6.86751	2.20364	6.93418	0.97076
1.5	5	0.00833	3.0546	6.73603	2.31408	6.65781	1.16119
1.5	5	0.00833	3.17413	6.82203	2.22694	6.87335	0.75231
2.0	5	0.00833	4.16787	8.88444	3.01506	8.92640	0.47232
2.0	5	0.00833	3.95161	8.67011	3.18007	8.53011	1.61480
2.0	5	0.00833	3.97449	8.70368	3.16176	8.57179	1.51527
2.0	5	0.00833	4.03937	8.77684	3.11098	8.69049	0.98388
2.0	5	0.00833	3.82897	8.50679	3.28192	8.32665	2.11765
2.5	5	0.00833	4.90999	10.62467	3.99898	10.50121	1.16201
2.5	5	0.00833	5.12970	11.01976	3.82770	10.90852	1.00946
2.5	5	0.00833	5.02351	10.78447	3.90861	10.71130	0.67848
2.5	5	0.00833	5.18173	11.05944	3.78927	11.00538	0.48881
2.5	5	0.00833	5.16244	11.00824	3.80343	10.96945	0.35237

Table 4.4: Comparison between total scattering cross sections of approximate equivalent elliptical cylinder and random cylinder, for constant variance.

error between the two values in this table is less than 6%.

Table 4.5 shows same parameters, as given in Table 4.4, for some more sample random cylinders. The mean radius of these cylinders is different and their variance is relatively large. Maximum value of the absolute relative error in this table is about 10%. The values of absolute relative error in Table 4.5 are slightly higher than similar values of Table 4.4. This is because the variance of sample random cylinders in Table 4.5 is high and their cross sectional shape can deviate markedly from any canonical shape. Hence the above stated differences in the predicted values of total scattering cross section are not considered large.

The total scattering cross section of random cylinder and its predicted value obtained from the elliptical cylinder, given in above Tables, are also compared with the total scattering cross sections of circular cylinder and strip. This comparison helps to show that which of the three structures is a better equivalent structure, for a given lateral width. Figure 4.3 shows σ_T^c and σ_T^{ecp} , for ensembles given in Tables 4.4 and 4.5, as scatter points. Solid and dotted lines on the scatter plot represent total scattering cross sections of a circular cylinder and a strip, respectively. Rectangular blocks on the plot mark total scattering cross section of random cylinder and triangular points are their predicted values. It can be observed that most of the scatter points in Figure 4.3 lie near the solid line, i.e., total scattering cross section of circular cylinder. This observation is consistent with the earlier conclusion, section 3.5, i.e., a circular cylinder is a better equivalent than a strip for random cylinder. It can also be observed that the predicted values of total scattering cross section, σ_T^{ecp} , are closer to the actual values as compared to that of circular cylinder. Hence total scattering cross section of a random cylinder can be better predicted with an approximate elliptical

r_d	N	σ_p^2	$L_M = l_w$	σ_T^{rc}	l_m	σ_T^{ecp}	Rel Error (%)
0.7	6	0.36000	2.70965	5.68205	0.56811	5.60835	2.33466
0.7	6	0.36000	2.09073	4.20041	0.73629	4.44169	10.33969
0.7	6	0.36000	1.74978	4.05764	0.87976	3.82497	10.32155
0.7	6	0.36000	2.18386	4.78158	0.70489	4.61391	6.31211
0.7	6	0.36000	2.80135	5.90842	0.54951	5.78385	3.79515
1.0	10	0.01667	2.17496	4.73707	1.44444	4.78895	1.97116
1.0	10	0.01667	2.16066	4.91588	1.45399	4.76378	5.56937
1.0	10	0.01667	2.29237	4.76893	1.37046	4.99716	8.61428
1.0	10	0.01667	2.00120	4.65268	1.56985	4.48676	6.41897
1.0	10	0.01667	2.36305	5.15376	1.32947	5.12382	1.04575
1.0	5	0.03333	2.38947	5.36657	1.31476	5.17140	6.54642
1.0	5	0.03333	2.24514	4.96538	1.39929	4.91305	1.89712
1.0	5	0.03333	2.29603	5.14710	1.36827	5.00369	5.01528
1.0	5	0.03333	2.33596	5.25353	1.34488	5.07516	6.11127
1.0	5	0.03333	2.12070	4.83616	1.48140	4.69375	5.30052
1.0	15	0.02500	2.37922	5.20048	1.32043	5.15293	1.64588
1.0	15	0.02500	2.28353	5.02313	1.37576	4.98138	1.49622
1.0	15	0.02500	2.46652	5.09313	1.27370	5.31083	7.69364
1.0	15	0.02500	2.25852	5.01581	1.39100	4.93683	2.83410
1.0	15	0.02500	2.33416	5.16706	1.34592	5.07194	3.31364
1.5	10	0.01667	3.47855	7.37816	2.03205	7.43009	1.26685
1.5	10	0.01667	3.18020	6.78845	2.22269	6.88435	2.54309
1.5	10	0.01667	3.23217	6.88728	2.18695	6.97864	2.38773
1.5	10	0.01667	3.52001	7.37644	2.00812	7.50645	3.17270
1.5	10	0.01667	3.25328	6.85649	2.17276	7.01705	4.21486

Table 4.5: Comparison between total scattering cross sections of approximate equivalent elliptical cylinder and random cylinder.

cylinder than a circular cylinder, if the lateral width and mean radius of the random cylinder are known.

4.4 Summary

In this chapter analytical expression as well as numerical formulation has been given to determine the total scattering cross section of an elliptical cylinder. Analytic expression is given as an infinite series in terms of Mathieu functions. MM formulation has been given to numerically determine the scattered field and total scattering cross section of elliptical cylinder. An equivalent elliptical cylinder is obtained on the basis of total scattering cross section of random cylinder. Major axis of equivalent elliptical cylinder is kept equal to the average lateral width of an ensemble. Minor axis of equivalent elliptic cylinder is obtained numerically using iterative method.

Geometric parameters such as eccentricity and equivalent radii ratio of equivalent elliptical cylinder are obtained. These parameters are compared with the equivalent radii ratio of random cylinders. No correspondence has been observed between the eccentricity or equivalent radii ratio of equivalent elliptical cylinder with the equivalent radii ratio or other input parameters of the ensemble. It has been observed that the two axes of the equivalent elliptical cylinder are inversely proportional to each other and the area of mean radius circular cylinder is the proportionality constant. A hypothesis is developed to approximately determine the minor axis of equivalent elliptical cylinder. The mean radius and lateral width of a random cylinder are needed to be known in order to use the hypothesis.

Finally in this chapter, the hypothesis is tested on individual random cylinders.

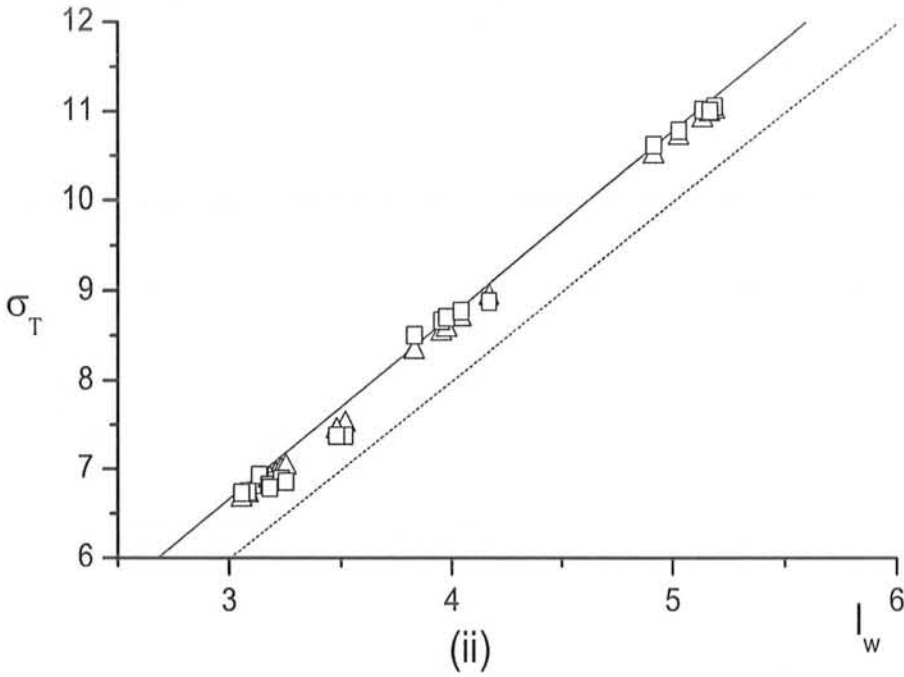
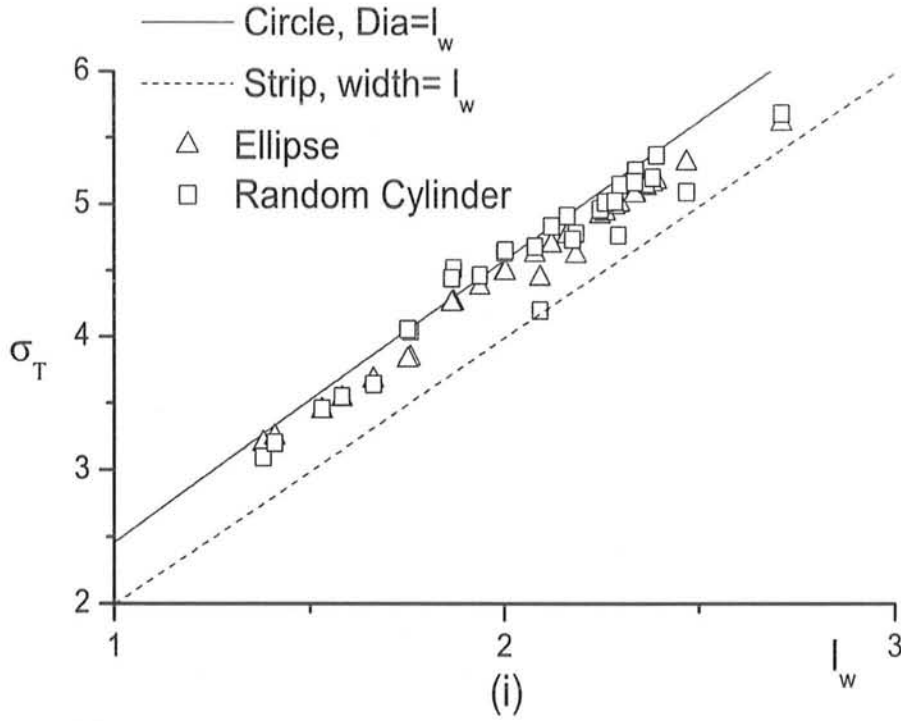


Figure 4.3: A comparison of total Scattering cross section of random cylinders and their predicted values with that of a circular cylinder and flat strip. (i) Lateral width between $1\lambda - 3\lambda$. (ii) Lateral width between $3\lambda - 6\lambda$.

The total scattering cross section of random cylinder is compared with total scattering cross section of approximate equivalent elliptical cylinder and circular cylinder of diameter equal to lateral width. This comparison revealed that approximated equivalent elliptical cylinder is a better equivalent than a circular cylinder. It has also been seen that the relative error between the actual total scattering cross section and that obtained from approximate equivalent elliptical cylinder is small. Hence an approximate elliptic cylinder can be used to predict the total scattering cross section of any cylinder with random cross section.

Chapter 5

Conclusion

In general the scattering properties of a perfectly electrically conducting but arbitrarily shaped object are difficult to determine as these properties are highly dependent on the shape of the object. Non resemblance of these structures with any canonical shape makes it impossible to apply analytical methods for determination of their scattering properties. In such cases numerical methods have to be used. In addition to error introduced by a numerical method, the numerical procedure has to be repeated for a new shape. Therefore, an engineering insight is needed to predict scattering properties of arbitrarily shaped objects. Scientists have made efforts to approximate certain electrical characteristics of an arbitrarily shaped object with the help of its non-electrical parameters. It is relatively easy to determine scattering due to canonically shaped objects hence attempts have been made to equate an electrical property of arbitrarily shaped object with that of a canonically shaped structure. The resultant canonically shaped structure is said to be an equivalent structure. Work on determining an equivalent canonically shaped object with the help of chosen geometrical parameters of arbitrarily shaped structures is also found in literature [40, 60].

Papas has shown that total scattering cross sections of a circular cylinder and

a strip are related to their cross sectional widths [56, 57]. Jaggard and Papas [40] have determined that if the capacitance between an arbitrarily shaped cylindrical structure and a cylinder at infinity is taken as invariant parameter then radius of equivalent circular cylinder can be obtained from the geometrical parameters of the arbitrarily shaped cylinder [40]. It has also been shown by Jaggard [60] that the radius of an equivalent circular cylinder can be approximated from the bounding values. These results give a source of motivation to explore the possibility of predicting total scattering cross section of arbitrarily shaped cylindrical structure from its geometrical parameters.

In this work scattering properties of arbitrarily shaped cylindrical structures have been studied. The motivation has been to obtain an engineering insight for their scattering properties. Arbitrarily shaped cylindrical structure considered in this thesis is an angularly corrugated cylindrical structure, i.e., a structure whose cross section does not vary along cylindrical axis. The study has been focused on scattering properties due to arbitrariness of the shape therefore the complexities in a scattering problem introduced by surrounding of the scatterer, its material and incident field are kept at minimum, i.e., the scatterer is assumed to be placed in free space, consists of PEC material and a linearly polarized plane wave with E vector along the cylindrical axis, is incident on the cylinder.

There are many challenges posed by arbitrary shape of scatterer. First of all it is difficult to mathematically describe it. The term arbitrary cross section describes an infinite set of cross sections. It gives rise to following questions: what parameters will define a certain class of arbitrary cross sections? How many samples of a certain class of arbitrary cross sections should be studied before developing any hypothesis? As far

as electromagnetic scattering is concerned arbitrariness of the cross section does not give any intuitive insight to the scattered field. In short, challenges in this problem exist right from the beginning till the end, i.e., from modelling of an arbitrary cross section to determining and analyzing its scattered field.

An arbitrary cross section can be mathematically modelled with the help of a random process. The resulting cylinder is referred to as random cylinder. In this thesis two random cylinder models are defined using an auxiliary random process. The auxiliary process is a finite Fourier series with uniformly varying random coefficient and phase. Finite number of terms in the Fourier series help to limit the number of crests and troughs of the process. Variance of zero mean random coefficient controls deviation from the mean value of the random process and random phase makes the resultant process stationary. It has been shown that for five or more number of terms the pdf of auxiliary random process is approximately Gaussian. One model of random cylinder is obtained by simply shifting the mean of the auxiliary random process. This model is called as Gaussian cylinder. The other model is obtained by taking auxiliary process equal to log of radius. It is referred to as Lognormal cylinder.

Analytic expression for mean and variance of radius, mean square area and circumference due to rms differential length are obtained for both the random cylinder models. These parameters help to better visualize the ensemble characteristics of the models. It has been observed that for a given value of mean, variance of radius and number of terms in the Fourier sum, the equivalent radii ratio of lognormal cylinder is greater than that of Gaussian cylinder. This fact discloses that lognormal model has higher tendency to deviate from a circular cross section than the Gaussian model and it is therefore not used any further, in this thesis.

Geometrical features of the selected cylinder model are further investigated. Maximum radius and lateral width of the random cylinder are considered important geometrical parameters in study of electromagnetic scattering from random cylinders. Therefore, probability densities of these two parameters are approximated. It is difficult to obtain exact pdfs of these features hence few assumptions are used. Number of maxima in each realization of a Gaussian cylinder will be equal to the number of terms used in Fourier sum and all of them are located independent of each other, are the assumptions used to approximate pdf of maximum radius. The assumption used to approximate pdf of lateral width is that the points, where the confining planes are tangent to random cylinder are statistically independent of each other. Analytic expressions of the pdfs are complicated and numerical procedures are employed to determine them. These approximated pdfs are compared with the simulated data and are found to be in good agreement with each other.

An ensemble of random cylinder consists of around fifty thousand random cylinders. Scattered field from each random cylinder is determined numerically using method of moment. Weighting and testing function as well as total number of segments for MM are carefully chosen to ensure fast processing and reliability of the resultant scattered field. Scattered field from a circular cylinder is first obtained and is compared with analytic results to ensure reliability of the code. Ensemble average of the scattered field at every angle is also determined and compared with earlier documented results. In the end optical theorem is used to show that scattered field obtained using MM is reliable.

It has been numerically determined that average total scattering cross section of random cylinder is bounded within the total scattering cross section of a strip

and a circle. The lateral widths of bounding structures are equal to average lateral width of the ensemble. It has also been observed that total scattering cross section of mean radius circular cylinder can also be used to define lower bound on average total scattering cross section. A tighter lower bound depends on the variance of the radius, if the variance is large than total scattering cross section of a strip defines a tighter bound.

The radius of equivalent circular cylinder is closer to the average lateral width than the width of an equivalent strip. Hence it is concluded that a circular cylinder is a better equivalent model for random cylinders than a strip. It has been also observed that both equivalent radius and half of average lateral width are bounded within an equivalent area radius and equivalent circumferential radius. The approximation, given by Jaggard [60], to determine the equivalent radius from its bounding values is applied. The value of approximate equivalent radius is greater than the actual equivalent radius and difference between the two increases with increase in variance and number of terms of the Fourier series.

Two dimensional scatter plots between lateral width and total scattering cross section show a petal shaped regular pattern. It is inferred from these plots that these two quantities are highly correlated and majority of the points lie in region between the twice lateral width of sample cylinder and total scattering cross section of circular cylinder with diameter equal to lateral width. The density of the points is also determined to estimate their joint pdf. Estimated pdf is compared with bivariate Gaussian distribution and they are found to be in good agreement with each other.

An elliptical cross section is introduced as an equivalent model for random cylinder, in this thesis. Two parameters are required to define an elliptic cross section.

These are its major and minor axes, if it is represented in cartesian coordinates. Both analytical and MM solutions are obtained for the scattered field due to an elliptical cylinder in free space. Two parameters of random cylinders needed to obtain an equivalent elliptical model are taken to be the lateral width and total scattering cross section of random cylinder. The major axis of equivalent elliptic cylinder is kept equal to lateral width of random cylinder. Minor axis is determined such that the total scattering cross section of elliptical cylinder is equal to that of random cylinders.

In an effort to predict the minor axis of equivalent elliptic cylinder it is observed that the product of the two axis of equivalent cylinder almost remains constant for a given mean radius. It is further determined that the proportionality constant is the area of mean radius circular cylinder. The proportionality constant can be easily obtained from input statistics of random cylinders. Lateral width either can be approximated from input characteristics or can be obtained by generating random cylinders. It can therefore be said that total scattering cross section of an ensemble of random cylinders can be approximated without solving electromagnetic problem for the ensemble. It is important to note that this hypothesis does not remain valid if there is no randomness in the cylinder.

It has been numerically shown the approximation to predict the minor axis of equivalent elliptical cylinder is valid even for a single random cylinder. The hypothesis is applied on few individual random cylinders of different input characteristics. Total scattering cross section predicted by the equivalent model is found very close to actual total scattering cross section of individual random cylinder. These results are very encouraging as one can now predict total scattering cross section of a given random cylinder. Lateral width of the individual sample random cylinder can be obtained

from its cross section and angle of incidence. Assuming stationarity of the radius of random cylinder, its time averaged radius is taken to be its ensemble average radius. With the help of these two parameters of random cylinder an equivalent elliptical cylinder can be approximated and its total scattering cross section can be obtained. Hence total scattering cross section of random cylinder can be predicted without solving electromagnetic problem for random cylinder.

Appendix A

Sum of Stationary Processes

Let \mathbf{X} and \mathbf{Y} be two random processes and their joint density function is given as

$$f_{\mathbf{XY}}(x_1, t_1; x_2, t_2; \cdots; x_n, t_n; y_1, t_1; y_2, t_2; \cdots; y_m, t_m). \quad (\text{A.0.1})$$

If processes \mathbf{X} and \mathbf{Y} are independent processes, then their joint density can be written as product of the individual densities,

$$f_{\mathbf{X}}(x_1, t_1; x_2, t_2; \cdots; x_n, t_n) f_{\mathbf{Y}}(y_1, t_1; y_2, t_2; \cdots; y_m, t_m) \quad (\text{A.0.2})$$

If these processes are also stationary, then their density functions will become

$$f_{\mathbf{X}}(x_1, \cdots x_n; t_2 - t_1, \cdots, t_n - t_1) f_{\mathbf{Y}}(y_1, \cdots y_m; t_2 - t_1, \cdots, t_m - t_1) \quad (\text{A.0.3})$$

Let the sum of these random processes be $\mathbf{P} = \mathbf{X} + \mathbf{Y}$. Density function of \mathbf{P} can be written as

$$f_{\mathbf{P}}(p_1, t_1; p_2, t_2; p_3, t_3; \cdots; p_n, t_n) \quad (\text{A.0.4})$$

$$f_{\mathbf{P}}(x_1 + y_1, t_1; x_2 + y_2, t_2; x_3 + y_3, t_3; \cdots; x_n + y_n, t_n) \quad (\text{A.0.5})$$

where $p_1 = x_1 + y_1, p_2 = x_2 + y_2, \cdots, p_n = x_n + y_n$. It is important to note that the number of samples and their respective sampling time of both the processes, \mathbf{X} and \mathbf{Y} ,

are same. Let \mathbf{Q} be another random process defined as $\mathbf{Q} = \mathbf{X}$. The transformation of pair of random variables (\mathbf{X}, \mathbf{Y}) into a pair of (\mathbf{P}, \mathbf{Q}) is defined as

$$f_{\mathbf{PQ}}(p_1, \dots, p_n, q_1, \dots, q_n) = \frac{f_{\mathbf{XY}}(x_1, \dots, x_n, y_1, \dots, y_n)}{\left| J \begin{pmatrix} p_1 & \dots & p_n & q_1 & \dots & q_n \\ x_1 & \dots & x_n & y_1 & \dots & y_n \end{pmatrix} \right|} \quad (\text{A.0.6})$$

where $J()$ is the Jacobian matrix. The Joint density of \mathbf{X} and \mathbf{Y} can be written in terms of \mathbf{p} and \mathbf{q} as

$$f_{\mathbf{X}}(q_1, \dots, q_n; t_2 - t_1, \dots, t_n - t_1) f_{\mathbf{Y}}(p_1 - q_1, \dots, p_n - q_n; t_2 - t_1, \dots, t_n - t_1) \quad (\text{A.0.7})$$

Jacobian determinant of this transform is unity. The density of process \mathbf{P} can be obtained by integrating the joint density of (\mathbf{P}, \mathbf{Q}) over all values of \mathbf{Q} , i.e.,

$$f_{\mathbf{P}} = \int_{-\infty}^{\infty} \dots \int_{-\infty}^{\infty} f_{\mathbf{X}}(q_1, \dots, q_n; t_2 - t_1, \dots, t_n - t_1) f_{\mathbf{Y}}(p_1 - q_1, \dots, p_n - q_n; t_2 - t_1, \dots, t_n - t_1) dq_1 \dots dq_n \quad (\text{A.0.8})$$

Above integrals are convolution integrals and as all q 's will be integrated out, it will be function of p 's and time differences $t_2 - t_1, \dots, t_n - t_1$ only. The density function of \mathbf{P} depends on $n - 1$ time parameters hence it is also stationary. So the sum of two independent stationary processes is also a stationary.

References

- [1] J.J. Bowman, T.B.A. Senior and P.L.E. Uslenghi. *Electromagnetic and Acoustic Scattering by Simple Shapes*. North-Holland Pub. Co., Amsterdam, 1969.
- [2] S.O. Rice. Reflection of em waves from slightly rough surfaces. *Comm. Pure Appl. Math.*, 4:361–378, 1951.
- [3] D.E. Cartwright and M.S. Longuet-Higgins. The statistical distribution of the maxima of a random function. *Proceedings of the Royal Society of London, Series A, Mathematical and Physical Sciences*, 237(1209):212–232, 1956.
- [4] J. Nakayama, H. Ogura and B. Matsumoto. A probabilistic theory of scattering from a random rough surface. *Radio Science*, 15:1049–1057, 1980.
- [5] J. Nakayama, H. Ogura and M. Sakata. Scattering of a scalar wave from a slightly random surface. *Journal of Mathematical Physics*, 22:471–477, 1981.
- [6] J. Nakayama, H. Ogura and M. Sakata. A probabilistic theory of electromagnetic wave scattering from a slightly random surface– 1. horizontal polarization. *Radio Science*, 16:831–845, 1981.
- [7] J. Nakayama, M. Sakata and H. Ogura. A probabilistic theory of electromagnetic wave scattering from a slightly random surface– 2. vertical polarization. *Radio Science*, 16:847–853, 1981.
- [8] J. Nakayama. Anomalous scattering from a slightly random surface. *Antennas and Propagation Society International Symposium*, 20:312–315, 1982.

- [9] H. Ogura and N. Takahashi. Green function and radiation over a random rough surface. *Journal of Optical Society of America A*, 2(12):2208–2224, 1985.
- [10] H Ogura, T Kawanishi, N Takahashi and Z L Wang. Scattering of electromagnetic waves from a slightly random surface—reciprocal theorem, cross-polarization and backscattering enhancement. *Waves Random Media*, 5(12):461–495, October 1995.
- [11] H. Ogura and N. Takahashi. Scattering, radiation and propagation over two-dimensional random surface stochastic functional approach. *Progress In Electromagnetics Research*, PIER 14:89180, 1996.
- [12] A.T. Manninen. Multiscale surface roughness and backscattering. *Progress In Electromagnetics Research*, PIER 16:175203, 1997.
- [13] T. Chiu and K. Sarabandi. Electromagnetic scattering interaction between a dielectric cylinder and a slightly rough surface. *IEEE Trans. on Antennas and Propagation*, 47(5):902–913, 1999.
- [14] Y. Tamura and J. Nakayama. Mass operator for wave scattering from a slightly random surface. *Waves Random Media*, 9.
- [15] V.I. Tatarskii and V.V. Tatarskii. Statistical non-gaussian model of sea surface with anisotropic spectrum for wave scattering theory. part i. *Progress In Electromagnetics Research*, PIER 22:259291, 1999.
- [16] V.I. Tatarskii and V.V. Tatarskii. Statistical non-gaussian model of sea surface with anisotropic spectrum for wave scattering theory. part ii. *Progress In Electromagnetics Research*, PIER 22:293313, 1999.
- [17] Chin-Yuan Hsieh. Polarimetric bistatic scattering from random rough surfaces along azimuth angle. *Journal of Microwaves and Optoelectronics*, 1(5):65–87, 1999.

- [18] X. Luo, J. Askne, G. Smith and P. Dammert. Coherence characteristics of radar signals from rough soil. *Progress In Electromagnetics Research*, PIER 31:69–88, 2001.
- [19] C. Bourlier and G. Berginc. Microwave analytical backscattering models from randomly rough anisotropic sea surface—comparison with experimental data in c and ku bands. *Progress In Electromagnetics Research*, PIER 37:31–78, 2002.
- [20] G. Soriano and M. Saillard. Modelization of the scattering of electromagnetic waves from the ocean surface. *Progress In Electromagnetics Research*, PIER 37:101128, 2002.
- [21] C. Macaskill and P. Cao. A new treatment of rough surface scattering. *Proc. Roy. Soc. London Ser. A*, 452(1955):2593–2612, 1996.
- [22] R.L. Wagner, J. Song and W.C. Chew. Monte carlo simulation of em scattering from 2-d random rough surfaces. *IEEE Transactions on Antennas and Propagation*, 45(2):235–246, Feb 1997.
- [23] Y. Zhang, Y.E. Yang, H. Braunisch and J.A. Kong. Electromagnetic wave interaction of conducting object with rough surface by hybrid spm/mom technique. *Progress In Electromagnetics Research*, PIER 22:315335, 1999.
- [24] D.J. Donolve, H.C. Ku and D.R. Thompson. Application of iterative mm solution to ocean surface radar scattering. *IEEE Trans. on Antennas and Propagation*, AP-46(1):748–756, 1998.
- [25] C. Baudier and R. Dusseaux. Scattering of an e//–polarized plane wave by one-dimensional rough surfaces: Numerical applicability domain of a rayleigh method in the far-field zone. *Progress In Electromagnetics Research*, PIER 34:1–27, 2001.

- [26] R. Dusseaux and R. de Oliveira. Scattering of a plane wave by a 1-dimensional rough surface study in a nonorthogonal coordinate system. *Progress In Electromagnetics Research*, PIER 34:6388, 2001.
- [27] L. Tsang, J. A. Kong, K. Ding and C.O. Ao. *Scattering of Electromagnetic Waves: Numerical Simulations*. John Wiley & Sons, New York, 2001.
- [28] G. Granet, K. Edee and D. Felbacq. Scattering of a plane wave by rough surfaces: A new curvilinear coordinate system based approach. *Progress In Electromagnetics Research*, PIER 37:235250, 2002.
- [29] H. Ogura and N. Takahashi. Scattering of waves from a random spherical surface—mie scattering. *Journal of Mathematical Physics*, 31(1):61–75, 1990.
- [30] A.K. Fung, M.R. Shah and S. Tjuatja. Numerical simulation of scattering from 3d randomly rough surfaces. *IEEE Transactions on Geoscience and Remote Sensing*, 32(5):986–994, Sep 1994.
- [31] L. Tsang, J. A. Kong and K. Ding. *Scattering of Electromagnetic Waves: Theories and Applications*. John Wiley & Sons, New York, 2000.
- [32] N. Blaunstein, D. Censor and D. Katz. Radio propagation in rural residential areas with vegetation. *Progress In Electromagnetics Research*, PIER 40:131153, 2003.
- [33] S.H. Tseng, A. Taflove, D. Maitland, V. Backman and J.T. Walsh Jr. Investigation of the noise-like structures of the total scattering cross-section of random media. *Optics Express*, 13(16):6127–6132, 2005.
- [34] Cornel Eftimiu. Electromagnetic scattering by rough conducting circular cylinders—i: Angular corrugation. *IEEE Transactions on Antennas and Propagation*, 36(5):651–658, May 1988.

- [44] A. Papoulis. *Probability, Random Variables and Stochastic Processes*. McGraw-Hill, New York, third edition, 1995.
- [45] Bilal M. Ayyub and Richard H. McCuen. *Probability, Statistics and Reliability for Engineers*. CRC Press, Boca Raton–New York, 1997.
- [46] M.I. Mischenko, J.W. Hovenier and L.D. Travis, editors. *Light Scattering by Nonspherical Particles: Theory, Measurements, and Applications*. Academic Press, New York, 2000.
- [47] Sverre Gran. *A Course in Ocean Engineering*. Elsevier Science Pub., Amsterdam, 1992.
- [48] S.O. Rice. Mathematical analysis of random noise. *Selected Papers on Noise and Stochastic Processes*, Ed. Nelson Wax, Dover Pub. Inc., NY.:133–294, 1954.
- [49] Atif Raza. *Scattering from Random Boundaries*. M.Phil. Thesis, Department of Electronics, Quaid-i-Azam Univerisity, Islamabad, 2003.
- [50] R.F. Harrington. *Field Computation by Moment Methods*. IEEE Press, New York, 1993.
- [51] J.J.H. Wang. *Generalized Moments Method in Electromagnetics*. John Wiley & Sons, New York, 1991.
- [52] C. A. Balanis. *Advanced Engineering Electromagneteics*. John Wiley & Sons, New York, 1989.
- [53] M. Abramowitz and I. A. Stegun. *Handbook of Mathematical Functions*. National Bureau of Standards, Washington DC, 1964.
- [54] K.F. Warnick and W.C. Chew. Accuracy of the method of moments for scattering by a cylinder. *IEEE Transactions on Microwave Theory and Techniques*, 48(10):1652–1660, 2000.